

Electronic Thesis and Dissertation Repository

7-14-2021 1:00 PM

Characterizing The Cellular, Molecular, And Behavioural Pathology Of Repetitive mTBI In A Human Tau Transgenic Mouse

Morgan A. Walker, *The University of Western Ontario*

Supervisor: Brown, Arthur, *The University of Western Ontario*

A thesis submitted in partial fulfillment of the requirements for the Master of Science degree in Neuroscience

© Morgan A. Walker 2021

Follow this and additional works at: <https://ir.lib.uwo.ca/etd>



Part of the [Pathological Conditions, Signs and Symptoms Commons](#)

Recommended Citation

Walker, Morgan A., "Characterizing The Cellular, Molecular, And Behavioural Pathology Of Repetitive mTBI In A Human Tau Transgenic Mouse" (2021). *Electronic Thesis and Dissertation Repository*. 8002.
<https://ir.lib.uwo.ca/etd/8002>

This Dissertation/Thesis is brought to you for free and open access by Scholarship@Western. It has been accepted for inclusion in Electronic Thesis and Dissertation Repository by an authorized administrator of Scholarship@Western. For more information, please contact wlsadmin@uwo.ca.

Abstract

After an episode of repetitive mild traumatic brain injury (rmTBI), many cellular and molecular cascades are initiated that result in the disruption of the structural and chemical integrity of the components in the brain, leading to the development of various cognitive deficits. The goal of this thesis was to evaluate a mouse model of concussion in order to study the relationship between rmTBI, GSK3 β and tau phosphorylation, and behavioural outcomes in a transgenic mouse line expressing solely human tau. We found that there was increased phosphorylation of the two main regulatory sites on GSK3 β , Tyr216 and Ser9, in the C57BL/6 mice. When investigating the pathology and behaviour in the *MAPT* KI mice, there was positive silver staining, pathological tau staining (AT8), and increased Iba1 staining compared to shams, with animals displaying cognitive deficits upon behavioural testing. Overall, this study supports the use of *MAPT* KI transgenic mice in rmTBI studies.

Keywords

Repetitive mild traumatic brain injury (rmTBI), concussions, Chronic Traumatic Encephalopathy (CTE), tauopathy, glycogen synthase kinase 3 (GSK3), glycogen synthase kinase 3-beta (GSK3 β), tau, *MAPT* KI mice

Summary for Lay Audience

Traumatic brain injuries (TBIs) are injuries that affect the structural integrity of the brain which, in turn, has a negative impact on brain functions and influences the behaviour of those affected. The least severe form of TBIs, known as mild TBIs (mTBIs) includes concussions and sub-concussive closed head injuries. When the exposure to mTBIs becomes repetitive, in other words repetitive mild traumatic brain injuries (rmTBI), there is an increased risk for the development of a neurodegenerative disease known as Chronic Traumatic Encephalopathy (CTE). The main characteristic of this disease is the presence of abnormal tau protein aggregates in the brain. One protein that has been implicated in the process of formation of these abnormal protein aggregates is called glycogen synthase kinase 3-beta (GSK3 β).

There is always the struggle of taking results from scientific studies involving animal models and then applying them to human beings. However, technological advancements have allowed the development of genetic tools that have been applied to rodents in order to create ideal models with greater clinical relevance to human disease. In this thesis I investigate a novel mouse model in which the entire mouse tau gene has been replaced with the human tau gene. I use this mouse model to characterize the structural damage, at the cellular and molecular levels, that occur post-rmTBI, as well as the behavioural outcomes, in order to validate the use of this model in future research.

This study demonstrates that the novel mouse model is capable of developing the cellular and molecular injuries typical of rmTBIs. The mice also demonstrate behavioural deficits that correlate with rmTBI injury, similar to that seen in humans. Overall, this study supports the use of these mice for future rmTBI studies, as these mice are more clinically relevant and therefore more desirable models. This study will hopefully serve as a stepping stone for future studies of rmTBI with a focus on further characterizing the pathology and developing and applying potential therapeutics.

Acknowledgments

First, I would like to thank Dr. Brown for giving me the opportunity to work within his lab. I have had the chance to grow as a graduate student within the lab, as well as a person outside of the lab. This experience has really opened my eyes as to what graduate school is all about and what it takes to succeed. Dr. Brown served both as a leader, guiding me throughout my Master's by action, and as a mentor, helping me understand the types of questions I should be asking as I move through experiments. He is a supportive and positive role model, and I will be forever grateful for all of the lessons that I have learned, both within and outside of the academic setting.

Next, I would like to individually thank the various members of the Brown Lab. I would like to thank Dr. Kathy Xu for teaching me how to conduct the live animal surgeries, upon which the entire project is based, and for guiding me throughout the process of starting up and maintaining my colony. It was amazing to be able to learn the ins and outs of the breeding and genetics that goes on behind the scenes. I also appreciate all of her mentorship in teaching me how to properly dissect specific brain regions for analyses, and for helping me during the COVID-19 pandemic. I would like to thank Dr. Todd Hryciw for taking the time to show me how to conduct various protein assays and how to properly organize and run western blots; in addition, he helped in running some of my samples during the pandemic. I learned a lot and became more aware of how to choose the appropriate internal and external controls in order to properly compare across different western blots. Lastly, I would like to thank Dr. Nicole Geremia for teaching me how to conduct my behavioural experiments and lending me a helping hand in running them. She has always been a positive light throughout this experience, offering constant words of encouragement. Although she was a part of the Brown lab for only a brief time period as a lab volunteer, I would also like to thank Carla Du Toit for helping me run some of the many westerns that were a part of this project.

A gracious thank you goes out to the members of my Advisory Committee, and those who had to step in as my committee members throughout my degree: Dr. Greg Dekaban, Dr. Vania Prado, Dr. Stephen Pasternak, and Dr. Brian Corneil. Thank you for all of the guidance and feedback that was provided during our gatherings, for without it I would not have gained new perspectives and ideas to implement into my thesis.

With regard to my personal life outside of the lab, I would like to take the time to thank my amazing friends/teammates/roommates: Dagmar Wallsten, Olivia Bechberger, and Bry Muir. Without these lovely ladies I probably would have lost my focus due to overthinking. I definitely would have never seen the light of day or had the chance to get out of my shell and learn to get an outside perspective. Together, they have been the best support system, pushing me to be a better version of myself. I honestly do not know what I would have done without them.

Of course, I would like to appreciate and thank my parents for always having my back and believing in my abilities. They both have been so supportive and encouraging throughout this entire experience. I honestly appreciate all of the sacrifices that they have made to help me get to where I am today, and the sacrifices they continue to make as I prepare for my PhD. These efforts do not go unnoticed and I promise to work hard to make their sacrifices worth it.

Finally, I would like to thank all of my boys: Jasveer Dhindsa (my boyfriend), Atlas (my dog), and Oscar (my cat). It is great to have the three of them in my corner constantly cheering me on or offering me cuddles after a long day in the lab. They serve as my constant motivation to keep moving forward and to push through and become a better student/person. Again, I could not have done it without their constant support.

Overall, this Masters has put me through a lot more than I expected. I knew it was going to be tough, as research tends to be; however, what I did not expect was how much I would learn about myself as a person. This, in turn, allowed me to grow and focus on becoming a better version of myself. I honestly cannot wait to see what the future holds; there will definitely be more research, but thanks to this experience, I will be able to tackle anything that comes my way with greater ease.

Funding Sources:

I would like to thank the following organizations, on behalf of the Brown Lab and myself, for funding this project: the Canadian Institutes of Health Research (CIHR) and the Steve Moore Foundation. Without their generosity this project would have never been possible.

COVID-19 Impact Statement

Due to the unfortunate circumstances surrounding the COVID-19 outbreak I was forced to shut down my second experiment right as it was taking off. Before the shut down began, I was actively breeding my colonies in order to increase the numbers so that my experimental groups had sufficient n's. It took a lot of effort to breed the colony up to the point where I had enough mice to conduct the second phase of experiments, and unfortunately those efforts were in vain. In order to comply with the new health regulations surrounding the pandemic, I had to halt the second phase of experiments entirely. The new regulations prohibited my attendance in the lab and therefore put a stop to all data collection. In order to remain productive throughout the shut down, I focused on the writing portion of my thesis; however, only so much can be written without sufficient data collected. Upon returning to the lab, I had to start over from scratch with what was left of my colony.

The pandemic not only interrupted my work, but also affected my overall thesis outline. I had plans to start a lithium study once the second experiment was started. Unfortunately, like I stated before, I had to halt the breeding of the mice as the shut down began and was forced to use the mice that were left over in the colony to start up the experiments from scratch again. This means there were no mice of age/not enough born to conduct the lithium experiments. The importance of this lithium study is that lithium is known to inhibit GSK3 β activity and, therefore, potentially inhibit tau phosphorylation. It would have been very interesting to have observed how lithium would have acted in the treated *MAPT* KI mice, a more clinically relevant model of tauopathy.

Four months off of research takes a toll not only on the research itself, but on the opportunity to share that research with others in the field and to communicate one's findings. It is unfortunate that the timeline of my thesis was thrown off due to the pandemic shut down, and it is unfortunate that the conferences followed suit. Although it is understandable why conferences were cancelled, it is always sad when an opportunity is missed.

Despite the drawbacks of the pandemic, I am grateful for the chance that Dr. Brown and his lab gave me to remain on as a graduate student so that I may finish up my work and produce a quality thesis.

List of Abbreviations

Abbreviations	Terms
rmTBI	Repetitive mild traumatic brain injury
mTBI	Mild traumatic brain injury
TBI	Traumatic brain injury
CTE	Chronic Traumatic Encephalopathy
GSK3	Glycogen synthase kinase 3
GSK3 β	Glycogen synthase kinase 3-beta
GSK3 α	Glycogen synthase kinase 3-alpha
BBB	Blood brain barrier
DAI	Diffuse Axonal Injury
DTI	Diffusion Tensor Imaging
CHIMERA	Closed-Head Impact Model of Engineered Rotational Acceleration
ROS	Reactive oxygen species
RNS	Reactive nitrogen species
DNA	Deoxyribonucleic acid
SalB	Salvianolic acid
GAD	Generalized anxiety disorder
OCD	Obsessive compulsive disorder
mRNA	Messenger ribonucleic acid
PTSD	Posttraumatic stress disorder
PCS	Post-concussive syndrome
AD	Alzheimer's disease
ALS	Amyotrophic lateral sclerosis
TDP-43	Transactive response DNA-binding protein of 43 kDa
SIS	Second-impact syndrome
<i>NEP</i>	Neprilysin gene
A β	Amyloid beta
ACE	Angiotensin-converting enzyme
CACNA1A	Calcium channel subunit gene
MAP	Microtubule-associated protein
MAPT	Microtubule-associated protein tau
NFT	Neurofibrillary tangles
PHF	Paired helical filament
FPI	Fluid percussion injury
CCI	Controlled cortical impact injury
GFAP	Glial fibrillary acidic protein
Iba-1	Ionized calcium-binding adapter molecule 1
EPM	Elevated Plus Maze
MWM	Morris Water Maze
MAPK	Mitogen-activated protein kinase
CK1 δ	Casein kinase 1 delta
cdk	Cyclin dependent kinase

Table of Contents

Abstract.....	ii
Summary for Lay Audience.....	iii
Acknowledgments.....	iv
COVID-19 Impact Statement	vii
List of Abbreviations	viii
Table of Contents.....	ix
List of Tables	xi
List of Figures.....	xii
Chapter 1.....	1
1 Introduction.....	1
1.1 Concussion.....	2
1.2 Chronic Traumatic Encephalopathy	10
1.3 Tau	12
1.4 Glycogen Synthase Kinase 3	16
1.5 Glycogen Synthase Kinase 3-beta and Tau	18
1.6 Models of Traumatic Brain Injury	20
1.7 Rationale, Goals and Aims for Thesis	22
Chapter 2.....	24
2 Materials and Methods.....	24
2.1 Animals.....	24
2.2 Repetitive Mild Traumatic Brain Injury Procedure	24
2.3 Silver Staining.....	25
2.4 Tissue Preparation for Western Blots	25
2.5 Glycogen Synthase Kinase 3 Western Blots.....	25

2.6 Tissue Preparation for Immunohistochemistry	27
2.7 Immunohistochemistry	27
2.8 Elevated Plus Maze Test.....	28
2.9 Morris Water Maze Test.....	29
2.10 Experiment 1: Pilot Study.....	30
2.11 Experiment 2: GSK3 Study	31
2.12 Experiment 3: <i>MAPT</i> KI Study.....	33
Chapter 3.....	36
3 Results	36
3.1 Pilot Study: To validate a closed head, closed skin model of rmTBI.....	36
3.2 Aim #1: To determine the kinetics of GSK3 β phosphorylation post-rmTBI in the C57BL/6 mice.....	39
3.3 Aim #2: To characterize the cellular and molecular pathology triggered by rmTBI in the <i>MAPT</i> KI mice	45
3.4 Aim #3: To characterize the behavioural outcomes triggered by rmTBI in the <i>MAPT</i> KI mice	57
Chapter 4.....	61
4 Discussion and Conclusions.....	61
4.1 Pilot Study.....	61
4.2 Kinetics of GSK3 β Phosphorylation triggered by rmTBI	62
4.3 Characterization of Cellular and Molecular Pathology triggered by rmTBI	64
4.4 Characterization of the Behavioural Outcomes triggered by rmTBI.....	67
4.5 Conclusions.....	68
4.6 Significance.....	68
References.....	70
Curriculum Vitae	95

List of Tables

Table 1. Table outlining the experimental plan for the Pilot Study.	30
Table 2. Table outlining the experimental plan for the GSK3 Study.....	32
Table 3. Table outlining the experimental plan for the <i>MAPT</i> KI Study.	34
Table 4. Table outlining the experimental plan for the aged <i>MAPT</i> KI and C57BL/6 mice.	35

List of Figures

- Figure 1.** Timeline of the GSK3 Study. Timeline showing the various timepoints at which the male C57BL/6 mice were sacrificed, along with their relative sample sizes (n's). 31
- Figure 2.** Timeline of the *MAPT* KI Study. Timeline showing the various timepoints at which the male and female *MAPT* KI mice were sacrificed, along with their relative sample sizes (n's). 33
- Figure 3.** Silver staining during the pilot study. (A) Silver staining of the corpus callosum of a naïve animal (n=2). (B) Silver staining of the optic tract of a naïve animal. (C) Silver staining of the corpus callosum of a closed skin injured animal (n=3). (D) Silver staining of the optic tract of a closed skin injured animal. (E) Silver staining of the corpus callosum of an open skin injured animal. (F) Silver staining of the optic tract of an open skin injured animal. All images were taken at 40x. 38
- Figure 4.** Western blot data for the cortex samples across all timepoints. (A) Graph shows all treatment groups (naïve, sham and injured) for each timepoint looking at the total amount of GSK3 β , GSK3 TOT, relative to β -actin and then compared to the naïve sample. (B) Graphs focus on the amount of phosphorylation at the Tyr216 site on GSK3 β relative to β -actin and then compared to the naïve sample. (C) Graphs focus on the amount of phosphorylation at the Ser9 site on GSK3 β relative to β -actin and then compared to the naïve sample. (D) Representative Western blots. Data were presented as mean \pm SEM. SEM was presented as the error bars. One-way ANOVA statistical tests were performed with Tukey's multiple comparisons test, $p < 0.05$. "*" represents treatment groups that significantly differ from the naïve animals. "#" represents significant differences between the sham and injured groups of the same timepoint. 40
- Figure 5.** Western blot data for the hippocampal samples across all timepoints. (A) Graph shows all treatment groups (naïve, sham and injured) for each timepoint looking at the total amount of GSK3 β , GSK3 TOT, relative to β -actin and then compared to the naïve sample. (B) Graphs focus on the amount of phosphorylation at the Tyr216 site on GSK3 β relative to β -actin and then compared to the naïve sample. (C) Graphs focus on the amount of

phosphorylation at the Ser9 site on GSK3 β relative to β -actin and then compared to the naïve sample. (D) Representative Western blots. Data were presented as mean \pm SEM. SEM was presented as the error bars. One-way ANOVA statistical tests were performed with Tukey’s multiple comparisons test, $p < 0.05$. “*” represents treatment groups that significantly differ from the naïve animals. “#” represents significant differences between the sham and injured groups of the same timepoint. 42

Figure 6. Western blot data comparing the amount of phosphorylation at the regulatory sites on GSK3 β to the total amount of GSK3 β protein. (A) Cortex samples for all treatment groups across all the timepoints analyzed focusing on the amount of phosphorylation at the Tyr216 regulatory site, relative to the total amount of protein. (B) Cortex samples for all treatment groups across all the timepoints analyzed focusing on the amount of phosphorylation at the Ser9 regulatory site, relative to the total amount of protein. (C) Hippocampus samples for all treatment groups across all the timepoints analyzed focusing on the amount of phosphorylation at the Tyr216 regulatory site, relative to the total amount of protein. (D) Hippocampus samples for all treatment groups across all the timepoints analyzed focusing on the amount of phosphorylation at the Ser9 regulatory site, relative to the total amount of protein. (E) Hippocampus samples from (D) excluding the naïve animals. Data were presented as mean \pm SEM. SEM represented as the error bars. One-way ANOVA statistical tests were performed with Tukey’s multiple comparisons test, $p < 0.05$. “*” represents treatment groups that significantly differ from the naïve animals. “#” represents significant differences between the sham and injured groups of the same timepoint. 44

Figure 7. Silver staining for the short term timepoints of the *MAPT* KI study. (A) Silver staining of the corpus callosum of a naïve animal (n=6). (B) Silver staining of the corpus callosum of a sham animal sacrificed at the 1 day timepoint. (C) Silver staining of the corpus callosum of an injured animal sacrificed at the 1 day timepoint. (D) Silver staining of the corpus callosum of a sham animal sacrificed at the 7 day/1 week timepoint. (E) Silver staining of the corpus callosum of an injured animal sacrificed at the 7 day/1 week timepoint. All images were taken at 40x. 47

Figure 8. Silver staining for the longer term timepoints of the *MAPT* KI study. (A) Silver staining of the corpus callosum of a sham male sacrificed at the 4 week timepoint. (B) Silver

staining of the corpus callosum of an injured male sacrificed at the 4 week timepoint. (C) Silver staining of the corpus callosum of a sham female sacrificed at the 4 week timepoint. (D) Silver staining of the corpus callosum of an injured female sacrificed at the 4 week timepoint. (E through H) Same order of images as the ones above, except taken from the animals sacrificed at the 10 week timepoint. All images were taken at 40x. 48

Figure 9. Silver staining of the variability of the injuries delivered by the controlled cortical impactor (CCI). (A through D) Snippets of the corpus callosum of the injured male animals sacrificed at the 10 week timepoint. (E through H) Snippets of the corpus callosum of the injured females sacrificed at the 10 week timepoint. Images on the left most side have negligible silver staining and as the images move towards the right most side there is significant amounts of silver staining. Images in the middle vary in the degree of silver staining. Images were taken at 40x. 49

Figure 10. Silver staining of the aged animals. (A) Silver staining of the corpus callosum of an aged *MAPT* KI male sacrificed at 14 months old. (B) Silver staining of the corpus callosum of an aged *MAPT* KI female sacrificed at 12 months old. (C) Silver staining of the corpus callosum of an aged C57BL/6 male sacrificed at 14 months old. (D) Silver staining of the corpus callosum of an aged C57BL/6 female sacrificed at 14 months old. All images were taken at 40x. 50

Figure 11. AT8 staining in the prefrontal cortex of the injured animals. (A) Representative ATLAS image of the brain sections that were stained and imaged. The black box represents the approximate area in which the photos were taken. AT8 staining is red and DAPI staining is blue. (B) Image of a C57BL/6 sham animal donated by Dr. Kathy Xu for comparison to the *MAPT* KI. (C) Image of a C57BL/6 injured animal donated by Dr. Kathy Xu for comparison to the *MAPT* KI. (D) Image of a naïve *MAPT* KI animal. (E) Image of a sham *MAPT* KI animal. (F) Image of an injured *MAPT* KI animal. Numbers in the top right corner represent the n's for each group. All images were taken at 40x. 51

Figure 12. AT8 staining in the prefrontal cortex of the aged animals. (A) Representative ATLAS image of the brain sections that were stained and imaged. The black box represents the approximate area in which the photos were taken. AT8 staining is red and DAPI staining is blue. (B) Image of an aged C57BL/6 male sacrificed at 14 months old. (C) Image of an

aged C57BL/6 female sacrificed at 14 months old. (D) Image of a naïve *MAPT* KI animal. (E) Image of an aged *MAPT* KI male sacrificed at 14 months old. (F) Image of an aged *MAPT* KI female sacrificed at 12 months old. Numbers in the top right corner represent the n's for each group. All images were taken at 40x..... 53

Figure 13. GFAP and Iba1 staining in the corpus callosum area for the injured animals. (A) Representative ATLAS image of the brain sections that were stained and imaged. The black box represents the approximate area in which the photos were taken. GFAP staining is green, Iba1 staining is red and DAPI staining is blue. (B and D) Images of the GFAP and Iba1 staining for a C57BL/6 sham animal donated by Dr. Kathy Xu. (C and E) Images of the GFAP and Iba1 staining for a C57BL/6 injured animal donated by Dr. Kathy Xu. (F and I) Images of the GFAP and Iba1 staining for a naïve *MAPT* KI animal. (G and J) Images of the GFAP and Iba1 staining for a sham *MAPT* KI animal. (H and K) Images of the GFAP and Iba1 staining for an injured *MAPT* KI animal. Numbers in the top right corner represent the n's for each group. All images were taken at 40x..... 54

Figure 14. GFAP and Iba1 staining in the corpus callosum area for the aged animals. (A) Representative ATLAS image of the brain sections that were stained and imaged. The black box represents the approximate area in which the photos were taken. GFAP staining is green, Iba1 staining is red and DAPI staining is blue. (B and D) Images of the GFAP and Iba1 staining of an aged C57BL/6 male. (C and E) Images of the GFAP and Iba1 staining of an aged C57BL/6 female. (F and I) Images of the GFAP and Iba1 staining for a naïve *MAPT* KI animal. (G and J) Images of the GFAP and Iba1 staining of an aged *MAPT* KI male. (H and K) Images of the GFAP and Iba1 staining of an aged *MAPT* KI female. Numbers in the top right corner represent the n's for each group. All images were taken at 40x. 56

Figure 15. Behavioural data from the Elevated Plus Maze (EPM) Test. (A) Time spent in the closed arms of the EPM for sham and injured *MAPT* KI males. (B) Time spent in the open arms of the EPM for sham and injured *MAPT* KI males. (C) Time spent in the centre area of the EPM for sham and injured *MAPT* KI males. (D) Time spent in the closed arms of the EPM for sham and injured *MAPT* KI females. (E) Time spent in the open arms of the EPM for sham and injured *MAPT* KI females. (F) Time spent in the centre area of the EPM for sham and injured *MAPT* KI females. Data were presented as mean±SEM. SEM was

represented as the error bars. “*” represents significant differences between the treatment groups. Student’s t-test was performed for the EPM data, $p < 0.05$ 58

Figure 16. Mean speed and total distance travelled in the Elevated Plus Maze (EPM) Test. (A) Mean speed of sham and injured *MAPT* KI males. (B) Total distance travelled for sham and injured *MAPT* KI males. (C) Mean speed of sham and injured *MAPT* KI females. (D) Total distance travelled for sham and injured *MAPT* KI females. Data were presented as mean±SEM. SEM was represented as the error bars. “*” represents significant differences between the treatment groups. Student’s t-test was performed for the EPM data, $p < 0.05$ 59

Figure 17. Behavioural data from the Morris Water Maze (MWM) Test. (A) Escape latency for each of the four training days of the MWM for both sham and injured *MAPT* KI males. (B) Time spend in both the non-target (Q1-3) and target (Q4) quadrants of the MWM during the probe trial for both sham and injured *MAPT* KI males. (C) Mean swim speed for sham and injured *MAPT* KI males. (D) Escape latency for each of the four training days of the MWM for both sham and injured *MAPT* KI females. (E) Time spend in both the non-target (Q1-3) and target (Q4) quadrants of the MWM during the probe trial for both sham and injured *MAPT* KI females. Data were presented as mean±SEM. SEM was represented as the error bars. “*” represents significant differences between the treatment groups. One-way ANOVA statistical tests were performed for A, B, D, and E with Tukey’s multiple comparisons test. Student’s t-test were performed for C and F, $p < 0.05$ 60

Chapter 1

1 Introduction

After an episode of repetitive mild traumatic brain injury (rmTBI), also referred to as concussions, many cascades are initiated that result in the deterioration of neurons, leading to degeneration within the brain and the development of cognitive deficits. Chronic traumatic encephalopathy (CTE) is a neurodegenerative disease that develops from repetitive impacts sustained to the head causing concussions (Lucke-Wold et al., 2014). This has been observed in both athletes, those in contact sports, and military personnel (Lucke-Wold et al., 2014). It is characterized as a tauopathy as one of the major defining features of the disease involves tau, a microtubule-associated protein. Abnormally phosphorylated tau within neurons begins to form aggregates, fibrils, and tangles, which disrupts normal cell functions such as microtubule assembly and the ability to maintain stable structure within the cell (Kolarova et al, 2012). Abnormal phosphorylation of tau not only causes pathology within neurons, but it also results in cognitive impairments due to the degeneration within the brain itself (Kolarova et al, 2012). This leads to progressive cognitive impairments/dementia such as memory deficits, depression, and increased anxiety/anxiety related behaviours (Luo et al., 2014), observed in CTE. I sought to develop a clinically relevant mouse model of concussion/rmTBI to study the pathophysiological mechanisms that lead to CTE. One mechanism that has been put forward to explain the development of CTE following rmTBI focuses on the tau kinase, glycogen synthase kinase 3-beta (GSK3 β) (Dash et al., 2011; Moszczynski et al., 2018). It has been proposed that GSK3 β is responsible for the abnormal phosphorylation of tau in tauopathies, such as CTE (Hooper, Killick, and Lovestone, 2008). This abnormal phosphorylation of tau is what leads to the pathological formation of aggregates/fibrils/tangles leading to neuronal death (Polydoro et al., 2009).

A model of concussion needs to mimic the tell-tale features of human injury including the cellular pathologies, molecular pathologies, and behavioural outcomes post-injury. The accumulation of all of these features is what ultimately leads to the eventual development of CTE. It is the goal of this thesis to develop and evaluate a mouse model of concussion

in order to study the relationship between rmTBI, GSK3 β activity, tau phosphorylation and the development of cognitive deficits in a transgenic mouse line expressing solely human tau.

1.1 Concussion

Traumatic Brain Injuries (aka Primary Injuries)

Traumatic brain injuries (TBIs) are a devastating set of injuries that affect the structural and chemical integrity of the brain which, in turn, influences the behaviour of those affected (Bramlett & Dietrich, 2015; Kokiko-Cochran et al., 2018; Shultz et al., 2020). When severe, TBIs affect the rest of the central nervous system and cause permanent damage to the brain or even death (Ling et al., 2015). TBIs have recently become of more interest due to the increasing awareness of the general public, as they are a huge health concern (Yap et al., 2017). The complications that arise, post-TBI, create a ripple effect in the health care system, the economy, and cause strain in those closest to the individuals who are injured (Siebold et al., 2018). Anyone can be affected by a TBI, however, some individuals are more at risk than others. Individuals who partake in contact sports, are enrolled in the military, or have careers that increase the probability of injury, are all examples of individuals that are at a higher risk of incurring a TBI (McKee et al., 2009).

TBIs may be classed based on their severity as mild, moderate or severe. Several clinical assessment tools have been developed and used in order to assess the severity of a sustained TBI including various imaging techniques, timing and/or presence of loss of consciousness, presence and/or absence of amnesia, and finally the Glasgow Coma Scale (Siebold et al., 2018). The least severe classification of TBIs, known as mild TBI (mTBI), includes injuries referred to as concussions and sub-concussive injuries, which involve acceleration, deceleration and rotational mechanical forces transmitted to the brain upon impact resulting in shearing of brain tissues (Montenigro et al., 2017). Concussions and sub-concussive injuries are typically closed head injuries which do not involve penetrating forces (Tagge et al., 2018). Specifically, concussions can be defined as any impact that directly or indirectly involves the head producing a number of

symptoms which can recover over a variable length of time, depending on the individuals' circumstance (Montenigro et al., 2017). However, sub-concussions can be defined similarly to that of concussions, with the exception that sub-concussions fail to produce visible symptoms (Bailes et al., 2013; Erlanger, 2015; Montenigro et al., 2017). When repetitive, the pathological sequelae of rmTBIs can accumulate and activate secondary injury cascades and potentially the development of neurological disease (Bailes et al., 2013).

There are many external factors that influence the severity of an mTBI. It has been proposed that acceleration and deceleration forces play an important role in the outcome of the severity of injury (Ling et al., 2015). These forces can act on the brain either in a linear or non-linear/rotational manner, depending on the mechanism or method of delivery for the injury (Ling et al., 2015). The result is the brain, consisting of all of the neurons, glia cells, and other components, being mechanically disarrayed (Ling et al., 2015). The location of the insult, the magnitude of the force behind the injury, the amount of surface area affected, and the amount of freedom of the head to move during impact are also factors to consider (Bolton-Hall et al., 2019).

There are instances in which individuals experience more than one mTBI in a given period of time, referred to as repetitive/repeated mild traumatic brain injury (Donovan et al., 2014). Repetitive mTBI can potentially lead to the development of second-impact syndrome (SIS) (Cobb & Battin, 2004) in which there can be serious consequences including death. It has been shown that there is a window of time in which the brain is more vulnerable to a second potential impact after the initial injury (Laurer et al., 2001; Longhi et al., 2005) contributing to the development of SIS. With each injury, the pathological cascades and behavioural symptoms become additive (Cobb & Battin, 2004).

TBI is often described as having two components: a primary injury and a secondary injury. The primary injury/TBI involves the physical disruption of the brain and includes various mechanical disruptions such as the shearing and stretching of axons (Cernak et al., 2004). However, not all primary injuries/TBIs are the same and this makes treatment

difficult as the nature of these injuries are very heterogenous (Siebold et al., 2018; Washington et al., 2012). The primary injury/TBI initiates many secondary injury cascades, such as, diffuse axonal injury, apoptosis, and ionic disturbances (Cernak et al., 2004). The intensity and duration of these secondary injury cascades depends ultimately on the severity of the initial injury.

Secondary Injuries

Secondary injuries are considered to be any and all pathological cascades that occur after the initial insult to the brain (Cernak et al., 2004). Secondary injuries can roughly be sorted into two major categories: secondary cellular injuries and secondary molecular injuries, which both lead to the development of behavioural deficits (Krishnamurthy K & Laskowitz DT, 2016; Washington et al., 2012). It is worthy to note that certain cases of cellular injury, such as immediate cell death or direct damage to brain tissues, can be considered by some to be primary injuries as they are a result originating directly from the impact (Abdul-Muneer et al., 2015). Behavioural outcomes, on the other hand, are a result of the additive effects of both the secondary cellular and molecular injuries produced from the initial trauma (T. Chen et al., 2011; Davis, 2000).

Secondary Cellular Injuries

Secondary cellular injuries result in mechanical damage to the various structures within the brain (J. R. Hay et al., 2015), as well as damage to cells and/or organelles within the central nervous system (Haber et al., 2017; Mbye et al., 2008). There have been several studies that have investigated the effect of TBIs on the integrity of the blood brain barrier (BBB) post-injury (J. R. Hay et al., 2015; Tomkins et al., 2011; Weissberg et al., 2014). Interestingly, one study investigating the effects of concussive and sub-concussive impacts on football players found that there was increased BBB permeability in both the gray and white matter areas in approximately 40% of the players that were analyzed (Weissberg et al., 2014). The authors postulated that this could be influenced by repeated exposures to sub-concussive events that go unnoticed at the time of the injury, or due to neglected or unreported concussive events (Weissberg et al., 2014). The vasculature within the brain is also at risk post-injury, as mTBIs cause damage to the blood vessels as

a whole and microstructural damage to the vascular cells which decreases and alters blood flow and brain function (Jullienne et al., 2016; Monson et al., 2019). Depending on the severity of the TBI, the location of the injury and the method of delivery, a beneficial or a harmful/prolonged inflammatory response may develop (Burda et al., 2016). With the integrity of the BBB being compromised post-TBI, there is the possibility of the inflammatory response to be sustained by incoming neutrophils, monocytes, and lymphocytes (Ziebell & Morganti-Kossmann, 2010).

The mechanical forces of TBIs also cause stretching, shearing and/or tearing of the neurons and axons of neurons within the brain which, in turn, results in diffuse axonal injuries (DAI) throughout the white matter (Yap et al., 2017). DAI is considered to be a hallmark of TBIs and is of great concern as it results in the disruption of axonal transport, production of retraction bulbs, and in more severe cases, axonal loss and degeneration (Haber et al., 2017). It was discovered that even under very mild axonal stretch conditions there was increased growth cone collapse and smaller growth cones within the tips of regenerative sprouts in developing axons (Yap et al., 2017). Another study, investigating the relationship between diffusion tensor imaging (DTI) and DAI in a Closed-Head Impact Model of Engineered Rotational Acceleration (CHIMERA) mouse model of TBI, discovered that there were DTI abnormalities, post-injury, indicating damage to several white matter tracts such as the optic tract and the corpus callosum (Haber et al., 2017). Silver staining of sections from injured brains was used to confirm the findings of the DTI results. Unfortunately, when cellular damage occurs it can result in various components within the cell to be damaged as well. Organelles, in particular the mitochondria which are essential to neuronal function, are also subject to injury upon TBI (Mbye et al., 2008). Upon injury, many cascades are thrown into disarray (such as Ca^{2+} homeostasis, activation of calpains and caspases, increases in oxidative stress), which results in mitochondrial dysregulation, and ultimately neuronal death (G. Cheng et al., 2012). All of these examples of cellular injury due to TBIs, and many more, are intimately related to various secondary molecular injuries that are initiated post-injury.

Secondary Molecular Injuries

There are many molecular cascades and pathways that are activated post-TBI that are classified as secondary molecular injuries such as the generation of reactive oxygen species (ROS)/reactive nitrogen species (RNS), proapoptotic signals, activation of various enzymes, and production of inflammatory signals (Bramlett & Dietrich, 2015), and many more. TBIs create an environment in which the balance of antioxidants and the generation of ROS/RNS becomes altered, favouring the production of the latter, thus resulting in oxidative stress (Abdul-Muneer et al., 2015). The production of these free radicals, in this case ROS/RNS, poses a serious threat to the maintenance of cellular homeostasis as these radicals are capable of interacting and reacting with any cellular components, therefore compromising cellular function (Tyurin et al., 2000). Oxidative stresses play a role in a number of other secondary injury processes, both cellular and molecular. Oxidative stress has been implicated in the increased permeability of the BBB and brain vasculature, further facilitating inflammation by directly/indirectly initiating the production of various neuroinflammatory signals, and damage to proteins, DNA, and mitochondrial function (Abdul-Muneer et al., 2015; Ansari et al., 2008).

Apoptosis, a form of programmed cell death, can be an early or delayed post-injury response that ultimately results in neuronal death (Uzan et al., 2006; X. Zhang et al., 2004). The initiation of apoptosis can occur via a number of different pathways, all of which are able to interact with one another (X. Zhang et al., 2004) to result in the completion of apoptosis. One method of apoptosis induction is through the activation of caspases, a family of proteases, initiated through intrinsic and/or extrinsic routes. Intrinsic activation signals consist of various stress signals from mitochondria contained within the cell, however, extrinsic signals consist of a number of signals binding to their respective receptors (Uzan et al., 2006). Both intrinsic and extrinsic pathways initiate the proteolytic cleavage of members of the caspase family which allow the enzymes to be able to interact with their substrates, resulting in DNA fragmentation, cytoskeletal disintegration, and ultimately apoptosis (X. Zhang et al., 2004). Another method of regulation for the process of apoptosis is through the balance of members of the B-cell lymphoma-2 (Bcl-2) family. The Bcl-2 family consists of both pro- and anti- cell death

signals, and the balance of these signals influence whether or not apoptosis will occur (Wong et al., 2005). Events, such as TBIs, can tip the scales in favour of apoptosis through the activation/imbalance of any of these pathways resulting not only in neuronal death, but the death of various glial cells as well (X. Zhang et al., 2004).

Once a TBI has occurred, there are many molecular pathways that are involved in the inflammatory process that are activated and are able to influence various cellular changes that occur throughout the inflammatory response (Ghirnikar et al., 1998). Some of these pathways include the release of several mediators such as prostaglandins, free radicals (ROS/RNS), and cytokines which facilitate the expression of chemokines (Ghirnikar et al., 1998). The production and levels of cytokines and chemokines play a role in the neuropathological outcome after TBIs. There is controversy surrounding the therapeutic value of inflammation post-injury, due to the fact that inflammation can benefit the central nervous system by clearing out damaged cells and debris, while a pro-longed inflammatory response can be detrimental (Morganti-Kossmann et al., 2001). In particular, cytokines involved in the inflammatory process can be divided into two subgroups, one being cytokines with pro-inflammatory properties and the other being cytokines with anti-inflammatory properties (T. Chen et al., 2011). One study investigating the effects of administration of salvianolic acid B (SalB) on TBI found that SalB blocked the activities of pro-inflammatory cytokines, thus preventing the infiltration of incoming inflammatory cells while increasing the expression of anti-inflammatory cytokines (T. Chen et al., 2011). The treatment with SalB resulted in various improvements post-TBI in the form of decreased lesion volumes, brain edema, and behavioural deficits with decreases in motor functional and spatial learning/memory impairments (T. Chen et al., 2011).

Behavioural Outcomes

There are many cognitive, behavioural, and emotional conditions that arise post-TBI/TBIs due to the accumulated actions of secondary cellular and molecular injury processes (Davis, 2000; Washington et al., 2012). The intensity, the number, and the

nature of the TBIs can influence the prevalence of these conditions post-injury (Washington et al., 2012).

The most common behavioural outcome occurring after TBIs is the development of depression, with a higher percentage of individuals developing some level of depression post-injury compared to anxiety (Leong Bin Abdullah et al., 2018; Mauri et al., 2014). One study investigating the prevalence of Axis I and II disorders (mental health/substance use disorders versus personality/mood disorders), post-TBI, discovered that the development of major depression was present at both the acute and chronic time points of the study, all the way up to the 30 year follow up checkpoint (Koponen et al., 2002). The onset of depression post-TBI can be attributed to the damage from the initial injury itself, various secondary injury pathways (example: decreased glucose metabolism), and external lifestyle factors (Fann et al., 2009). There is a possibility that individuals who experience TBIs, and develop depression, can also develop anxiety as well, on top of the depression, making treatment even more difficult (Barker-Collo et al., 2018).

Anxiety disorders are another common behavioural outcome after TBIs. There is an increased risk for the development of several anxiety disorders post-injury including generalized anxiety disorder (GAD), obsessive compulsive disorder (OCD), panic disorder, and others (Hiott & Labbate, 2002). In one study, the authors sought to investigate anxiety/anxiety-like behaviours in a rodent mild blast TBI model and aimed to correlate the behavioural outcomes to possible changes at the genetic level (Blaze et al., 2020). In this study there were significant increases in anxiety/anxiety-like behaviour at the acute time points studied and, while not statistically significant, there was a trend towards increased anxiety at chronic time points. This study also showed that there were significant changes in gene expression in the amygdala post-TBI at chronic time points by transcriptomic analyses (Blaze et al., 2020). Other reports have indicated changes in the structural features of the amygdala as well as differences in various molecular processes, such as levels of mRNA and protein expression (Almeida-Suhett et al., 2014; Tate et al., 2016).

The relationship between TBIs and posttraumatic stress disorder (PTSD) is both controversial and complex (Y.-F. Chen & Zhao, 2019). Scientists have proposed that in some circumstances TBIs, in particular mTBIs/rmTBIs, can be an important risk factor for the development of this anxiety disorder (Hoge et al., 2008). This could be in large part due to the fact that individuals who suffer mTBIs/rmTBIs in a traumatic scenario are able to remember the traumatic event due to lack of loss of consciousness and are more likely to develop PTSD (Gil et al., 2005). Situations that typically give rise to PTSD tend to also involve the potential for incurring TBIs, such as active military personnel or abuse victims (Y.-F. Chen & Zhao, 2019). Both TBIs and PTSD lead to the development of several undesirable and harmful behavioural traits including depression, violence, substance abuse, and suicidal tendencies (Y.-F. Chen & Zhao, 2019).

Cognition, memory, and learning processes are all negatively affected by TBIs. There is decreased spatial information processing, and decreased learning and memory processing, all of which are dependent on the hippocampus (Pierce et al., 1998; Rola et al., 2006). There are many underlying pathological pathways that are initiated, post-TBI, that could play a role in the cognitive/learning/memory deficits observed. In particular, one study looking into the effects of TBIs on neurogenesis in the hippocampus found evidence of cell loss/death, changes in cell fates, and evidence of persisting inflammation (Rola et al., 2006). Another study revealed that TBI increases the production of ROS (corresponding to oxidative stress) and decreases antioxidant and synaptic protein levels (Ansari et al., 2008), most likely contributing to cellular dysfunction/cell death in the hippocampus and behavioural deficits. Overall, the nature of TBIs is quite heterogeneous as is the patient population therefore making behavioural deficits difficult to predict.

Outcomes Post-Concussion

Ultimately there are four possible outcomes after an episode(s) of TBI. First, a concussed individual can have symptoms acutely that then resolve within days or weeks (Alexander, 1995). Second, a concussed individual may develop post-concussive syndrome (PCS), in which the symptoms take longer, months or even years, to resolve (Maroon et al., 2012). PCS is a very complex phenomenon in which the composition of symptoms can vary

within the same individual over time (Maroon et al., 2012). Third, an unfortunate subgroup of concussed individuals may go on to develop a neurodegenerative disease known as Chronic Traumatic Encephalopathy (CTE) (McKee et al., 2013). Concussions have been shown to be a risk factor for the development of CTE in several studies (McKee et al., 2009, 2013; Roberts et al., 1990). There is also a possibility to further develop other neurodegenerative characteristics or diseases alongside CTE such as CTE with Alzheimer's Disease (AD) (Turner et al., 2016; Yuan & Wang, 2018), CTE with Amyotrophic Lateral Sclerosis (ALS) (Moszczynski et al., 2018; Walt et al., 2018), and CTE with other pathological protein deposits, such as transactive response DNA-binding protein of 43 kDa (TDP-43) (Heyburn et al., 2019; McKee et al., 2010). The fourth possible outcome after TBI is death, either from complications post-injury, SIS (Cobb & Battin, 2004), and eventual death from the development of CTE.

1.2 Chronic Traumatic Encephalopathy

History of Chronic Traumatic Encephalopathy

In 1928, an initial description of what is now known to be CTE was first described by Dr. Martland as he analyzed the brain pathology and behaviours of boxers known to be “punch drunk” who had developed both mild and severe symptoms (Martland, 1928). He proposed that the development of the “punch drunk” syndrome was the result of multiple injuries to the head (Martland, 1928). In 1934, Dr. Parker expanded upon the work of Dr. Martland and referred to the syndrome as “traumatic encephalopathy” (Parker, 1934). Dr. Parker confirmed that repeated injuries to the head sustained during the sporting careers of boxers leads to the development of numerous symptoms, which he referred to as a ‘medley’ of symptoms (Parker, 1934). Later, in 1937, another scientist named Millspaugh observed similar symptoms and behaviours as Martland, mostly in boxers, and used a different term, “dementia pugilistica” (Baugh et al., 2012). Many other scientists and researchers over time have looked into this phenomenon and many names were put forward (Stein et al., 2014). It was during the 1940s that the term “Chronic Traumatic Encephalopathy” (CTE) was coined, and it is now widely used and accepted (Montenigro et al., 2015). Since then, the study of CTE has advanced and the natural progression of CTE has been characterized (McKee et al., 2013).

Risk Factors for Chronic Traumatic Encephalopathy

Both environmental and genetic risk factors, and the interaction between these risk factors, play a role in the development of CTE (Gavett et al., 2010). The most obvious environmental risk factor for the development of CTE is the exposure to mTBI (Gavett et al., 2010, 2011; McKee et al., 2009). As mentioned previously, individuals who participate in contact sports, are enrolled in the military, suffer from domestic abuse, or have any instance where exposure to repeated concussive or sub-concussive impacts is increased, have a greater risk of developing CTE (Baugh et al., 2012). Individuals who experience frequent falls, vehicular accidents, or have epilepsy are also populations at risk for the development of CTE (Gavett et al., 2010).

Genetic background also plays a role in the recovery from TBI and may explain some of the variability seen in the recovery process (McAllister, 2010). Candidate genes and their respective alleles, as well as various epigenetic factors acting on these genes, can act alone or interact and therefore influence the outcome(s) post-injury (McAllister, 2010). There are several known genetic risk factors associated with a poorer outcome post-injury (J. Hay et al., 2016). Individuals with the *APOE* ϵ 4 allele and/or the longer microsatellite polymorphism repeat located in the promoter in the neprilysin gene (*NEP*) are subject to a greater risk for the development of amyloid beta ($A\beta$) plaques, and neurological impairment post-TBI (J. Hay et al., 2016). Polymorphisms in TP53, angiotensin-converting enzyme (*ACE*), and calcium channel subunit gene (*CACNA1A*), are also associated with a poorer outcome post-TBI (McAllister, 2010). The involvement of many genes in the molecular cascades activated by secondary injury mechanisms is believed to explain why so many genes may influence the level of risk for developing neurodegenerative disease following TBI (McAllister, 2010).

Progression of Chronic Traumatic Encephalopathy

In 2013, McKee and colleagues set out to characterize the progression and spectrum of the neuropathological changes associated with CTE (McKee et al., 2013). The results demonstrate that the brains of concussed subjects analyzed could be sorted into one of four stages with a distinct pattern of pathological protein and other microscopic changes.

Stage I is the mildest of the stages of CTE progression. Brains classified as stage I CTE show little ventricular enlargement with focal perivascular pathological tau protein located in the depths of cortical sulci. Brains classified as stage II (mild CTE) show ventricular enlargement, increases in pathological tau protein that penetrate the superficial layers of the cortex, and small amounts of pathological tau in areas such as the hippocampus, entorhinal cortex, and thalamus. Brains classified as stage III (moderate CTE) show areas of brain atrophy, axonal loss in subcortical white matter, and increased pathological tau spread throughout the cortices, hippocampus, entorhinal cortex and amygdala. The final stage of CTE, Stage IV, is the most severe stage. This stage includes significant brain atrophy in several brain areas, decreased overall brain weight, significant ventricular enlargement, significant neuronal death and widely distributed pathological tau protein. The complete characterization of the progression of CTE can be found in the paper of McKee et al. (2013), with more information found in the work of Stein and fellow colleagues (Stein et al., 2014). Overall, the pathology of CTE increases as the stages progress from Stage I (very mild) to Stage IV (severe). Although CTE can be present alongside other neurodegenerative diseases and have other pathological proteins/processes present, CTE is characterized as a tauopathy due to the fact that the main pathological hallmark is the deposition of pathological phospho-tau aggregates.

1.3 Tau

The Microtubule-Associated Protein Tau (MAPT)

Tau proteins are members of the microtubule-associated protein (MAP) family (Binder et al., 1985; Brandt et al., 2005). The main function of tau is to help stabilize, bind, and regulate microtubule dynamics in the axons of neurons (Arendt et al., 2016). However, there are many other functions of tau within cells, such as interacting with other cellular components, like the mitochondria and the plasma membrane, and potentially playing a role in various signaling processes (Kolarova et al., 2012).

Tau proteins are expressed both in the peripheral nervous system and in the central nervous system (Arendt et al., 2016), with trace amounts of tau mRNA in several peripheral tissues (Buée et al., 2000). Within the central nervous system, tau proteins are

expressed predominantly in neurons (Kolarova et al., 2012). Tau can also be found both within oligodendrocytes (Arendt et al., 2016) as well as in astrocytes (Arena et al., 2020). In healthy neuronal cells tau is localized in the axonal compartment, where its primary function is to interact with microtubules (M Goedert & Jakes, 1990). With regard to human tau proteins, the single gene responsible for the production of all of the tau family members is located on chromosome 17, position 17q21 (Kolarova et al., 2012). There are a total of 16 exons contained within this gene, of those, 11 are involved in alternative splicing (Brandt et al., 2005; M Goedert et al., 1988). Three of the exons are not transcribed in the brain at all, specifically, exons 4A, 6 and 8 (Park et al., 2016). The alternative splicing generates six unique tau isoforms that differ with respect to the number of binding domain repeats at the C-terminal end and either the presence or absence of two N-terminal amino acid inserts (Arendt et al., 2016). Specifically, the regions subjected to alternative splicing, that create the unique isoforms in the brain, are encoded by exons 2, 3, and 10 (M Goedert et al., 1989; Park et al., 2016). Exons 2 and 3 can be spliced so that neither of them, exon 2, or both exon 2 and 3 can be included in the structure of the isoforms, resulting in a 0N, 1N, or 2N isoform (Arendt et al., 2016; Park et al., 2016). The alternative splicing of exon 10 results in either the exclusion of this exon, 3R tau isoforms, or the inclusion of this exon, resulting in 4R tau isoforms (Brandt et al., 2005). As a result, of these combined alternative splicing's, six tau isoforms are generated and are referred to as 0N3R, 1N3R, 2N3R, 0N4R, 1N4R, and 2N4R (Kolarova et al., 2012). It is important to note that the previously described tau isoforms apply to the tau isoforms located in the central nervous system, as the peripheral nervous system has an additional tau isoform, referred to as "big tau" (Brandt et al., 2005; M Goedert et al., 1992).

The Structure and Developmental Expression of Tau

Tau is a natively unfolded protein with little secondary structure (Arendt et al., 2016; Kolarova et al., 2012). However, the differences between the various tau isoforms dictate the functional outcome of each of the proteins, and therefore influence their interactions with microtubules, especially during development (Kolarova et al., 2012). During development, the tau isoforms are differentially regulated and expressed (Kosik et al.,

1989). In the fetal brain, only 3R isoforms are expressed, whereas in the adult human brain, both 3R and 4R isoforms are expressed equally at a ratio of approximately 1:1 (M Goedert & Jakes, 1990; Hanes et al., 2009). It has been demonstrated that the 4R isoform is capable of binding microtubules more efficiently than their 3R counterparts (M Goedert & Jakes, 1990). This seems to reflect the change in plasticity within the brain as it ages, as 3R tau's weak binding to microtubules will allow for greater neuroplasticity during neuronal development while the strong microtubule binding of 4R tau will decrease neuroplasticity by enhancing microtubule stability (Arendt et al., 2016).

Post-Translational Modifications of Tau

Tau proteins are not only regulated by alternative splicing throughout development, but also by various post-translational modifications. These modifications influence tau's ability to bind and stabilize microtubules (Sergeant et al., 2005). Tau can be modified through the process of O-glycosylation, glycation, ubiquitination, SUMOylation, nitration, methylation, acetylation, truncation, and more, all of which affect tau's ability to function and potentially become pathogenic (Arendt et al., 2016). The most studied and well-known modification of tau is its phosphorylation at regulatory sites. Tau itself is considered a phosphoprotein (Trinczek et al., 1995), as there are approximately 80 sites available for potential phosphorylation on the longest tau isoform (Sergeant et al., 2005). Pathological phosphorylation of tau leads to the deposition of tau aggregates and disease.

Tau and Tauopathies

Tauopathies are a group of heterogeneous neurodegenerative diseases characterized by filamentous tau aggregates consisting of hyperphosphorylated tau proteins (Kovacs, 2018; V. M.-Y. Lee et al., 2001). Tauopathies may be classified based on the unique composition of their tau aggregates (Sergeant et al., 2005). Tauopathies can be further subdivided into either sporadic or familial tauopathies, in which sporadic tauopathies arise spontaneously and familial tauopathies arise due to inherited mutations (Arendt et al., 2016). Tauopathies may also be classified as either primary or secondary, depending on how significant the tau pathology is, and the severity of other coincident pathological features (Kovacs, 2018). Each tauopathy is unique, as the distribution of tau, isoforms

present, isoform ratio balance, and presence/absence of other pathological features is specific to each respective disease (Arendt et al., 2016; Sergeant et al., 2005).

Familial Tauopathies

Over 30 genetic mutations have been implicated in the development of familial tauopathies (Engel et al., 2006; Michel Goedert & Jakes, 2005). Missense, deletion, and silent mutations involving the exons of the tau gene can influence the outcomes of alternative splicing, as can various mutations in the intron sequences (Niblock & Gallo, 2012). When the regulation of alternative splicing becomes altered, the production of 3R and 4R tau isoforms becomes unbalanced, affecting the normal physiological isoform ratio (Niblock & Gallo, 2012). Besides mutations to the introns, exons, or both the introns and exons, there can also be genetic alterations involving the entire sequence of the tau gene. The genetic inversion of the DNA region containing the tau *MAPT* gene results in the production of two haplotypes, H1 and H2, with the H1 haplotype having several sub-haplotypes, some of which are associated with the development of tauopathies (Niblock & Gallo, 2012; Sánchez-Juan et al., 2019).

Sporadic Tauopathies

Typically, sporadic tauopathies originate in a vulnerable area of the brain and subsequently the pathological tau aggregates spread throughout the rest of the brain through the neuronal pathways connecting them (Sergeant et al., 2005). When the ratios of 3R:4R isoforms become unbalanced or the modifications influencing tau's activity become dysregulated, or external triggers, such as substance abuse or brain injuries, occur, sporadic tauopathies may emerge (Arendt et al., 2016; Irwin et al., 2013).

Tau as a Prion Protein

A proposed mechanism for the propagation of pathological tau throughout the brain is via a prion-like mechanism. This mechanism involves the corruption of native proteins into pathological proteins and aggregates using a template-dependent manner from pathological tau (Kumar & Udgaonkar, 2018). The forms of pathological tau, in this case, are referred to as “strains” and each strain has a distinct fibrillar structure (Sanders

et al., 2014). The characteristics of each strain determines the characteristics of the disease that manifests. These strains of pathological tau are stable and are able to propagate from cell-to-cell through synapses (Mudher et al., 2017). This could explain how tau is able to spread from vulnerable brain regions to connecting brain areas.

Imbalance of Post-translational Phosphorylation of Tau

There have been several studies that have investigated various post-translational modifications of tau and how these modifications play into aggregate formation and/or disease progression (Arendt et al., 2016; Morris et al., 2015). Of particular interest is the post-translational phosphorylation of tau. As mentioned above, tau is known to be a phosphoprotein in which the level of phosphorylation naturally influences and regulates tau function (Buée et al., 2000; Trinczek et al., 1995). However, diseases may arise when tau becomes pathologically hyperphosphorylated (Kolarova et al., 2012). It has been proposed that an imbalance in the activities and regulations of protein kinases and phosphatases results in the hyperphosphorylation of tau, either through an increase in kinase activity or a decrease in phosphatase activity (Buée et al., 2000).

1.4 Glycogen Synthase Kinase 3

Overview

Glycogen synthase kinase 3 (GSK3) is a ubiquitously expressed proline-directed serine/threonine kinase that is constitutively active (Beurel et al., 2015; Hooper et al., 2008). It consists of two important functional domains: a primed substrate binding domain and a kinase domain (Beurel et al., 2015). Initially discovered in the 1970s for its role in the phosphorylation and regulation of glycogen synthase, GSK3 has since been implicated in many other cellular and signaling pathways (Cohen & Goedert, 2004). GSK3 is involved in glycogen metabolism, gene transcription, apoptosis, inflammation, and microtubule stability, just to name a few cellular processes (Cohen & Goedert, 2004; Hooper et al., 2008). There are two unique aspects to GSK3 activity: 1) GSK3 is constitutively active and 2) GSK3 may phosphorylate both primed and un-primed substrates (Beurel et al., 2015; Hooper et al., 2008). The “priming” of the substrates

involves the phosphorylation of a site approximately 4 residues to the C-terminal side of the target site, which allows the substrate to bind to the GSK3 primed substrate binding domain (Beurel et al., 2015). GSK3 is regulated by a number of kinases and phosphatases and the breakdown of these regulations has been implicated in the increased risk of disease (Hooper et al., 2008).

Regulation of Glycogen Synthase Kinase 3

There are many post-translational regulatory mechanisms that keep the activity of GSK3 in check. Post-translational modifications, substrate priming, association with protein complexes, and regulation of expression and degradation are all mechanisms that are capable of regulating GSK3 (Beurel et al., 2015). Post-translational acetylation of GSK3 can influence whether GSK3 activity is increased or decreased. When acetylated, the activity of GSK3 proteins is suppressed, however, when the proteins become deacetylated, the levels of activity increase (Monteserin-Garcia et al., 2013). Much more work needs to be done in order to tease apart the effect that other non-phosphorylation dependent post-translation modifications have on GSK3 activity (Beurel et al., 2015). Substrate priming is another method of controlling the levels of activity of GSK3. This method is more complex than mere post-translational modifications, as not only does the substrate have to be pre-phosphorylated at the correct site, thus being primed for GSK3 proteins, but activated GSK3 proteins must be in the vicinity of the primed substrate (Beurel et al., 2015). The priming of the substrate requires that other signaling pathways be active and phosphorylating the desired substrate at approximately 4 residues C-terminal to the target motif (Beurel et al., 2015). One way to directly influence the activities of GSK3 phosphorylation is to incorporate GSK3 into a number of different protein complexes, depending on the desired substrates and outcomes. For example, one of the most well known protein complexes involving GSK3 is the destruction complex of the Wnt signalling pathway (Kim et al., 2009). GSK3 forms a destruction complex with various other proteins in order to phosphorylate and target β -catenin for degradation (Kim et al., 2009). In addition to these methods of regulating GSK3 activity, GSK can also be regulated by its cellular sequestration to the mitochondria, the nucleus or the cytosol, of the cell (Beurel et al., 2015). In the next section I will discuss the regulation of GSK3

activity by phosphorylation of GSK3's main regulatory sites that vary depending on the isoform/paralog of interest (Beurel et al., 2015).

Isoforms of Glycogen Synthase Kinase 3

There are two major paralogs, sometimes referred to as isoforms, of GSK3, one is glycogen synthase kinase 3-alpha (GSK3 α) and the other is glycogen synthase kinase 3-beta (GSK3 β) which are each produced from their respective genes (Beurel et al., 2015; Soutar et al., 2010). There is a final form of GSK3, which is the product of a splice variant of GSK3 β , a protein known as GSK3 β 2. This splice variant is known to be enriched within the neurons of the central nervous system, in particular the brain (Soutar et al., 2010). The activity of GSK3 α and GSK3 β can be regulated by several different mechanisms, however, the phosphorylation of two specific residues, a tyrosine residue and a serine residue, are of the greatest importance. When tyrosine 279 (Tyr279) is phosphorylated (pTyr279) in GSK3 α the activity of GSK3 α is increased and when serine 21 (Ser21) is phosphorylated (pSer21) the activity is decreased (Fang et al., 2000; Medina & Wandosell, 2011). Similarly, if tyrosine 216 (Tyr216) on GSK3 β is phosphorylated (pTyr216) the activity is increased, and when the serine 9 (Ser9) residue is phosphorylated (pSer9) the activity is decreased (Fang et al., 2000; Krishnankutty et al., 2017). Although the isoforms are similar, they have distinct substrate preferences (Soutar et al., 2010). GSK3 β has the most predicted substrates than any other kinase, with over 500 predicted substrates (Beurel et al., 2015; Linding et al., 2007). One of the substrates of interest, tau (the microtubule-associated protein), has been shown to be a substrate for GSK3 β , and in the case of disease development, the hyperphosphorylation of this protein by GSK3 β has been associated with increased pathological outcomes (Avila et al., 2012).

1.5 Glycogen Synthase Kinase 3-beta and Tau

Phosphorylation of Tau by Glycogen Synthase Kinase 3-beta

Many studies have investigated the relationship of tau, its phosphorylation by GSK3 β , and the risk of disease. In tauopathies, tau is abnormally phosphorylated, above the

physiological levels resulting in the production of toxic conformations which form aggregates leading to neurofibrillary tangle (NFTs) development (Hanger et al., 2009). GSK3 β is capable of phosphorylating tau at both primed and un-primed sites (Cho & Johnson, 2003), therefore creating more opportunity for increased tau phosphorylation. GSK3 β displays more activity towards tau and is known to co-localize with hyperphosphorylated tau proteins (Tsujiro et al., 2000). The overall levels of GSK3 are also increased within Alzheimer's diseased brains by at least 50% (Tsujiro et al., 2000). One study investigated the activities of kinases acting on recombinant tau using nanoelectrospray mass spectrometry and demonstrated that GSK3 β is capable of phosphorylating tau at several known sites contained within paired helical filament (PHF) tau aggregates (Reynolds et al., 2000). A desirable goal might be to disrupt or halt the process of tau phosphorylation entirely by administering inhibitors to block kinase activity (Hanger et al., 2009).

Inhibitors Prevent Kinase Activity

The foregoing discussion of GSK3 β 's role in tau phosphorylation and the role of pathological tau phosphorylation in disease suggests that GSK3 β inhibition might be an attractive strategy for the treatment or prevention of tauopathies. GSK3 β inhibitors can be classified into two main categories, one being ATP competitive inhibitors, and the other being non-ATP competitive inhibitors (Eldar-Finkelman et al., 2010). Since ATP binding sites are very highly conserved domains in kinases, it is ideal to use non-ATP competitive inhibitors in order to increase the specificity for GSK3 proteins and minimizing any off-target effects (Eldar-Finkelman et al., 2010). The most appealing non-ATP competitive inhibitors for targeting GSK3 proteins are ones that compete with GSK3 substrates for binding, termed substrate competitive inhibitors (Eldar-Finkelman et al., 2010). However, the production of GSK3 inhibitors includes many types of chemicals with many different modes of action. Some of the main groups of inhibitors are the maleimides derivatives, aminopyrimidines, the amino thiazoles, and the thiadiazolidinones (TDZD) (Cohen & Goedert, 2004; Eldar-Finkelman et al., 2010). One group investigating the effects of GSK3 inhibition on a double transgenic mouse line that develops AD-like pathology found that upon inhibition of GSK3 β with NP12 (a TDZD,

non-ATP competitive), there were decreased levels of phosphorylated tau, and decreased cell death (Serenó et al., 2009) among other molecular, cellular, and cognitive benefits. Another study investigated the mechanism of GSK3 β activation, through the phosphorylation of tau at Thr175, that leads to the subsequent phosphorylation of tau at Thr231, fibril formation, and cell death (Moszczynski et al., 2015). Four inhibitors of GSK3 β were used; lithium chloride, AR-A014418, Tideglusib (aka NP12), and TWS-119; all of which successfully prevented pathological fibril formation and cell death (Moszczynski et al., 2015).

1.6 Models of Traumatic Brain Injury

Invertebrate Models

Caenorhabditis elegans (*C. elegans*) are nematodes that are considered to be a valued model organism (Hill et al., 2000). These metazoans have had their entire genome completely sequenced in the 1990s, therefore making genetic studies possible and easily accessible (Hill et al., 2000). One group has studied the effects of surface acoustic waves (SAW) in producing similar pathologies in *C. elegans* comparable to blast induced TBIs seen in military and civilians affected by war (Miansari et al., 2019). This group saw that there was decreased mobility and short-term memory impairment upon SAW injury. Another model organism are the flies known as *Drosophila melanogaster* (Adams et al., 2000). One team of researchers set out to develop a closed head model of TBI using *Drosophila melanogaster* and discovered that these flies face similar post-TBI injuries compared with humans that have suffered from TBI (Katzenberger et al., 2013). These models offer the benefits of being cheap to maintain, time efficient (with short lifespans), and significant knowledge of their genetic backgrounds has been developed (Katzenberger et al., 2013; Miansari et al., 2019). Although these models of TBI have useful insights into pathological mechanisms and molecular and cellular cascades that are initiated post-injury, there are several drawbacks that must be considered. For example, there are limited tests available to evaluate complex behaviours in these organisms (Shah et al., 2019). Second, these model organisms are too small to administer potential therapeutic drugs and observe the effects on behavioural outputs, thereby limiting their clinical relevance (Shah et al., 2019).

Vertebrate Models

The effects of TBIs have been investigated using different methods of delivering injuries (fluid percussion injury, FPI; controlled cortical impact injury, CCI; weight drop models, and blast injuries) and using different animal models (cats, dogs, sheep, rabbits, pigs, ferrets, and monkeys) (Xiong et al., 2013). Although the possible combinations may offer a lot of insight into the mechanisms behind the pathology of TBIs and disease development, there are some drawbacks to consider in using large animal models. For instance, it is difficult to find suitable equipment in order to deliver consistent, precise injuries to larger animals. It is also difficult to find enough space to house the animals (Cernak, 2005). Larger animals also mean larger costs for proper housing, care and enrichment. Large animal experiments in TBI may also raise more ethical issues (Cernak, 2005).

Rodent Models

There is always the struggle of taking results from scientific studies involving animal models and then applying them to human beings (Risling et al., 2019). However, technological advancements have allowed the development of genetic tools that have been applied to rodents in order to create ideal transgenic models with greater clinical relevance to human disease. Rodents are also ideal models due to the fact that they are small, and therefore space efficient, and also able to quickly increase their numbers through reproduction to repeatedly run morphological, cellular, biochemical, and behavioural analyses (Cernak, 2005). Several transgenic mouse models have already been created in order to tease apart the interactions between rmTBI, GSK3 β , and tau. The downside of the previous transgenic models is that they fail to express all tau isoforms in the same proportions as found in humans, a ratio of ~1:1 for 3R:4R respectively (Hanes et al, 2009). As previously mentioned, the balance of the 3R:4R ratio of tau isoforms is critical for models of tauopathies, as a disruption to this balance can result in tau pathology, without the addition of other factors, and ultimately CTE (Hanes et al, 2009; Sergeant, Delacourte, and Buée, 2005). A rat model of hypertension was shown to have different ratios of 3R:4R tau isoforms depending on the brain area of

interest (Cortex 1:9, Hippocampus 1:7, and Brainstem 1:6) (Hanes et al, 2009) compared to the htau mouse model with an isoform imbalance leaning towards more 3R tau than 4R tau (Andorfer et al., 2003). However, a group of scientists have created a brand new, improved mouse model of tauopathy, the *MAPT* knock-in mouse (*MAPT* KI mice) (Saito et al, 2019). Overall, the new mouse strain was created by replacing the entire murine *Mapt* genetic sequence with the human *MAPT* sequence (exons 1-14) through homologous recombination. The targeting construct, including the neomycin-resistant gene (*neo*) flanked with *loxP* sites, was injected into ES-R1 cells, and once selected the positive clones were injected into C57BL/6 blastocysts. The resulting chimeric mice were then crossbred with EIIa CRE mice in order to get rid of the *neo* gene, and the mice were then backcrossed with C57BL/6 mice for 5 generations. This mouse strain was developed in order to express all six human tau isoforms without any expression of murine tau, resulting in a tau isoform ratio of approximately 1:0.66 3R:4R (Saito et al, 2019), which is much closer to that seen in humans. Therefore, this new mouse strain serves as an ideal model for studying the mechanisms of tau phosphorylation in tauopathies, and potential avenues for therapeutic targets. In order to ensure that this study is able to capture a more realistic outcome of tau pathology in humans, and therefore be more clinically relevant, the *MAPT* KI mouse strain (Saito et al, 2019) will be used.

1.7 Rationale, Goals and Aims for Thesis

Rationale

Repetitive mild traumatic brain injury (rmTBI) is known to be a risk factor for the development of neurodegenerative diseases such as Chronic Traumatic Encephalopathy (CTE) (Ojo et al., 2013). It is also known to influence the activity of glycogen synthase kinase 3-beta (GSK3 β), a kinase with many functions, one of which is to phosphorylate tau (Moszczynski et al, 2018). Previous studies have shown that the activation of GSK3 β , as a result of brain injury, leads to many detrimental cascades including abnormal increases in tau phosphorylation (Moszczynski et al, 2018). These increases in tau phosphorylation are above the natural levels found within cells, and lead to the pathology seen in diseased states. Hyperphosphorylated tau is prone to misfolding,

aggregation, fibril formation, and tangle formation, leading to neuron death and other pathologies (Polydoro et al., 2009). The need for a more clinically relevant model of rmTBI is an important milestone that must be reached. By using the newly generated humanized *MAPT* KI mice in this model of closed skull/closed skin rmTBI, we are taking one step further towards better understanding the relationships between all of these phenomena.

Goals and Aims for this Thesis

The overarching goal of this thesis is to validate and characterize a closed skull, closed skin model of rmTBI using the *MAPT* KI mouse. This work will set the stage for future studies to evaluate the pathophysiology of rmTBI and to test possible therapeutic strategies.

Goal

To develop and evaluate a mouse model of concussion in order to study the relationship between rmTBI, GSK3 β activity, tau phosphorylation, and the development of cognitive deficits in a transgenic mouse line expressing solely human tau.

Aims

1. To investigate the time course of GSK3 β activity in different regions of the brain in wildtype rmTBI mice.
2. To characterize the cellular and molecular pathology in rmTBI *MAPT* KI mice.
3. To characterize the behavioural outcomes of rmTBI in the *MAPT* KI mice, using the Elevated Plus Maze (to test for anxiety/anxiety-like behaviours) and the Morris Water Maze (to test for spatial learning/memory).

Chapter 2

2 Materials and Methods

2.1 Animals

All experiments were approved by the Western University Animal Care Committee which adheres to the Canadian Use of Experimental Animal Guidelines. Male and female C57BL/6 mice were purchased from Charles River (Quebec, Canada). Male and female *MAPT* KI mice, obtained from Dr. Hashimoto et al. (2019), were bred in house. All mice were kept on a 12 hour light : 12 hour dark cycle, and had free access to food and water. All experiments were performed during the light cycle. Mice were housed together, with a maximum of four mice per cage.

2.2 Repetitive Mild Traumatic Brain Injury Procedure

To model concussion in mice in a clinically relevant way, we performed an injury in which the skin and skull were kept intact. Mice were randomly assigned to receive either a repetitive mild traumatic brain injury (rmTBI), a sham procedure, or to act as naïve controls. Before any injuries were delivered, the controlled cortical impact (CCI) device (TBI 0310, Precision Systems and Instrumentation) was calibrated to the desired experimental parameters. Mice were then anesthetized using 3% isoflurane for induction and maintained on 2% isoflurane using a nose-cone. The hair on the scalp was shaved before the concussion or sham procedure and the mice, along with the nose-cone for anesthetic administration, were transferred directly under the CCI device (TBI 0310, Precision Systems and Instrumentation) that was used to deliver a mild traumatic brain injury. The tip of the impactor was aligned with the approximate center of bregma. The impact was then delivered with a custom-made silicone impactor tip of 4 mm diameter, at a programmed velocity of 3.5 m/s, at 1.0 mm depth, and with 500 msec dwell time. Mice were subjected to 5 concussions with a 24 hour inter-injury interval time in order to achieve an rmTBI model. Sham mice underwent 5 minutes of isoflurane anesthesia each day for 5 days with a 24 hour interval between sham procedures. Naïve mice were not

manipulated. Mice were sacrificed at various time points after the final concussion or sham procedure.

2.3 Silver Staining

The silver staining procedure followed was provided by the manufacturer of the FD Neurosilver™ Kit II (FD NeuroTechnologies, Ellicott City, MD). After the coronal brain sections (50 µm thickness) were stained, they were then promptly mounted on VWR microslides (25x75 mm, 1.0 mm thick) and allowed to air dry in the fume hood. Once dry, the slides were rinsed in a xylene solution three times, for three minutes each time, and then sealed by a cover-slip. Two slides per animal, containing approximately five sections per slide, were selected for analysis. In total, approximately 3-4 sections per animal were visually inspected for positive silver staining. Slides were imaged using an Olympus BX50 brightfield microscope. Images were taken along the corpus callosum. Images were taken for all animals in each experimental group (n's specified in the experimental timelines below).

2.4 Tissue Preparation for Western Blots

The mice that were assigned to be used for Western blot analyses were transcardially perfused using a chilled saline solution. Once perfused, brains were extracted and the regions of interest, the cortex and the hippocampus, were dissected free of the rest of the brain. The cortex and hippocampus samples were sonicated in RIPA lysis buffer supplemented with Halt protease and phosphatase inhibitor cocktail (Life Technologies; #78440) at a dilution of 1:100. The sonicated mixture was then centrifuged at 6000 rpm for 20 minutes at 4 °C. Afterwards, the supernatants were aliquoted into separate tubes for storage at -80 °C. Protein concentrations were determined by a Bradford protein assay for each sample in order to load an equal concentration of protein to each lane in the Western blots (10 µg/lane).

2.5 Glycogen Synthase Kinase 3 Western Blots

Mice were sacrificed at various time points after the last impact/sham injury was delivered (Refer to Figure 1 and Table 2). A group of naïve mice were also sacrificed to

provide an additional control. A standard Western blot protocol was followed (Abcam), in which a 10% acrylamide gel was used as the resolving gel, with a 4% acrylamide stacking gel. The protein gels ran for approximately one hour at 80 V until samples entered the bottom resolving, gel, at which time the voltage was increased to 100 V. Western blots were then transferred from the gel to Millipore Immobilon-FL PVDF membranes for approximately 1.5-2 hours at 110 V. Membranes were then dried, trimmed, and stored at 4 °C overnight. Membranes were then blocked in Intercept Blocking Buffer (TBS) from LI-COR for approximately an hour, and then incubated in a primary antibody overnight. To detect β -actin we used either a rabbit anti- β -actin from LI-COR Biosciences (#926-42210; Waller et al., 2017) or a mouse anti- β -actin from LI-COR (#926-42212; Almanzar et al., 2016), each at a dilution of 1:5000, depending on the primary antibody used to detect the GSK3 β proteins. To detect total GSK3 (GSK3 TOT) we used a mouse anti-GSK3 β from BD Transduction Laboratories at a dilution of 1:5000 as the primary antibody (Lucas et al., 2001). To detect GSK3 β phosphorylated on tyrosine 216 (pTyr216) we used a mouse anti-GSK3 β pTyr216 from BD Transduction Laboratories at a dilution of 1:1000 as the primary antibody (Bhat et al., 2000). To detect GSK3 β phosphorylated on Serine 9 (pSer9) we used a rabbit anti-GSK3 β pSer9 from Biorad at a dilution of 1:1000 as the primary antibody (Stambolic & Woodgett, 1994). Membranes were then washed in TBST three times, ten minutes each time, and incubated in secondary antibody (either a donkey anti-mouse (680; red) or a donkey anti-rabbit (800; green) antibody (LI-COR Bioscience) as appropriate) for an hour. Afterwards, membranes were washed in TBST three times (ten minutes each time), and TBS for ten minutes. Membranes were imaged using the Odyssey Imaging System (LI-COR Bioscience) imaging software. The relative optical densities of the proteins of interest were quantified using ImageStudio Plus software. Densitometric values for target proteins (GSK3 TOT, pTyr216, pSer9) were normalized to the densitometric values for β -actin, and then compared to the values obtained for naïve animal samples that were present on each blot. Each set of animals, shams and injured, were run on the same set of gels. Each set of gels were produced with alternating orders of samples to prevent position bias within the gels, which were referred to as “Formats”. Each gel that was

produced had the same naïve sample to act as a control across all blots to ensure that results could be compared across all gels, and therefore across all time points.

2.6 Tissue Preparation for Immunohistochemistry

MAPT KI mice were sacrificed at various time points after the last impact or sham procedure (Refer to Figure 2, Table 3, and Table 4). A group of naïve mice were also sacrificed to provide an additional control. Mice were perfused with saline, followed by 4% paraformaldehyde. Brains were dissected and post-fixed in 4% paraformaldehyde overnight at 4 °C and then transferred to 20% sucrose solution the next day and left in at 4 °C overnight. Brains were then patted dry, transferred into plastic brain moulds, immersed in OCT, and then stored in the -80 °C freezer.

The fixed brains were sectioned in the coronal plane on a cryostat. For silver staining floating sections at 50 µm thickness were collected. For immunohistochemistry 18 µm thick sections were thaw-mounted directly onto slides. Thirty slide sections and ten floating sections were collected in an alternating fashion until the desired amount of sections were collected. Floating sections were stored in six-welled plates in 8% sucrose/0.5% sodium azide solution and later transferred to 4% paraformaldehyde once all of the brains were processed. The floating sections were then processed according to the silver staining protocol, mounted on slides, and allowed to dry overnight in the fume hood before being sealed by a cover-slip (see above for more details). Slide sections were stored in a labelled box in the -80 °C freezer until they were used for immunohistochemical staining.

2.7 Immunohistochemistry

AT8, GFAP and IBA1

Slides were removed from the -80 °C in order to thaw to room temperature for 30 minutes. Once thawed, slides were washed in 1xPBS (Phosphate Buffered Saline) twice for five minutes each. Slides were then covered in blocking medium (1xPBS, Goat Serum, Triton-X-100) for approximately 2 hours and left at room temperature. The primary antibodies, which were diluted in blocking medium, were applied. To detect

pathologically phosphorylated tau (phospho-tau (Ser202, Thr205) monoclonal mouse AT8 (1:100 dilution) from Invitrogen was used (Y. Zhang et al., 2019). To detect glial fibrillary acidic protein (GFAP) a marker of activated astrocytes a mouse anti-GFAP (1:500 dilution) from Sigma was used (Lazarus et al., 2015). To detect Iba1, a marker of microglia, a rabbit anti-Iba1 (1:1000 dilution) from Novus Biologicals was used (Schultz et al., 2018). The slides were then “cover-slipped” with a section of parafilm and incubated at 4 °C. The following day, the slides were washed in 1xPBS, three times, for 30 minutes each. The slides were then incubated in the appropriate secondary antibody (either donkey anti-mouse 595 (Life Technologies) or donkey anti-mouse 488 (Invitrogen) or donkey anti-rabbit 594 (Invitrogen)) for 45 minutes at a 1:500 concentration while “cover-slipped” with a new section of parafilm. After the incubation, the slides were washed in 1xPBS three times for 30 minutes each time. The slides were briefly washed in double distilled water before applying VectaShield Hardset Antifade Mounting Medium with DAPI (Vector Laboratories, Inc.) and stored at 4 °C.

Image Analyses

Two slides, containing approximately five sections per slide, were made for each animal in each treatment group. Out of those sections, 2-3 sections were visually analyzed for positive staining. Slides were imaged using an Olympus BX50 brightfield microscope. Images of the prefrontal cortex area were visually analyzed for positive AT8 staining. Images of the corpus callosum were visually analyzed for positive GFAP/Iba1 staining. All images were taken at 40x magnification, and images were taken of all animals in each experimental group (n's specified in experimental timelines and in related figures). Dr. Kathy Xu of the Brown Lab generously donated representative images of both sham and injured C57BL/6 male mice for comparison against the *MAPT* KI mice.

2.8 Elevated Plus Maze Test

Behaviours in both male and female *MAPT* KI mice were evaluated by the Elevated Plus Maze (EPM) test in order to assess anxiety/anxiety-like behaviours (Broussard et al., 2018). Eight and a half weeks after the last concussion injury or sham procedure mice were placed in the centre of the maze platform facing one of the closed arms and allowed

to freely explore for a total of five minutes. Each mouse had one trial and after the trial was concluded the maze was sanitized with 70% ethanol. The behaviour of each mouse in the maze was video recorded and then analyzed using ANY-Maze (Stoelting Co. Wood Dale, IL) for the time spent in each of the 3 defined areas (closed arms, open arms, centre) as well as the speed, and distance travelled.

2.9 Morris Water Maze Test

During the ninth week after the last concussion injury or sham procedure both male and female *MAPT* KI mice underwent evaluation of spatial learning and memory using the Morris Water Maze (MWM) (Mannix et al., 2014; Xu et al., 2021). Training on the MWM occurred on four consecutive days (4 trials per training day per mouse). Each day of training had four trails that each had a different starting position corresponding to each of the four quadrants in the maze. The order of the starting positions was changed randomly on each training day to prevent repetition. Mice were placed in the water, facing the wall of the maze and allowed to freely swim/explore for a minute per trial. The goal of the maze is to locate the hidden transparent platform, placed 1 cm under the water, located in quadrant 4. Successful trials concluded when the mouse located the hidden platform and was removed from the maze. Unsuccessful trials, trials in which the mouse was unable to find/locate the hidden platform, concluded with the mouse being placed on the hidden platform for approximately 20 seconds and then being removed from the maze. After the four days of training was completed, a Probe Trial was conducted on the fifth day in which the hidden platform was removed from the pool and the mice were allowed to freely swim around the pool for one minute. One week after the first probe test, mice underwent a retention trial, again with the platform removed, and were allowed to swim freely for one minute. For both the probe and retention trials mice were placed in quadrant 2, across from the target quadrant, and were only tested for that one trial. The testing information was recorded with a video camera placed above the pool area, and analysis was conducted by the ANY-Maze software (Stoelting Co. Wood Dale, IL).

2.10 Experiment 1: Pilot Study

Five C57BL/6 mice were used for this study, 2 naïve mice and 3 rmTBI mice (Table 1). A depth of 1.0 mm was used during the pilot study in order to determine if this would be sufficient enough to cause the desired effect of a mild traumatic brain injury, without fracturing the skull. Silver staining was performed in order to assess physical axonal damage. Slides were imaged using an Olympus BX50 brightfield microscope. The corpus callosum was imaged and later assessed, visually, for positive silver staining.

Table 1. Table outlining the experimental plan for the Pilot Study.

Group #	Tests	Sample Size (n)	Timepoints	Age
I	IHC	2	naïve	2-3 month
II	IHC	3	10 day rmTBI	2-3 month

2.11 Experiment 2: GSK3 Study

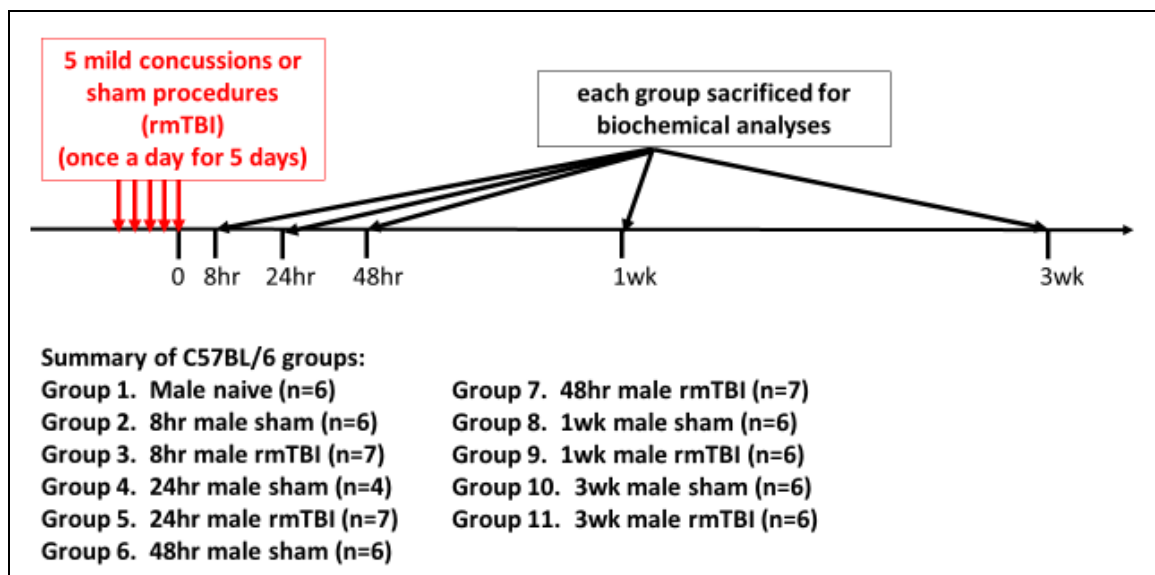


Figure 1. Timeline of the GSK3 Study. Timeline showing the various timepoints at which the male C57BL/6 mice were sacrificed, along with their relative sample sizes (n's).

67 male C57BL/6 mice were used in this study, 6 naïve, 28 sham, and 33 rmTBI mice. The outline of the experimental groups can be seen in both Figure 1 and Table 2. Mice were sacrificed at various timepoints, after the last impact or sham procedure, and Western blots were used to assess the total amount of GSK3 β protein (GSK3 TOT), the activation of GSK3 β (pTyr216), and the inactivation of GSK3 β (pSer9). Data organization was possible with the use of excel spreadsheets. Statistical analyses were performed using Graphpad Prism 8, and data is presented as mean \pm SEM. Western blot data were analyzed using a One-way ANOVA test in order to compare across the multiple time points that were assessed post-last injury. Correction for multiple comparisons was done using a Tukey's post hoc test. Statistical significance was set as $p \leq 0.05$.

Table 2. Table outlining the experimental plan for the GSK3 Study.

Group #	Tests	Sample Size (n)	Timepoints	Age
I	Western blots	6 naïve	naïve	2-3 months
II, III	Western blots	6 sham, 7 rmTBI	8hr	2-3 months
IV, V	Western blots	4 sham, 7 rmTBI	24hr	2-3 months
VI, VII	Western blots	6 sham, 7 rmTBI	48hr	2-3 months
VIII, IX	Western blots	6 sham, 6 rmTBI	1wk	2-3 months
X, XI	Western blots	6 sham, 6 rmTBI	3wk	2-3 months

2.12 Experiment 3: *MAPT* KI Study

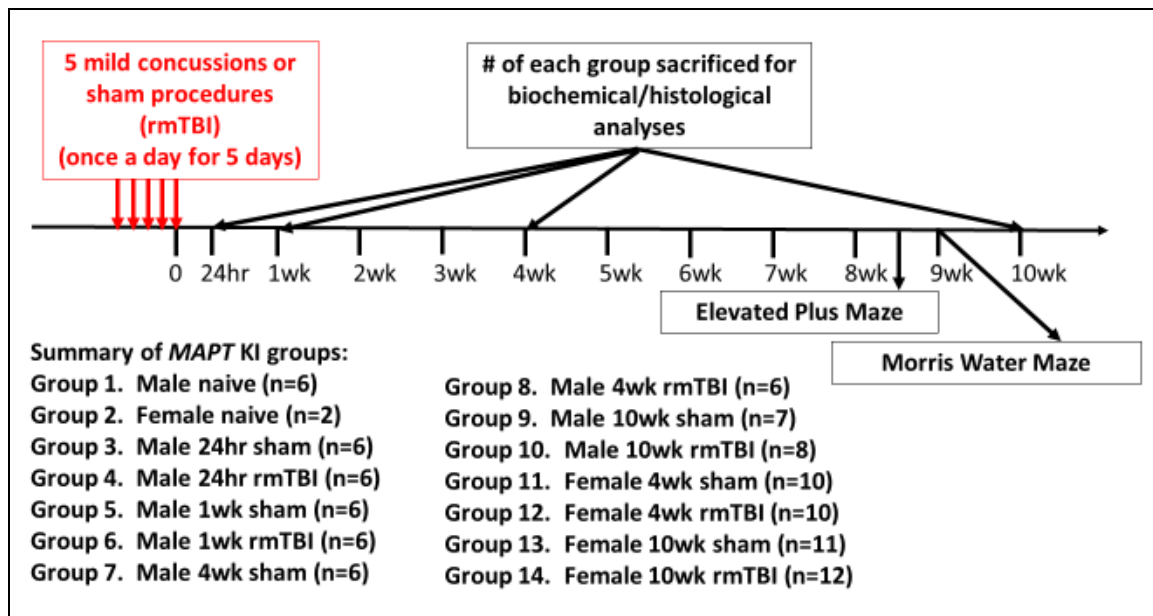


Figure 2. Timeline of the *MAPT* KI Study. Timeline showing the various timepoints at which the male and female *MAPT* KI mice were sacrificed, along with their relative sample sizes (n's).

102 *MAPT* KI mice were used in this study, 8 naïve, 46 sham, and 48 rmTBI mice. The outline of the experimental groups can be seen in both Figure 2 and Table 3. Mice were sacrificed at various timepoints, after the last impact or sham procedure, and various immunohistochemical staining were used to assess cellular and molecular pathology. Slides were imaged using an Olympus BX50 brightfield microscope and later assessed, visually, for positive silver staining/immunohistochemical staining. Groups 9, 10, 13, and 14 underwent evaluation through the use of various behavioural tests in order to assess possible changes in behavioural outcomes post-injury in addition to the various immunohistochemical staining. Data organization was possible with the use of excel spreadsheets. Statistical analyses were performed using Graphpad Prism 8, and data is presented as mean \pm SEM. Elevated Plus Maze results were compared using unpaired Student's t-test. The Morris Water Maze learning curves were analyzed using a Two-way ANOVA, whereas the time spent in the quadrants was analyzed using a One-way ANOVA. Correction for multiple comparisons was done using a Tukey's post hoc test. Statistical significance was set as $p \leq 0.05$.

Table 3. Table outlining the experimental plan for the *MAPT* KI Study.

Group #	Tests	Sample Size (n)	Timepoints	Age
I	IHC	Male: 6 naïve	naïve	Male: 5-6 months
II		Female: 2 naïve		Female: 5-6 months
III, IV	IHC	Male: 6 sham, 6 rmTBI	24hr	Male: 5-6 months
V, VI	IHC	Male: 6 sham, 6 rmTBI	1wk	Male: 5-6 months
V11, V111	IHC	Male: 6 sham, 6 rmTBI	4wk	Male: 5-6 months
XI, XII		Female: 10 sham, 10 rmTBI		Female: 3-5 months
IX, X	IHC	Male: 7 sham, 8 rmTBI	10wk	Male: 3-5 months
X111, XIV	EPM	Female: 11 sham, 12 rmTBI		Female: 3-5 months
	MWM			

7 aged *MAPT* KI mice (5 males and 2 females) and 3 aged C57BL/6 mice (2 males and 1 female) were used in this study. The outline of the experimental groups can be seen in Table 4. Slides were imaged using an Olympus BX50 brightfield microscope and later assessed, visually, for positive silver staining/immunohistochemical staining.

Table 4. Table outlining the experimental plan for the aged *MAPT* KI and C57BL/6 mice.

Group #	Tests	Sample Size (n)	Age	Strain, Sex
I	IHC	5	14 months	<i>MAPT</i> KI, male
II	IHC	1	12 months	<i>MAPT</i> KI, female
III	IHC	2	14 months	C57BL/6, male
IV	IHC	1	14 months	C57BL/6, female

Chapter 3

3 Results

3.1 Pilot Study: To validate a closed head, closed skin model of rmTBI

The goal of this thesis was to characterize a mouse model of concussion that is as clinically relevant as possible. In order to accomplish this, it was important that both the skull and the skin of the mice remained intact during the entire procedure. Previously reported models of TBI in mice were either open skull, requiring a craniotomy (Popovitz et al., 2019) or a craniectomy (Giarratana et al., 2019), or closed skull but open skin (Bolton & Saatman, 2014; Rehman et al., 2019; Xu et al., 2021). While these methods have the advantage of allowing the site of injury to be precisely located, the fact that the skull and skin are not intact in these models makes them less clinically relevant than desired. The Brown laboratory has previously characterized a closed skull, open skin model of rmTBI in C57BL/6 mice (Xu et al., 2021). In this model, mice were placed in a Kopf mouse anesthesia mask under a traumatic brain injury device (TBI 0310, Precision Systems and Instrumentation, LLC). Following a 10 mm midline incision, the skin and fascia were reflected. Then the mice received a mild controlled cortical impact directly onto the skull, centered on the bregma, with a custom-made, 4mm-diameter pliant silicone tip. The impact device was programmed to impact at a depth of 1.0 mm at a velocity of 3.5 m/sec with a 500 millisecond dwell time. Each mouse in that study received 5 mTBIs (one a day for 5 consecutive days). The purpose of this pilot study was to determine if the same injury protocol, without the skin incision, would produce a similar level of injury as the open skin rmTBI as assessed by silver staining of the brain to detect diffuse axonal injury.

C57BL/6 mice ($n = 3$) were subjected to 5 mTBIs (one a day for 5 days) and sacrificed 10 days post-last injury. A group of unmanipulated mice ($n = 2$) acted as naïve controls. An examination of tissue sections from injured and naïve mice demonstrated that the injured mice had significant levels of silver stained axons within the corpus callosum (Figure 3C) and even more so in the optic tract (Figure 3D) compared to the naïve controls (Figure

3A and B). When compared to the mice injured in the same way but with the scalp reflected away (Figure 3E and F), there was less silver staining in the corpus callosum and more robust staining in the optic tract. This suggested that the rmTBI with closed skin produces a similar injury as the open skin injury with the impact device settings of 1.0 mm depth, 3.5 m/sec velocity and 500 millisecond dwell time, just in different regions of the brain. Therefore, the rmTBI with the skin intact, was shown to produce sufficient physical damage, as assessed by the silver staining.

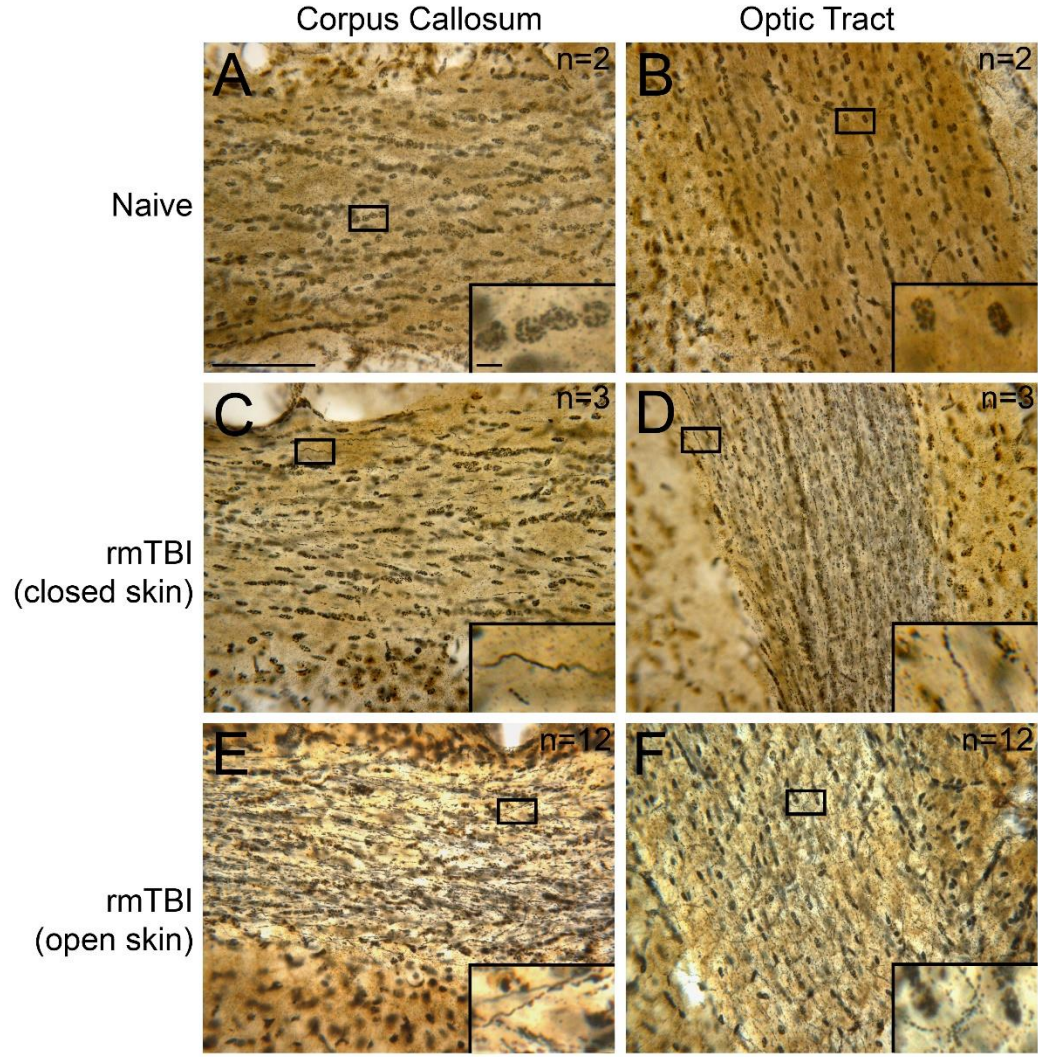


Figure 3. Silver staining during the pilot study. (A) Silver staining of the corpus callosum of a naïve animal (n=2). (B) Silver staining of the optic tract of a naïve animal. (C) Silver staining of the corpus callosum of a closed skin injured animal (n=3). (D) Silver staining of the optic tract of a closed skin injured animal. (E) Silver staining of the corpus callosum of an open skin injured animal. (F) Silver staining of the optic tract of an open skin injured animal. All images were taken at 40x.

3.2 Aim #1: To determine the kinetics of GSK3 β phosphorylation post-rmTBI in the C57BL/6 mice

GSK3 β has been identified as a kinase critical to the pathological phosphorylation of tau (Hooper et al., 2008; Moszczynski et al., 2018). *In vitro* GSK3 β inhibition prevents pathological tau phosphorylation and promotes cell survival (Moszczynski et al., 2015). The regulation of GSK3 β depends on the phosphorylation status of two regulatory sites, Tyr216 and Ser9. When Tyr216 becomes phosphorylated (pTyr216), the activity of GSK3 β is increased, however, when Ser9 becomes phosphorylated (pSer9), the activity of the kinase is blocked (Soutar et al., 2010). As one of the ultimate goals of this model development, to test whether GSK3 β inhibition may be a strategy to prevent pathological tau accumulations in the concussed brain, we sought to describe the kinetics of GSK3 β phosphorylation on both the Tyr216 and the Ser9 sites at various time points after rmTBI. In this study Western blots were used to assess the levels of GSK3 β protein (GSK3 TOT), pTyr216, and pSer9 in the cortex and hippocampus of naïve, sham, and rmTBI mice (n= 4-7 per group). The levels of GSK TOT, pTyr216 and pSer9 were analyzed relative to the levels of β -actin. The levels of pTyr216 and pSer9 were also analyzed as a ratio to GSK TOT.

Western blot analyses of cortical samples when protein levels were normalized to β -actin

Western blot analyses of total amount of GSK3 β protein in naïve, sham and rmTBI cortices revealed that the levels of GSK3 TOT were higher in shams than in naïves at 8 h and 1 week post-injury (Figure 4A). Similarly, the levels of GSK3 TOT were higher in rmTBI mice than in naïves at 8 h, 1 week and 3 week post-injury (Figure 4A). The Western blot analyses also showed higher pTyr216 levels in both shams and rmTBI mice compared to naïves across all time points with the exception of shams at 8 h post-procedure (Figure 4B). The Western blot analyses also showed increased levels of pSer9 in shams at 3 weeks post-procedure compared to naïves and at 48 h and 3 week post-injury in the rmTBI group compared to naïves (Figure 4C). There were no time points at which GSK TOT or pTyr216 levels were significantly different between sham and rmTBI

mice, however, pSer9 levels were significantly higher in rmTBI mice compared to shams at 48 h post-injury.

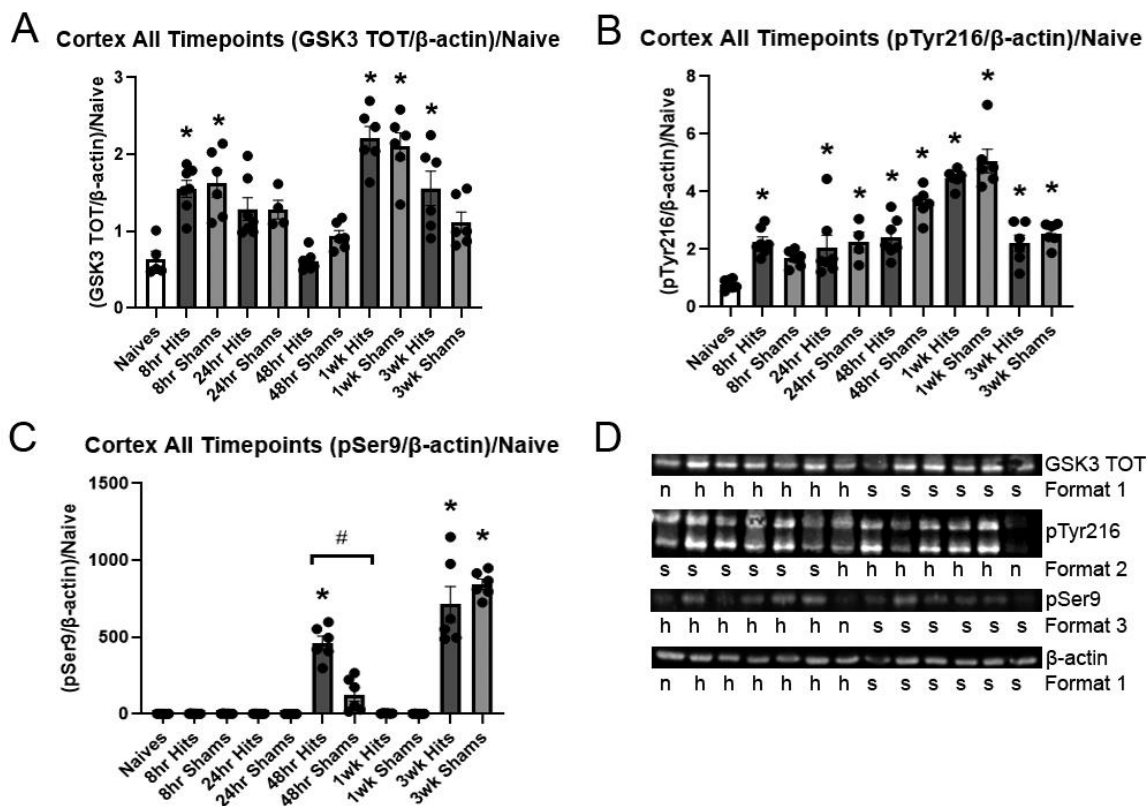


Figure 4. Western blot data for the cortex samples across all timepoints. (A) Graph shows all treatment groups (naïve, sham and injured) for each timepoint looking at the total amount of GSK3 β , GSK3 TOT, relative to β -actin and then compared to the naïve sample. (B) Graphs focus on the amount of phosphorylation at the Tyr216 site on GSK3 β relative to β -actin and then compared to the naïve sample. (C) Graphs focus on the amount of phosphorylation at the Ser9 site on GSK3 β relative to β -actin and then compared to the naïve sample. (D) Representative Western blots (n=naïve, s=sham, h=hit). Data were presented as mean \pm SEM. SEM was presented as the error bars. One-way ANOVA statistical tests were performed with Tukey's multiple comparisons test, $p < 0.05$. "*" represents treatment groups that significantly differ from the naïve animals. "#" represents significant differences between the sham and injured groups of the same timepoint.

Western blot analyses of hippocampal samples when protein levels were normalized to β -actin

Western blot analyses of total amount of GSK3 β protein in naïve, sham and rmTBI hippocampi revealed that the levels of GSK3 TOT were higher in sham and rmTBI hippocampi than in naïve hippocampi at 24 h post-injury or sham procedure (Figure 5A). The Western blot analyses also showed higher pTyr216 levels in both shams and rmTBI mice compared to naïves across all time points with the exception of the 3 week time point post-procedure (Figure 5B). Compared to naïves the levels of pSer9 was higher in shams at 48 h and 1 week post-sham procedure and in rmTBI mice at 1 week post-injury (Figure 5C). There were no time points at which GSK TOT or pTyr216 levels were significantly different between sham and rmTBI mice, however, pSer9 levels were significantly lower in rmTBI mice compared to shams at 1 week post-injury.

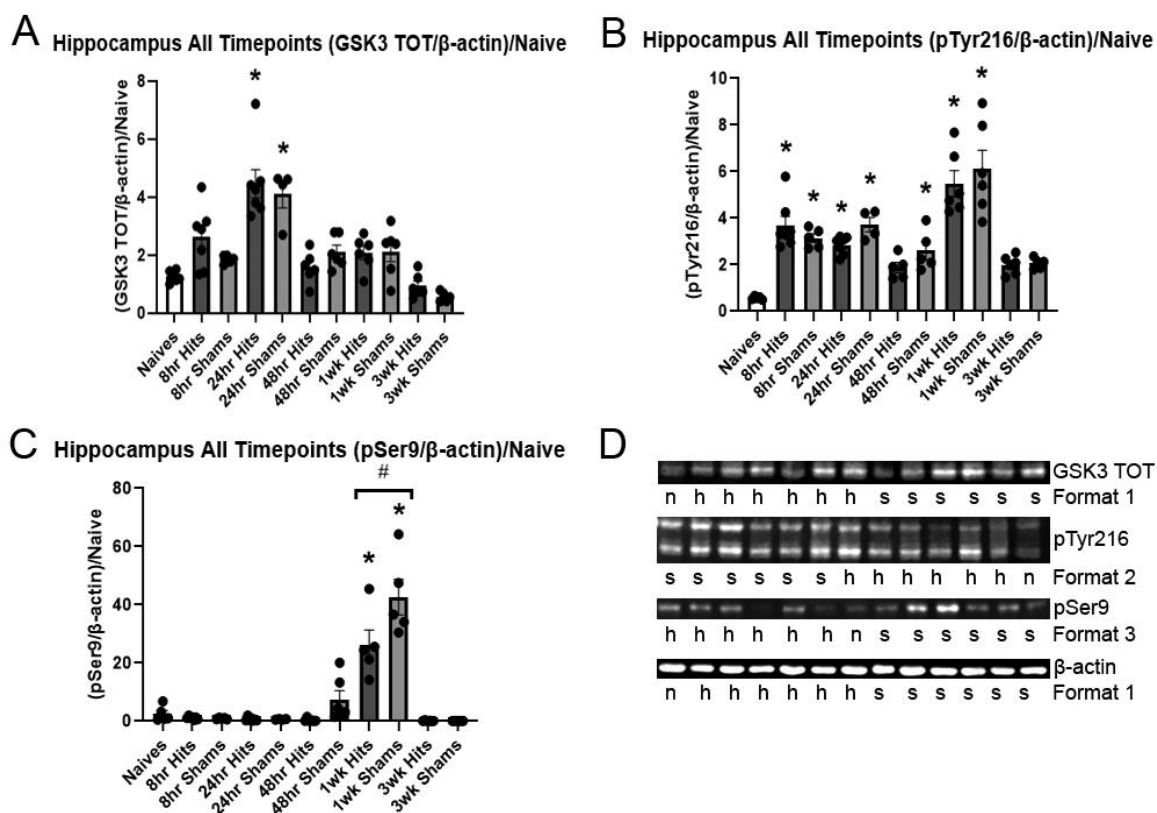


Figure 5. Western blot data for the hippocampal samples across all timepoints. (A) Graph shows all treatment groups (naïve, sham and injured) for each timepoint looking at the total amount of GSK3 β , GSK3 TOT, relative to β -actin and then compared to the naïve sample. (B) Graphs focus on the amount of phosphorylation at the Tyr216 site on GSK3 β relative to β -actin and then compared to the naïve sample. (C) Graphs focus on the amount of phosphorylation at the Ser9 site on GSK3 β relative to β -actin and then compared to the naïve sample. (D) Representative Western blots (n=naïve, s=sham, h=hit). Data were presented as mean \pm SEM. SEM was presented as the error bars. One-way ANOVA statistical tests were performed with Tukey's multiple comparisons test, $p < 0.05$. "*" represents treatment groups that significantly differ from the naïve animals. "#" represents significant differences between the sham and injured groups of the same timepoint.

Western blot analyses of cortical samples when protein levels were normalized to GSK TOT

To evaluate the relative level of GSK3 β activation in the cortex we also examined the ratio of pTyr216 levels to GSK TOT levels in cortical protein samples. These analyses

revealed that the levels of pTyr216, when normalized to GSK TOT levels, was significantly reduced by approximately 2-fold, in sham and rmTBI mice compared to naïves at all time points studied (except for the shams at 3 week post-procedure) (Figure 6A). To evaluate the relative level of GSK3 β inhibition we also examined the ratio of pSer9 levels to GSK TOT levels in cortical protein samples. We found that pSer9 levels in sham mice, when normalized to GSK TOT levels were significantly reduced (by 5 – 10 fold) compared to naïves at 8 h, 24 h, 48 h and 1 week post-procedure (Figure 6B). The pSer9 levels in the rmTBI mice, when normalized to GSK TOT levels, were significantly reduced (by 5 – 10 fold) compared to naïves at 8 h and 24 h, post-injury (Figure 6B).

Western blot analyses of hippocampal samples when protein levels were normalized to GSK TOT

To evaluate the relative level of GSK3 β activation in the hippocampus we examined the ratio of pTyr216 levels to GSK TOT levels in the hippocampal protein samples. This analyses revealed that the levels of pTyr216, when normalized to GSK TOT levels, was significantly reduced by approximately 4-5-fold, in sham and rmTBI mice compared to naïves at all time points studied (except for the 3 week post-injury or procedure time point) (Figure 6C). To evaluate the relative level of GSK3 β inhibition we also examined the ratio of pSer9 levels to GSK TOT levels in cortical protein samples. We also found that pSer9 levels in sham mice, when normalized to GSK TOT levels were significantly reduced (by 25 - 100 fold) compared to naïves at all time points (Figure 6D).

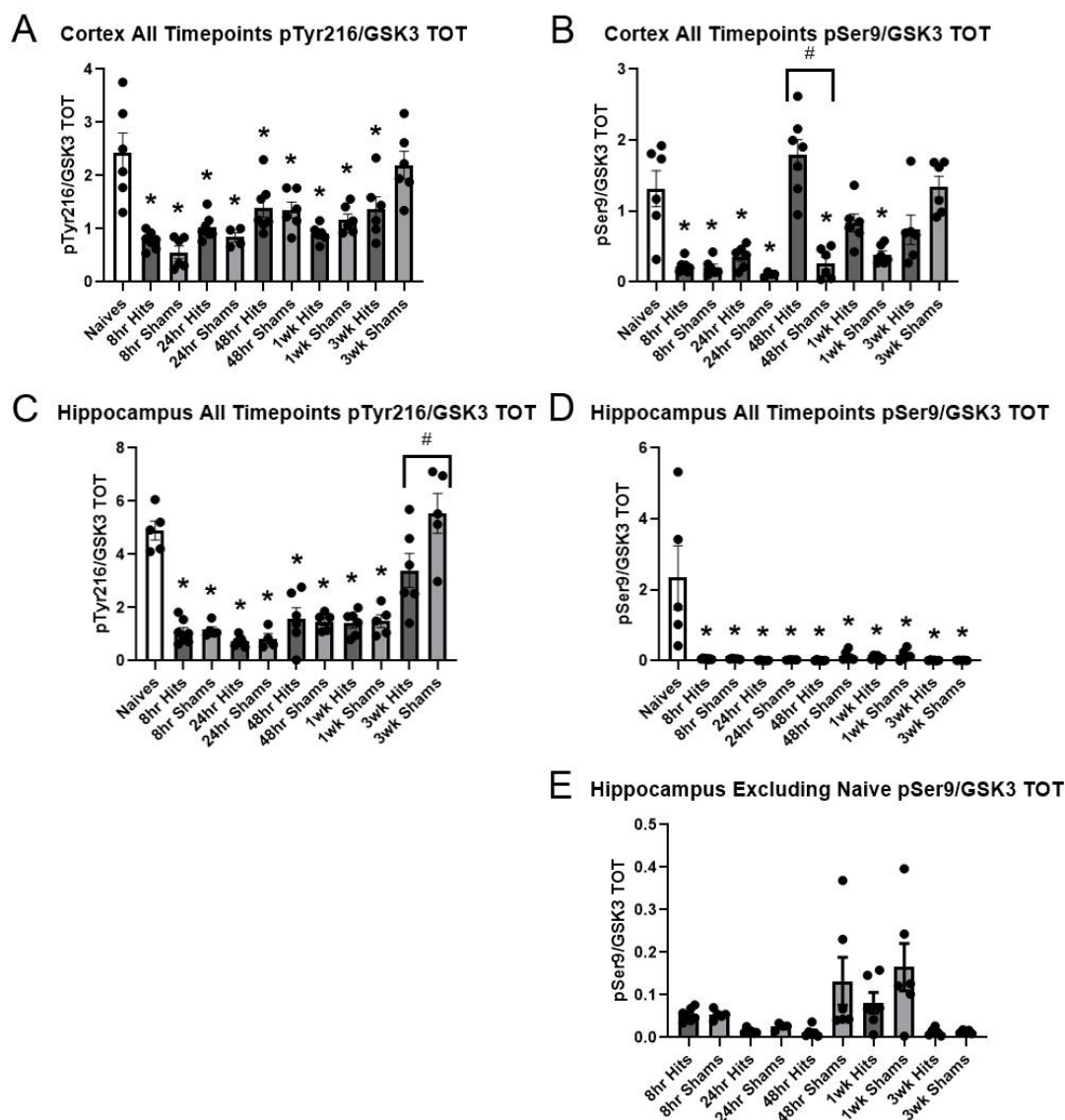


Figure 6. Western blot data comparing the amount of phosphorylation at the regulatory sites on GSK3 β to the total amount of GSK3 β protein. (A) Cortex samples for all treatment groups across all the timepoints analyzed focusing on the amount of phosphorylation at the Tyr216 regulatory site, relative to the total amount of protein. (B) Cortex samples for all treatment groups across all the timepoints analyzed focusing on the amount of phosphorylation at the Ser9 regulatory site, relative to the total amount of protein. (C) Hippocampus samples for all treatment groups across all the timepoints analyzed focusing on the amount of phosphorylation at the Tyr216 regulatory site, relative to the total amount of protein. (D) Hippocampus samples for all treatment groups across all the timepoints analyzed focusing on the amount of phosphorylation at the Ser9 regulatory site, relative to the total amount of protein. (E) Hippocampus samples from (D) excluding the naïve animals. Data were presented as mean \pm SEM. SEM represented as the error bars. One-way ANOVA statistical tests were performed

with Tukey's multiple comparisons test, $p < 0.05$. "*" represents treatment groups that significantly differ from the naïve animals. "#" represents significant differences between the sham and injured groups of the same timepoint.

3.3 Aim #2: To characterize the cellular and molecular pathology triggered by rmTBI in the *MAPT* KI mice

MAPT KI mice

As discussed in the introduction to this thesis (Chapter 1, pages 1-23), using *MAPT* KI mice to study rmTBI increases the clinical relevance of this model of rmTBI. The *MAPT* KI mice carry a fully humanized tau gene in place of the murine tau gene. Thus, pathological consequences of concussion due to the effects of rmTBI on tau would be predicted to be more reflective of human pathological changes consequent to concussion in the *MAPT* KI mice compared to C57BL/6 mice.

A COVID19 impact note concerning the histopathological and behaviour analyses below

*During the analyses phase of this study it became apparent that the controlled cortical impactor was not performing up to specifications, despite being calibrated by myself and others in the laboratory. There was a problem with the impactor itself, in that the speed and/or depth programming of the machine was incorrect and highly variable. The impactor was sent back to the company (Precision Instruments) for recalibration but was damaged in transit back to the Robarts Research Institute and we now are awaiting a replacement. I wanted to repeat the experiment with a properly calibrated impactor however, the combined effects of the COVID-19 restrictions on animal work instituted in March of 2020 and the impactor malfunction delayed my progress by 6 – 8 months making it impossible for me to repeat. Thus, I present my findings below with the admission that there was great variability in the injuries carried out in the *MAPT* KI mice that makes interpretations of the data challenging at best. However, I carried out the histopathological and behavioural analyses to the best of my ability and have, at the very least, provided baseline measurements for shams and naïves that will be useful when this project continues upon receipt of a new impactor.*

Histopathological analyses

To assess *MAPT* KI mice for histological changes after rmTBI that reflect diffuse axonal injury (DAI) we performed silver staining of brain sections from *MAPT* KI mice taken at various time points after injury using the FD Neurosilver™ Kit II silver staining kit (FD NeuroTechnologies, Ellicott City, MD) as previously described (Xu et al., 2021). Images of the corpus callosum were taken using a brightfield microscope at 40x and were visually inspected for black silver staining (Figure 7-10).

Short term analyses (naïve, 1 and 7 days)

Naïve animals had no intervention during the experiment, and as expected, had no evidence of silver stained axons when looking at the corpus callosum (Figure 7A). At 1 day and 7 days post-injury, brain sections from injured male *MAPT* KI (Figure 7C and E) demonstrated some silver staining, compared to shams (Figure 7B and D) that was particularly evident at high power magnification (insets in Figure 7C and E).

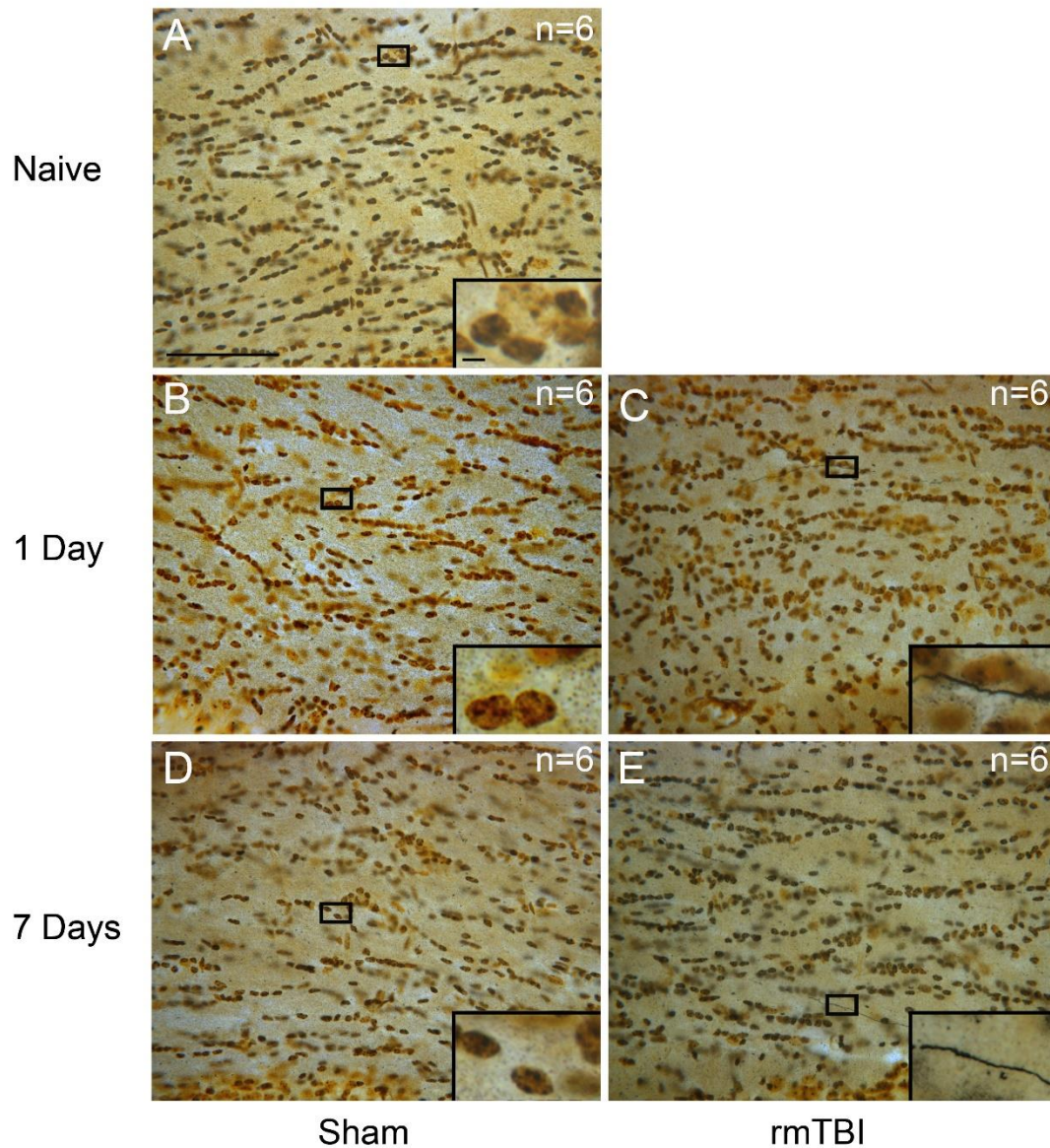


Figure 7. Silver staining for the short term timepoints of the *MAPT* KI study. (A) Silver staining of the corpus callosum of a naïve animal (n=6). (B) Silver staining of the corpus callosum of a sham animal sacrificed at the 1 day timepoint. (C) Silver staining of the corpus callosum of an injured animal sacrificed at the 1 day timepoint. (D) Silver staining of the corpus callosum of a sham animal sacrificed at the 7 day/1 week timepoint. (E) Silver staining of the corpus callosum of an injured animal sacrificed at the 7 day/1 week timepoint. All images were taken at 40x.

Long term analyses (4 and 10 weeks)

Sections from both male and female injured *MAPT* KI mice demonstrated some silver staining at 4 and 10 week post-injury compared to their sham counterparts (Figure 8). High power magnifications showed that the silver stained axons had the characteristic tortuous appearance suggestive of axonal damage (Shitaka et al., 2011).

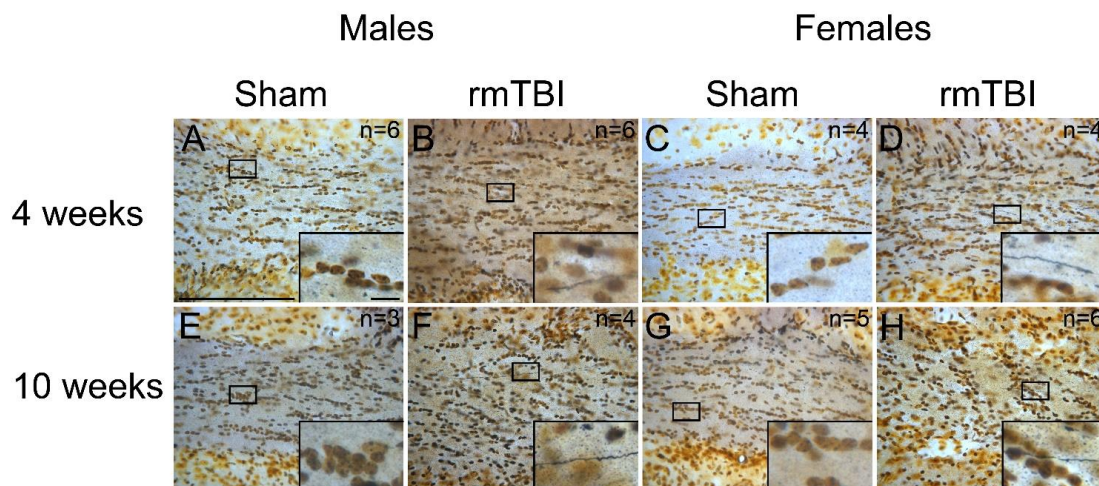


Figure 8. Silver staining for the longer term timepoints of the *MAPT* KI study. (A) Silver staining of the corpus callosum of a sham male sacrificed at the 4 week timepoint. (B) Silver staining of the corpus callosum of an injured male sacrificed at the 4 week timepoint. (C) Silver staining of the corpus callosum of a sham female sacrificed at the 4 week timepoint. (D) Silver staining of the corpus callosum of an injured female sacrificed at the 4 week timepoint. (E through H) Same order of images as the ones above, except taken from the animals sacrificed at the 10 week timepoint. All images were taken at 40x.

Variability in injury

While the histopathological staining of rmTBI *MAPT* KI mice showed the presence of silver-stained axons their number per section seemed greatly reduced compared to the number of silver-stained axons in the pilot project described above. Furthermore, we also observed a great degree of variability in the amount of silver staining in different mice. This variability can be seen in the images in Figure 9. Figure 9 shows the results of silver staining in sections from 4 different males and 4 different females 10 weeks after their

injury. Despite receiving the same injury, the silver staining revealed great variability in the number of silver stained axons between animals. Most of the animals studied had minimal silver staining (Figure 9A, B, C, E, F and G) suggesting lighter concussive hits, whereas a handful of injured animals had greater amounts of silver staining suggesting that they sustained more severe injuries (Figure 9D and H), resulting in more pathology. Naïve animals did not show signs of positive silver staining. This histopathology was the first inkling that the impactor was malfunctioning – a problem that was subsequently verified and prompted a return of the impactor to Precision Instruments for recalibration and repair.

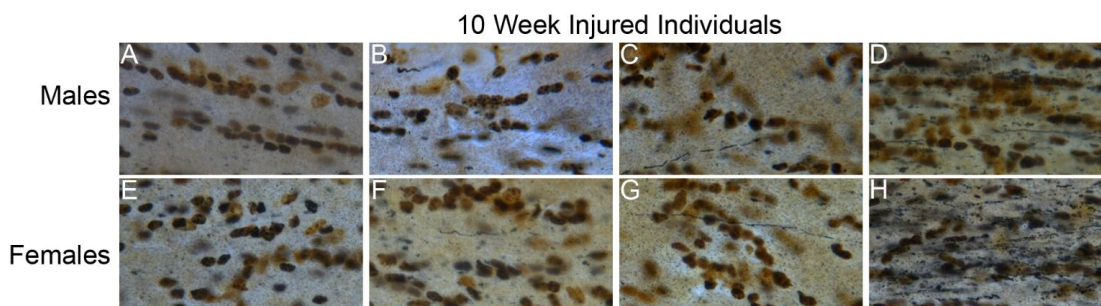


Figure 9. Silver staining of the variability of the injuries delivered by the controlled cortical impactor (CCI). (A through D) Snippets of the corpus callosum of the injured male animals sacrificed at the 10 week timepoint. (E through H) Snippets of the corpus callosum of the injured females sacrificed at the 10 week timepoint. Images on the left most side have negligible silver staining and as the images move towards the right most side there is significant amounts of silver staining. Images in the middle vary in the degree of silver staining. Images were taken at 40x.

Silver staining in sections from Aged MAPT KI mice

To fully characterize the usefulness of the *MAPT* KI mice for chronic studies of rmTBI there was a need to establish baseline histopathological measures in uninjured aged *MAPT* KI mice. All aged animals received no intervention during these experiments. Male *MAPT* KI mice were raised until they reached 14 months of age and were then

sacrificed. A single female *MAPT* KI mouse was raised until it reached 12 months of age and was then sacrificed. Greater numbers of *MAPT* KI mice were not available due to COVID-19 restrictions on animal breeding. Both aged male and female *MAPT* KI mice displayed minimal silver staining (Figure 10A and B) that was comparable to the amount of silver staining observed in aged (14 month old) C57BL/6 mice (Figure 10C and D).

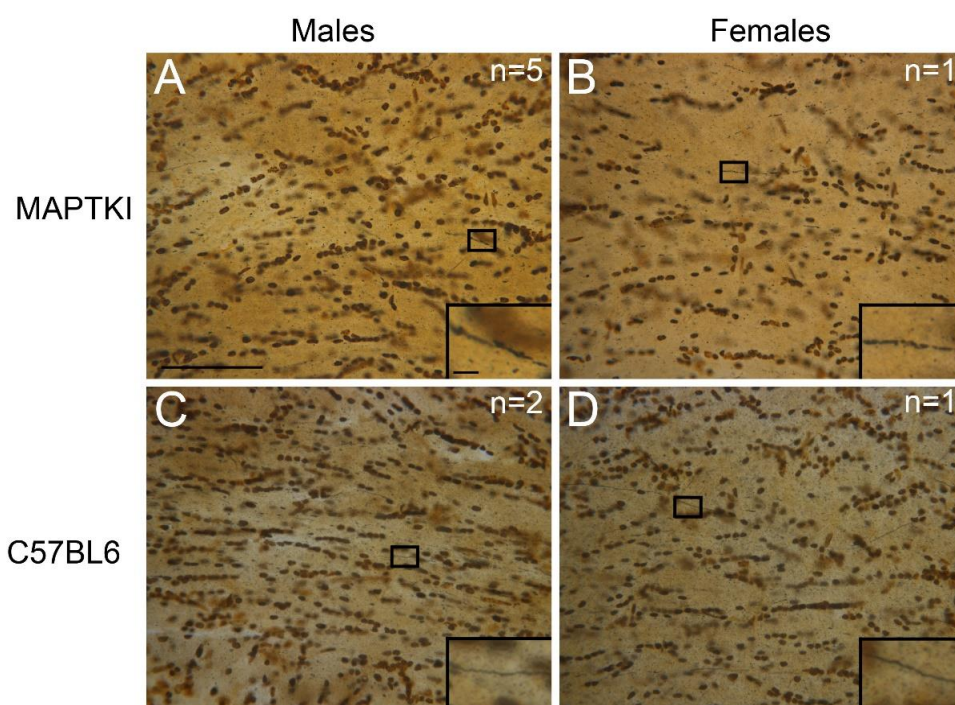


Figure 10. Silver staining of the aged animals. (A) Silver staining of the corpus callosum of an aged *MAPT* KI male sacrificed at 14 months old. (B) Silver staining of the corpus callosum of an aged *MAPT* KI female sacrificed at 12 months old. (C) Silver staining of the corpus callosum of an aged C57BL/6 male sacrificed at 14 months old. (D) Silver staining of the corpus callosum of an aged C57BL/6 female sacrificed at 14 months old. All images were taken at 40x.

Staining for pathologically phosphorylated tau in injured MAPT KI animals

Abnormal phosphorylation of tau has been reported in human brain samples from subjects with a history of concussion (McKee et al., 2009, 2013; Tagge et al., 2018) and

in rmTBI mice (Tagge et al., 2018; Xu et al., 2021). To characterize the levels of pathologically phosphorylated tau in rmTBI *MAPT* KI mice we immunostained sections from naïve, sham and rmTBI mice at 10 weeks post-injury or sham procedure with the AT8 antibody that recognizes phospho-tau (Ser202, Thr205) (Y. Zhang et al., 2019). Figure 11 shows a series of photomicrographs taken in the cortical/prefrontal areas of these sections. Naïve male *MAPT* KI did not display positive AT8 staining (Figure 11D). Injured male *MAPT* KI mice (Figure 11F) had significantly more AT8 positive staining compared to the shams (Figure 11E) and the naïve animals (Figure 11D) that was comparable to the AT8 staining seen in C57BL/6 rmTBI mice (Figure 11C).

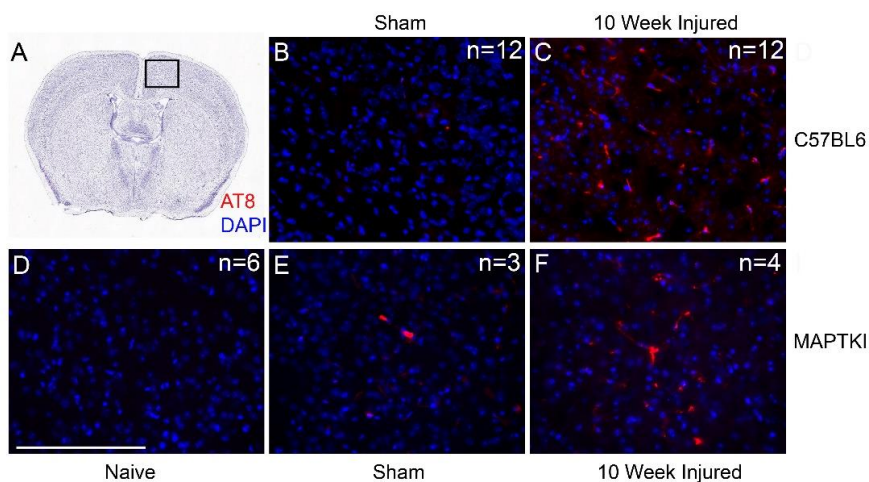


Figure 11. AT8 staining in the prefrontal cortex of the injured animals. (A) Representative ATLAS image of the brain sections that were stained and imaged. The black box represents the approximate area in which the photos were taken. AT8 staining is red and DAPI staining is blue. (B) Image of a C57BL/6 sham animal donated by Dr. Kathy Xu for comparison to the *MAPT* KI. (C) Image of a C57BL/6 injured animal donated by Dr. Kathy Xu for comparison to the *MAPT* KI. (D) Image of a naïve *MAPT* KI animal. (E) Image of a sham *MAPT* KI animal. (F) Image of an injured *MAPT* KI animal. Numbers in the top right corner represent the n's for each group. All images were taken at 40x.

Staining for pathologically phosphorylated tau in uninjured aged MAPT KI animals

To fully characterize the usefulness of the *MAPT* KI mice for chronic studies of rmTBI there was also a need to establish baseline levels for pathologically phosphorylated tau in aged *MAPT* KI mice. We immunostained brain sections from aged uninjured *MAPT* KI mice with the AT8 antibody. Figure 12 shows photomicrographs taken from the cortical/prefrontal areas of these sections (Figure 12A). Aged animals were not manipulated and left to age naturally over the course of this experiment. C57BL/6 male and female mice were aged to 14 months old, male *MAPT* KI mice were aged to 14 months old, and the sole female *MAPT* KI mouse was aged to 12 months. Naïve animals did not show any positive AT8 staining (Figure 12D). Uninjured, aged male and female C57BL/6 mice showed minimal AT8 staining (Figure 12B and C), whereas uninjured, aged male and female *MAPT* KI mice demonstrated more AT8 positive staining (Figure 12E and F).

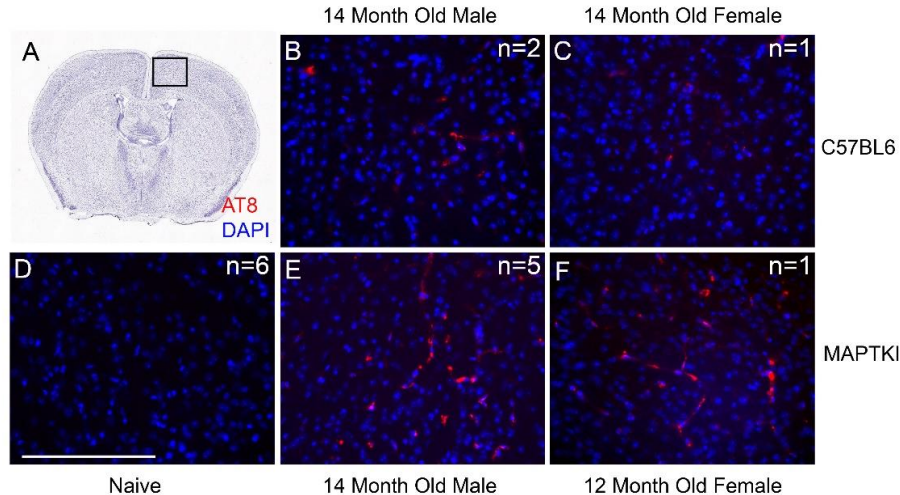


Figure 12. AT8 staining in the prefrontal cortex of the aged animals. (A) Representative ATLAS image of the brain sections that were stained and imaged. The black box represents the approximate area in which the photos were taken. AT8 staining is red and DAPI staining is blue. (B) Image of an aged C57BL/6 male sacrificed at 14 months old. (C) Image of an aged C57BL/6 female sacrificed at 14 months old. (D) Image of a naïve *MAPT* KI animal. (E) Image of an aged *MAPT* KI male sacrificed at 14 months old. (F) Image of an aged *MAPT* KI female sacrificed at 12 months old. Numbers in the top right corner represent the n's for each group. All images were taken at 40x.

Inflammation in the MAPT KI mice after rmTBI

To determine if the inflammatory response triggered by rmTBI in *MAPT* KI mice was similar to that triggered in rmTBI C57BL/6 mice we immunostained brain sections from rmTBI (C57BL/6 and *MAPT* KI) mice for GFAP and Iba1. Figure 13 shows photomicrographs from the cortex of these stained sections (Figure 13A). Injured male C57BL/6 and *MAPT* KI (Figure 13C and H) mice displayed increased levels of Iba1 immunostaining compared to sham animals (Figure 13B, D, G and J). Naïve male *MAPT* KI mice (and C57BL/6 mice, data not shown) did not show any significant Iba1 staining (Figure 13F), but did show moderate GFAP staining (Figure 13I) as did sections from sham (Figure 13D and J) and rmTBI mice (Figure 13E and K).

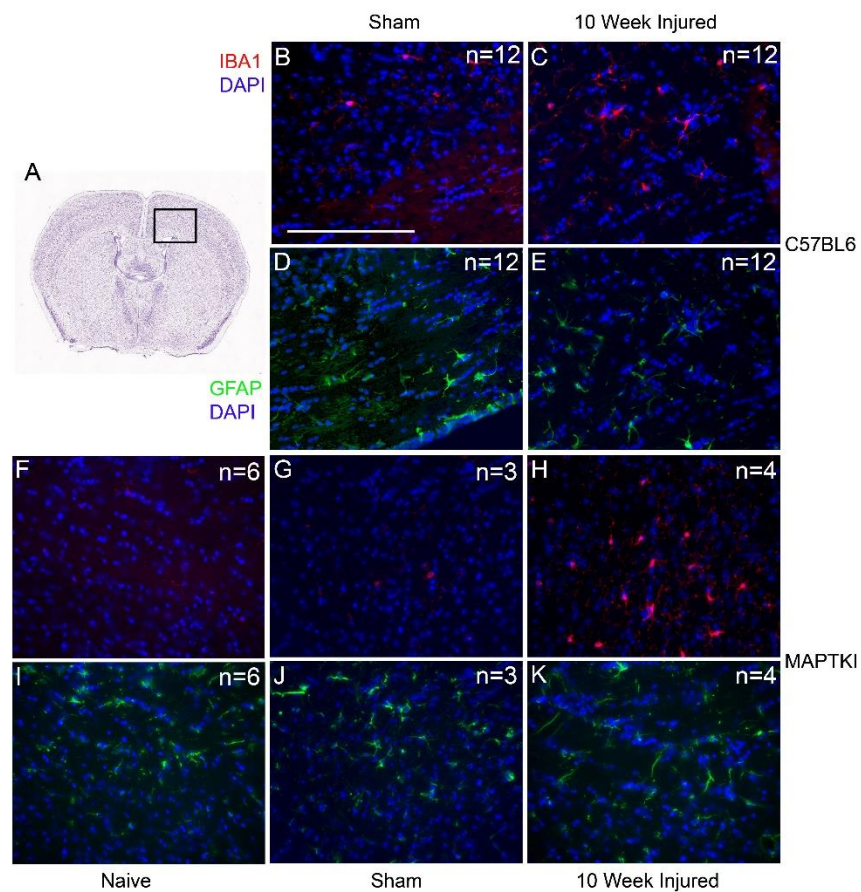


Figure 13. GFAP and Iba1 staining in the corpus callosum area for the injured animals. (A) Representative ATLAS image of the brain sections that were stained and imaged. The black box represents the approximate area in which the photos were taken. GFAP staining is green, Iba1 staining is red and DAPI staining is blue. (B and D) Images of the GFAP and Iba1 staining for a C57BL/6 sham animal donated by Dr. Kathy Xu. (C and E) Images of the GFAP and Iba1 staining for a C57BL/6 injured animal donated by Dr. Kathy Xu. (F and I) Images of the GFAP and Iba1 staining for a naïve *MAPT* KI animal. (G and J) Images of the GFAP and Iba1 staining for a sham *MAPT* KI animal. (H and K) Images of the GFAP and Iba1 staining for an injured *MAPT* KI animal. Numbers in the top right corner represent the n's for each group. All images were taken at 40x.

What does the GFAP and Iba1 staining look like in uninjured aged MAPT KI mice

To fully characterize the usefulness of the *MAPT* KI mice for chronic studies of rmTBI we investigated the baseline GFAP and Iba1 levels in brain sections from uninjured aged *MAPT* KI mice. Brain sections from uninjured, aged *MAPT* KI mice were immunostained for GFAP and Iba1 expression. Figure 14 shows photomicrographs taken from the cortex of these sections (Figure 14A). While aged, uninjured C57BL/6 and *MAPT* KI mice demonstrated very little Iba1 expression (Figure 14B, C, G and H) they did demonstrate moderate levels of GFAP immunostaining (Figure 14D, E, I, J and K).

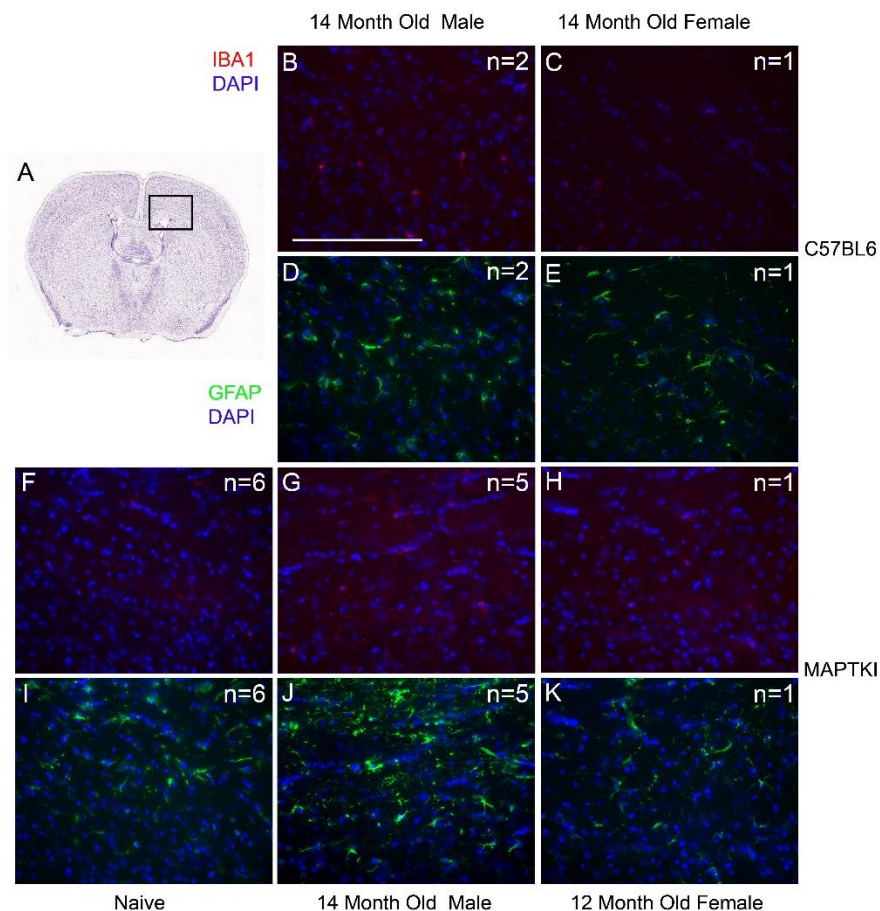


Figure 14. GFAP and Iba1 staining in the corpus callosum area for the aged animals. (A) Representative ATLAS image of the brain sections that were stained and imaged. The black box represents the approximate area in which the photos were taken. GFAP staining is green, Iba1 staining is red and DAPI staining is blue. (B and D) Images of the GFAP and Iba1 staining of an aged C57BL/6 male. (C and E) Images of the GFAP and Iba1 staining of an aged C57BL/6 female. (F and I) Images of the GFAP and Iba1 staining for a naïve *MAPT* KI animal. (G and J) Images of the GFAP and Iba1 staining of an aged *MAPT* KI male. (H and K) Images of the GFAP and Iba1 staining of an aged *MAPT* KI female. Numbers in the top right corner represent the n's for each group. All images were taken at 40x.

3.4 Aim #3: To characterize the behavioural outcomes triggered by rmTBI in the *MAPT* KI mice

The effects of rmTBI on behaviour of MAPT KI mice in the elevated plus maze

It has been previously shown that rmTBI can be associated with anxiety and anxiety-like behaviours post-injury (Broussard et al., 2017). We sought to investigate the potential effects of rmTBI on anxiety/anxiety-like behaviours at 8.5 weeks post-injury in the *MAPT* KI mice using the Elevated Plus Maze (EPM) test. Mice were placed into the centre portion of the maze and allowed to freely explore the maze as their behaviours were videotaped for five minutes. The amount of time each mouse spent in the closed arms, open arms, and in the centre of the maze was measured by ANY-Maze (Stoelting Co. Wood Dale, IL). Male rmTBI *MAPT* KI mice spent a significantly longer amount of time in the closed arms compared to the shams (Figure 15A), which spent more time in the open arms of the maze (Figure 15B). There were no significant differences in the amount of time spent in the centre part of the maze (Figure 15C). There were no significant differences in the mean speed, and total distance travelled between the male sham and rmTBI *MAPT* KI mice (Figure 16A and B).

An analysis of female rmTBI and sham *MAPT* KI mice demonstrated there were no significant differences in the amount of time spent in the closed and open arms of the maze (Figure 15D and E), however, there were significant differences in the amount of time spent in the centre part of the maze (Figure 15F). The female rmTBI mice spent a significantly longer time in the centre of the maze compared to shams. There were significant differences in the mean speed and total distance travelled (Figure 16C and D) with the female sham mice travelling at a faster mean speed than the injured females and travelling a greater distance within the EPM compared to injured individuals.

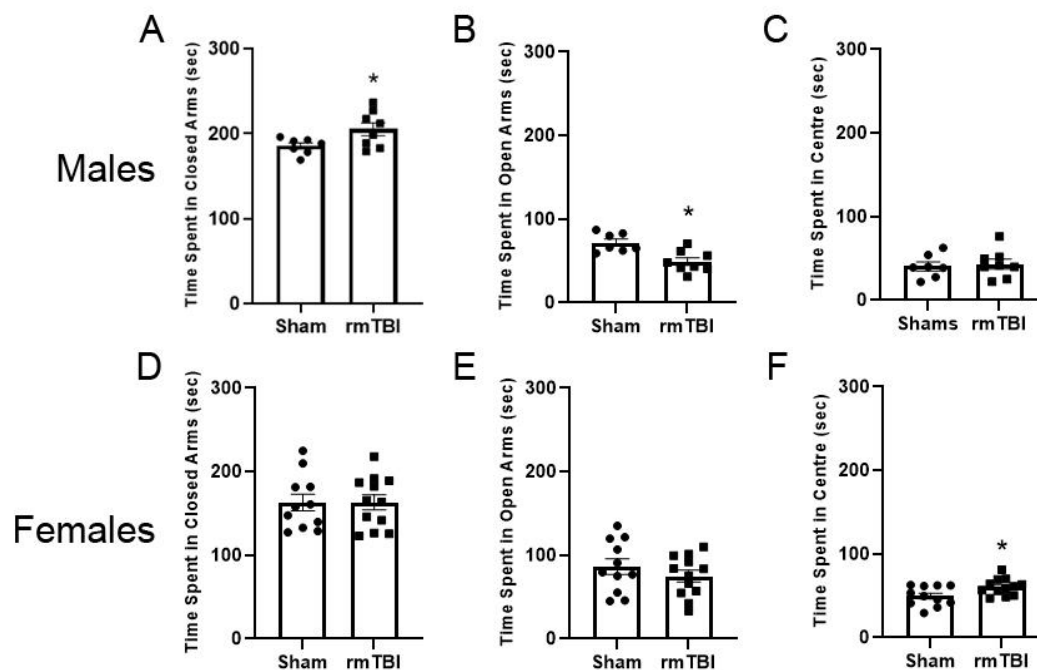


Figure 15. Behavioural data from the Elevated Plus Maze (EPM) Test. (A) Time spent in the closed arms of the EPM for sham and injured *MAPT* KI males. (B) Time spent in the open arms of the EPM for sham and injured *MAPT* KI males. (C) Time spent in the centre area of the EPM for sham and injured *MAPT* KI males. (D) Time spent in the closed arms of the EPM for sham and injured *MAPT* KI females. (E) Time spent in the open arms of the EPM for sham and injured *MAPT* KI females. (F) Time spent in the centre area of the EPM for sham and injured *MAPT* KI females. Data were presented as mean±SEM. SEM was represented as the error bars. “*” represents significant differences between the treatment groups. Student’s t-test was performed for the EPM data, $p < 0.05$

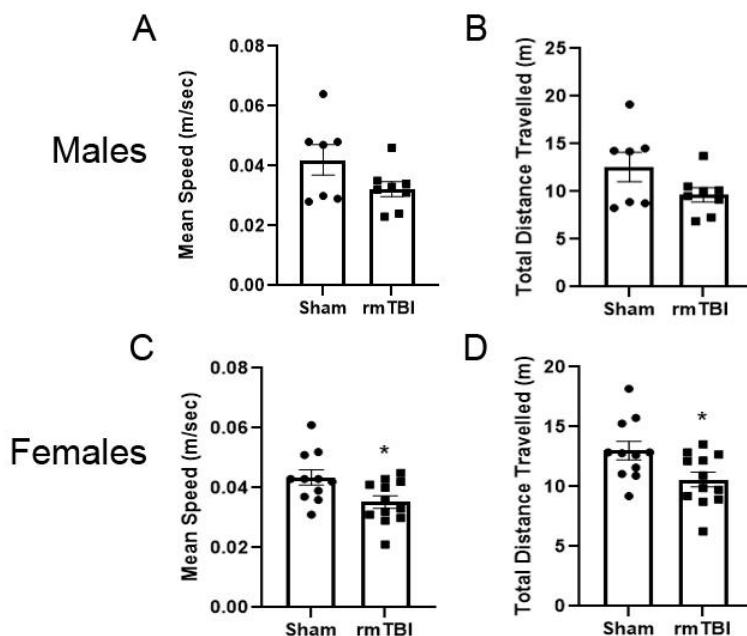


Figure 16. Mean speed and total distance travelled in the Elevated Plus Maze (EPM) Test. (A) Mean speed of sham and injured *MAPT* KI males. (B) Total distance travelled for sham and injured *MAPT* KI males. (C) Mean speed of sham and injured *MAPT* KI females. (D) Total distance travelled for sham and injured *MAPT* KI females. Data were presented as mean±SEM. SEM was represented as the error bars. “*” represents significant differences between the treatment groups. Student’s t-test was performed for the EPM data, $p < 0.05$

How does rmTBI influence spatial cognition and memory of MAPT KI mice?

Repetitive mTBI has been previously linked to spatial cognition and memory deficits using the Morris Water Maze test (MWM) (Mannix et al., 2014; Xu et al., 2021). The effects of rmTBI on spatial cognition and memory in male and female *MAPT* KI mice were assessed with the MWM. Male sham and rmTBI *MAPT* KI mice had difficulty learning the task, as demonstrated by the learning curves in Figure 17A [$F(3,48)=1.849$, $p=0.1510$]. During the Probe Trial, conducted on Day 5, there were no significant differences in the amount of time spent in the target quadrant versus non-target quadrants as assessed by one-way ANOVA (Figure 17B). There was a significant difference seen

in the mean swim speeds (m/sec) during the Probe Trial, with the injured males swimming significantly faster than the sham males (Figure 17C).

The learning curves for the female sham and rmTBI *MAPT* KI mice demonstrate that both groups were able to learn the task, with no significant differences in learning between groups throughout the four training days (Figure 17D). On the Probe Trial there were no significant differences in the amount of time spent in the target quadrant versus non-target quadrants as assessed by one-way ANOVA (Figure 17E), for sham or rmTBI *MAPT* KI females. There were no significant differences for swim speeds between groups during the Probe Trial (Figure 17F).

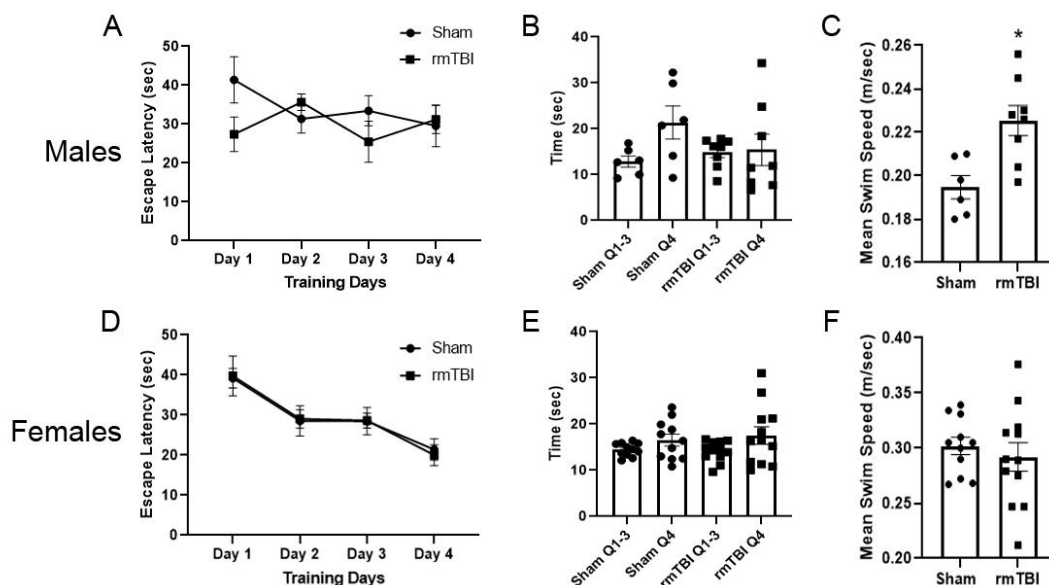


Figure 17. Behavioural data from the Morris Water Maze (MWM) Test. (A) Escape latency for each of the four training days of the MWM for both sham and injured *MAPT* KI males. (B) Time spend in both the non-target (Q1-3) and target (Q4) quadrants of the MWM during the probe trial for both sham and injured *MAPT* KI males. (C) Mean swim speed for sham and injured *MAPT* KI males. (D) Escape latency for each of the four training days of the MWM for both sham and injured *MAPT* KI females. (E) Time spend in both the non-target (Q1-3) and target (Q4) quadrants of the MWM during the probe trial for both sham and injured *MAPT* KI females. Data were presented as mean±SEM. SEM was represented as the error bars. “*” represents significant differences between the treatment groups. One-way ANOVA statistical tests were performed for A, B, D, and E with Tukey’s multiple comparisons test. Student’s t-test were performed for C and F, $p < 0.05$.

Chapter 4

4 Discussion and Conclusions

The objectives of this study were to characterize a time course of GSK3 β phosphorylation, using C57BL/6 mice, and to investigate the cellular/molecular pathology and behavioural outcomes in *MAPT* KI mice in order to validate their usefulness in concussion research as a more clinically relevant model. This study is going to be one of few, if not the first of its kind, to use the *MAPT* KI transgenic mice created from Saito et al. (2019) in a model of repetitive mild traumatic brain injury.

4.1 Pilot Study

Before the study began, a pilot study was conducted in order to determine if the same injury protocol, minus the skin incision, would produce similar injury levels compared to the injury protocol including the skin incision previously used by the Brown Lab (Xu et al., 2021). Silver staining revealed that both injury protocols produced abundant positive silver staining, but in different areas of the brain (Figure 3), proving that keeping the skin intact with the same injury parameters was sufficient to cause physical axonal damage. Clearly, the protocol excluding the skin incision was sufficient to produce some level of injury as indicated by the silver staining, however, in the future, there could be room for improvement. For instance, the parameters of the hit could be adjusted to account for the thickness of the skin and/or adjust the intensity of the injury delivered. One study investigating the physical and mechanical properties of mammalian skin in various animal models determined that smaller species, such as rodent models, have increased viscoelastic effects in the skin compared to larger species, such as humans (Wei et al., 2017). Other factors can also influence the properties of the skin, such as age, gender, and weight (Wei et al., 2017). In terms of the actual injury parameters, both the depth and the speed of the injury delivered could be adjusted in order to increase the severity of the hit. This could be done by increasing the depth or by increasing the speed, or by increasing both parameters at the same time.

4.2 Kinetics of GSK3 β Phosphorylation triggered by rmTBI

After an episode of rmTBI, many cascades are initiated that result in neurodegenerative changes that lead cognitive deficits. It has been proposed that GSK3 β is responsible for the abnormal phosphorylation of tau in tauopathies, such as CTE (Hooper, Killick, and Lovestone, 2008). This abnormal phosphorylation of tau is what causes the pathological formation of aggregates/fibrils/tangles leading to neuronal death (Polydoro et al., 2009). Moszczynski et al (2018) demonstrated this process, in a rodent model of moderate TBI, showing that both the activation of GSK3 β and tau pathology were increased 3 months post-injury. Many studies have evaluated the effects of preventing the activation of GSK3 β and abnormal tau phosphorylation (Dash et al., 2011). To plan how we might best deliver a GSK3 β inhibitor we sought to determine when and for how long, after rmTBI, GSK3 β is activated. In my study, several time points post-injury were analyzed to investigate the levels of phosphorylation on two of the main regulatory sites on GSK3 β , pTyr216 and pSer9 (Fang et al., 2000; Krishnankutty et al., 2017), relative to total GSK3 β . Western blot analyses revealed that in both the cortical and hippocampal protein samples GSK3 TOT levels when normalized to β -actin were increased in rmTBI mice compared to naïves at several timepoints (Figure 4 and 5). When looking at the relative phosphorylation on the regulatory sites compared to total GSK3 β protein (Figure 6), there is a higher ratio of pTyr216/GSK3 TOT compared to pSer9/GSK3 TOT, and, taken together with the increase in total GSK3 β protein, these results suggest that there may be increased activation of GSK3 β in the rmTBI groups. However, these two regulatory sites are not the only regulatory mechanisms acting on GSK3 β . For example, there is another known inhibitory site on GSK3 β , Ser389, that is phosphorylated by p38 mitogen-activated protein kinase (MAPK) (Thornton et al., 2008). In order to assess the actual activity of GSK3 β , kinase activity assays would need to be conducted, similar to that seen in the Noble et al. study (Noble et al., 2005). In the future, one could also assess the activity of multiple activation and inactivation pathways that converge on GSK3 β in order to get a clearer, more complete picture as to how active GSK3 β actually is during pathological processes. Two of the main signaling pathways that result in the inactivation of GSK3 proteins are the insulin and Wnt pathways (Beurel et al., 2015).

GSK3 β also requires substrate priming for the majority of its known substrates. Priming of target substrates is a method of controlling the specificity and targeting action of GSK3 β (Fiol et al., 1987). This priming mechanism involves the phosphorylation of GSK3 β substrates by another kinase at approximately 4 residues away from the target site for GSK3 β phosphorylation (Frame & Cohen, 2001). Therefore, it would be of great interest to investigate the priming kinases that phosphorylate before GSK3 β , as these kinases must act first in order for GSK3 β to perform the subsequent phosphorylation(s) (Frame & Cohen, 2001).

Another method of assessing the contribution of GSK3 β to the development of pathological hallmarks of disease would be to conduct inhibitory trials where the activity of GSK3 β is hindered or completely blocked. A potential candidate GSK3 β inhibitor, such as lithium, could be administered in order to mitigate these pathological mechanisms/pathways from occurring and deter cognitive impairments associated with multiple mild traumatic head injuries (concussions) (Dash et al, 2011). In a cell culture experiment using Neuro2A cells, Moszczynski et al (2015) demonstrated that lithium treated cultures showed reduced GSK3 β activity, decreased tau phosphorylation, reducing fibril formation and cell death.

It is worthy to note that other tau kinases may be responsible and contribute to the abnormal phosphorylation of tau. Each kinase involved in the phosphorylation of tau phosphorylates specific target sites that consequently result in unique physiological effects, some of which may be pathological (Dolan & Johnson, 2010). For example, a study investigating paired helical filament tau (PHF-tau) using mass spectrometry found that casein kinase 1 delta (CK1 δ) phosphorylated approximately 15 sites implicated in PHF-tau (Hanger et al., 2007). The number of sites that CK1 δ was capable of phosphorylating on PHF-tau was comparable to that of GSK3 β in this study, demonstrating that other tau kinases, or synergistic relationships between tau kinases, might be implicated in the generation of pathological tau aggregates (Hanger et al., 2007). Another kinase that may phosphorylate tau is cyclin dependent kinase 5 (cdk5) (Baumann et al., 1993). In this study, investigators evaluated cyclin dependent kinase (cdk) family members that are expressed within the brain and found a cdk-like kinase that

was able to phosphorylate tau in a similar manner to pathological tau present in Alzheimer's disease (AD) (Baumann et al., 1993). They discovered cdk5, confirming its presence with the use of cdk5 specific antibodies, and proposed that this kinase be considered as a serious contender for potential pathological phosphorylation of tau. Fyn, a tyrosine kinase, is also capable of phosphorylating human tau (at the tyrosine 18 (Tyr18) residue) (G. Lee et al., 2004). Fyn has been shown to co-localize with pathologically phosphorylated tau protein, in particular, PHF-tau that reacts positively with antibodies targeting the Tyr18 site (G. Lee et al., 2004). Therefore, Fyn is another important candidate for causing or contributing to the abnormal phosphorylation of tau.

It is important to recognize that both the sham and injured mice in this study displayed similar changes in the phosphorylation status of the two regulatory sites. It was discovered, upon conducting a literature search, that the anesthetic that was used in this study, isoflurane, is capable of influencing the phosphorylation status of GSK3 proteins. One study, investigating the effects of anesthetics on global protein phosphorylation in adult mouse hippocampi, found that there were 318 significant phosphorylation events with respect to 237 different proteins, one of which was GSK3 β (Kohtala et al., 2016). Another study using a rat model of Parkinson's Disease (PD) that was investigating the effects of brief isoflurane exposure on the phosphorylation of GSK3 β , found that there were increased levels of Ser9 phosphorylation in both the cortex and the striatum of the rats (Leikas et al., 2017). The effects of the isoflurane must be taken into account when designing and conducting experiments due to the confounding effects of its use. Appropriate experimental design must include shams for each timepoint analyzed in order to better distinguish between the effects of the anesthetic and the effects of the treatment.

4.3 Characterization of Cellular and Molecular Pathology triggered by rmTBI

In order to validate a clinically relevant model of concussion, rmTBI, we investigated whether the closed skin injury delivered by the CCI device generated diffuse axonal injury (DAI) using silver stained sections from rmTBI *MAPT* KI mice. In terms of the short term timepoints investigated (naïve animals, 1 day and 7 day timepoints), and the

long term timepoints (4 weeks and 10 weeks), the silver staining showed little positive silver staining in the injured groups compared to the shams, which is less than we were expecting (Figure 7 and 8). The variability in the injuries delivered by the CCI device can be seen in Figure 9, in which the level of silver staining in injured mice vary from very low levels to high levels of silver staining, despite the fact that all animals underwent the same injury protocol. These highly variable results may be explained by the fact that the controlled cortical impactor device that I was using throughout the *MAPT* KI study had been malfunctioning, despite being calibrated by myself and others in the lab. Although the outputs that were being read out by the machine itself were the desired parameters of the study, it was obvious that the machine was not matching those parameters, when the results were being analyzed, and the machine was then sent out to be re-calibrated. Therefore, the rmTBI mice in this study experienced inconsistent injuries of variable severity – a fact that must be kept in mind when interpreting the results.

When investigating the pathologically phosphorylated tau, recognized by the AT8 antibody that recognizes phospho-tau at Ser202/Thr205 (Invitrogen), both 10 week injured *MAPT* KI and C57BL/6 male mice were analyzed. Images were chosen to represent the average amount of staining for each group analyzed. Pathologically phosphorylated tau levels were comparable between the two strains of mice within the injured group (Figure 11). Similarly, both groups of injured mice had increased levels of Iba1 reactivity and comparable GFAP reactivity (Figure 13). Another set of *MAPT* KI and C57BL/6 mice were naturally aged to 12-14 months old. When analyzing the silver staining aged males and females had minimal positive silver staining which was comparable between the two strains (Figure 10). However, when investigating the pathologically phosphorylated tau, aged *MAPT* KI male and female mice had greater AT8 staining compared to their C57BL/6 counterparts (Figure 12). When analyzing the staining for the Iba1 and GFAP, there was minimal Iba1 staining and moderate GFAP staining for both aged *MAPT* KI and C57BL/6 animals (Figure 14).

When this data is considered together, we conclude that the *MAPT* KI mice should be used for rmTBI studies over the C57BL/6 mice due to the observation that just as in aged

humans, abnormal tau phosphorylations increase with age in the *MAPT* KI mice. This observation may be attributed to the tau isoforms expressed in C57BL/6 and the *MAPT* KI mice. The C57BL/6 mice, do not express any 3R tau isoforms once adulthood is reached, with matured neurons expressing solely the 4R tau isoforms (Götz et al., 1995; Spillantini & Goedert, 1998). Adult human brains express all six tau isoforms, where both 3R and 4R isoforms are expressed equally at a ratio of approximately 1:1 (M Goedert & Jakes, 1990; Hanes et al., 2009). There are also some sequence differences between human and mouse tau that should be taken into consideration due to the fact that these sequence differences can have implications for tau function. For example, the N-terminal region of human tau contains 11 amino acids that are lacking in mouse tau (Hernández et al., 2020). This variation in the length of the N-terminal region has an impact on the potential for tau to form the “paperclip” formation, with the longer human tau more likely to form this conformation than its mouse tau counterparts. The “paperclip” conformation involves the folding of the C- and N-terminal ends into the microtubule binding repeat domains. One study combined FRET pair mutants with various phospho-mimicking mutations, known to be hyperphosphorylated in AD (AT8, PHF1, AT100), in order to investigate the global folding of tau and how the level of phosphorylation influences this folding and subsequent conformations (Jeganathan et al., 2008). It was determined that the compaction of the paperclip conformation reacted positively with the MC1 antibody, an antibody that recognizes pathological conformations of tau in the early stages of AD, suggesting that this conformation of tau is in fact pathological.

Improvements in the analysis of both the silver staining and immunohistochemistry could be implemented in the future. In this study, qualitative analysis was conducted, in which the sections were visually examined for positive staining. This approach was used seeing as the quantified data would have been variable due to the inconsistent injuries. However, using both qualitative and quantitative data would be desirable once the study has been repeated. One could use a computer-assisted image analysis system, similar to Williams et al. (2006), in order to calculate the optical density (OD) of the silver staining in the sections of interest (Williams et al., 2006). In terms of the immunohistochemical staining, one could use a program such as ImageJ, in order to analyze the photos taken

and calculate the percentage of positive staining in the sections of interest (Moszczynski et al., 2019).

4.4 Characterization of the Behavioural Outcomes triggered by rmTBI

The final aim of this study was to characterize the effect of rmTBI on the behaviour of *MAPT* KI mice using the Elevated Plus Maze (EPM) (to test for anxiety/anxiety-like behaviours) and the Morris Water Maze (MWM) (to test for spatial learning/memory). In terms of the EPM, injured male *MAPT* KI mice spent significantly more time in the closed arms compared to the shams, although this difference was small; whereas, there were no significant differences seen in the behaviours in the female *MAPT* KI mice (Figure 15). During the Probe Trial of the MWM, there were no significant differences in the amount of time spent in the target versus non-target quadrants for both the male and female *MAPT* KI mice (Figure 17), although a trend can be seen for the male and female shams to spend more time in the target quadrant. Unfortunately, during this study, COVID-19 interrupted the progression of this work and the numbers of mice in the colonies had to be decreased, meaning that we did not have the desired numbers for the behavioural studies. Coupled with the fact that the CCI device was malfunctioning, one must not over-analyze these results. Ideally, these experiments would have been replicated with higher n's and with a fully functioning CCI device. However, these results (the increased anxiety, as seen in the rmTBI males of the EPM, and trends for troubled spatial cognition seen in the rmTBI males/females in the MWM), do agree with other studies investigating the effects of rmTBI on behaviour post-injury (Broussard et al., 2018; W. H. Cheng et al., 2019). One study testing the hypothesis that rmTBI negatively impacts spatial memory and anxiety/anxiety-like behaviours suggested that rmTBI does indeed impair spatial memory, as assessed by the MWM, and increases anxiety/anxiety-like behaviours, as assessed by the EPM and the Open Field Tests (OFT) (Broussard et al., 2018). Another study utilizing the Closed-Head Impact Model of Engineered Rotational Acceleration (CHIMERA) model of rmTBI found that there were deficits in the Barnes Maze (BM), another test of spatial learning and memory; however,

contrary to this study, there were decreases in anxiety levels in the EPM coinciding with increased risk taking behaviour (W. H. Cheng et al., 2019).

4.5 Caveats of the Novel Mouse Model

This new mouse model presents potential caveats that should be considered. First, with the humanization of the tau gene, there is concern that the mice do not develop normally as they age. Second, there is the potential for other abnormalities to present themselves as the animals age, for example, poor interaction of the human tau with the other mouse proteins or accelerated neurodegeneration. However, there are currently a few papers published using these mice that can ease the concerns surrounding these potential limitations. The first study that generated these mice found that neuroinflammation, cell death, and overall brain atrophy were not altered or accelerated with the humanization of the tau gene in mice aged to 24 months (Hashimoto et al., 2019). The second paper to utilize these mice checked to see if the humanized tau protein was properly integrated into the nervous system of the mice. This study found that the humanized tau protein was properly integrated into the nervous system, as it was localized in the axons of the neurons, similar to that of the wild type mice (Saito et al, 2019).

4.6 Conclusions

The results of this study support the use of *MAPT* KI mice for rmTBI studies. Implications of this study for the future could include applying these results in preclinical trials studying the pathophysiological mechanisms activated during recovery from rmTBI. This model could also serve useful for testing inhibitors of GSK3 β activity in a more clinically relevant model, as human tau is more prone to pathological processes compared to wild type mouse tau. The *MAPT* KI mice can also be humanized further by targeting other genes of interest, such as β -amyloid, and mimicking the protocols used to humanize the tau gene.

4.7 Significance

Currently, CTE can only be properly diagnosed post-mortem (Turner et al, 2013), which is of no use to the individuals whose lives have already been lost. In order to improve the

lives of those affected by neurodegenerative diseases such as CTE, and those of their families/loved ones, studies must turn their attention towards the mechanisms and pathways that initiate the detrimental cascades, leading to the development of the disease. The number of people being affected by repetitive mild traumatic brain injuries is on the rise, leading to an increase in the number of individuals developing CTE, additionally, causing an increase in the burden/cost to health care systems (Luo et al., 2014). In order to effectively develop a treatment, the time course of pathological activity and contributing processes must first be established. The time of treatment administration could then be designed to coincide with the time of peak pathological activity post-injury. For example, correctly timed administration of a GSK3 β inhibitor might be predicted to prevent the abnormal phosphorylation of tau, the formation of tau aggregates/fibrils/tangles, and potentially the development of CTE later in life. This work is of significant value to both the health and scientific communities since it is one of the first, if not the very first, of its kind to explore concussion and tau pathology in a clinically relevant model of concussion using transgenic mice solely expressing human tau. This study will hopefully serve as a stepping stone for future preclinical studies of rmTBI with a focus on pathophysiology and potential therapeutics.

References

- Abdul-Muneer, P. M., Chandra, N., & Haorah, J. (2015). Interactions of Oxidative Stress and Neurovascular Inflammation in the Pathogenesis of Traumatic Brain Injury. *Molecular Neurobiology*, *51*(3), 966–979. <https://doi.org/10.1007/s12035-014-8752-3>
- Adams, M. D., Celniker, S. E., Holt, R. A., Evans, C. A., Gocayne, J. D., Amanatides, P. G., Scherer, S. E., Li, P. W., Hoskins, R. A., Galle, R. F., George, R. A., Lewis, S. E., Richards, S., Ashburner, M., Henderson, S. N., Sutton, G. G., Wortman, J. R., Yandell, M. D., Zhang, Q., ... Venter, J. C. (2000). The Genome Sequence of *Drosophila melanogaster*. *Science*, *287*(5461), 2185–2195. <https://doi.org/10.1126/science.287.5461.2185>
- Alexander, M. P. (1995). Mild traumatic brain injury : pathophysiology , natural history , and clinical management. *Neurology*, *45*(7), 1253–1260.
- Almanzar, G., Mayerl, C., Seitz, J. C., Höfner, K., Brunner, A., Wild, V., Jahn, D., Geier, A., Fassnacht, M., & Prelog, M. (2016). Expression of 11beta-hydroxysteroid-dehydrogenase type 2 in human thymus. *Steroids*, *110*, 35–40. <https://doi.org/10.1016/j.steroids.2016.03.019>
- Almeida-Suhett, C. P., Prager, E. M., Pidoplichko, V., Figueiredo, T. H., Marini, A. M., Li, Z., Eiden, L. E., & Braga, M. F. M. (2014). Reduced GABAergic inhibition in the basolateral amygdala and the development of anxiety-like behaviors after mild traumatic brain injury. *PloS One*, *9*(7), e102627–e102627. <https://doi.org/10.1371/journal.pone.0102627>
- Andorfer, C., Kress, Y., Espinoza, M., De Silva, R., Tucker, K. L., Barde, Y.-A., Duff, K., & Davies, P. (2003). Hyperphosphorylation and aggregation of tau in mice expressing normal human tau isoforms. *Journal of Neurochemistry*, *86*(3), 582–590. <https://doi.org/https://doi.org/10.1046/j.1471-4159.2003.01879.x>

- Ansari, M. A., Roberts, K. N., & Scheff, S. W. (2008). Oxidative stress and modification of synaptic proteins in hippocampus after traumatic brain injury. *Free Radical Biology and Medicine*, 45(4), 443–452. <https://doi.org/https://doi.org/10.1016/j.freeradbiomed.2008.04.038>
- Arena, J. D., Smith, D. H., Lee, E. B., Gibbons, G. S., Irwin, D. J., Robinson, J. L., Lee, V. M.-Y., Trojanowski, J. Q., Stewart, W., & Johnson, V. E. (2020). Tau immunophenotypes in chronic traumatic encephalopathy recapitulate those of ageing and Alzheimer's disease. *Brain*, 143(5), 1572–1587. <https://doi.org/10.1093/brain/awaa071>
- Arendt, T., Stieler, J. T., & Holzer, M. (2016). Tau and tauopathies. *Brain Research Bulletin*, 126, 238–292. <https://doi.org/https://doi.org/10.1016/j.brainresbull.2016.08.018>
- Avila, J., León-Espinosa, G., García, E., García-Escudero, V., Hernández, F., & DeFelipe, J. (2012). Tau Phosphorylation by GSK3 in Different Conditions. *International Journal of Alzheimer's Disease*, 2012, 578373. <https://doi.org/10.1155/2012/578373>
- Bailes, J. E., Petraglia, A. L., Omalu, B. I., Nauman, E., & Talavage, T. (2013). Role of subconcussion in repetitive mild traumatic brain injury. *Journal of Neurosurgery JNS*, 119(5), 1235–1245. <https://doi.org/10.3171/2013.7.JNS121822>
- Barker-Collo, S., Theadom, A., Jones, K., Starkey, N., Kahan, M., & Feigin, V. (2018). Depression and anxiety across the first 4 years after mild traumatic brain injury: findings from a community-based study. *Brain Injury*, 32(13–14), 1651–1658. <https://doi.org/10.1080/02699052.2018.1540797>
- Baugh, C. M., Stamm, J. M., Riley, D. O., Gavett, B. E., Shenton, M. E., Lin, A., Nowinski, C. J., Cantu, R. C., McKee, A. C., & Stern, R. A. (2012). Chronic traumatic encephalopathy: neurodegeneration following repetitive concussive and subconcussive brain trauma. *Brain Imaging and Behavior*, 6(2), 244–254. <https://doi.org/10.1007/s11682-012-9164-5>

- Baumann, K., Mandelkow, E.-M., Biernat, J., Piwnica-Worms, H., & Mandelkow, E. (1993). Abnormal Alzheimer-like phosphorylation of tau-protein by cyclin-dependent kinases cdk2 and cdk5. *FEBS Letters*, *336*(3), 417–424. [https://doi.org/https://doi.org/10.1016/0014-5793\(93\)80849-P](https://doi.org/https://doi.org/10.1016/0014-5793(93)80849-P)
- Beurel, E., Grieco, S. F., & Jope, R. S. (2015). Glycogen synthase kinase-3 (GSK3): Regulation, actions, and diseases. *Pharmacology & Therapeutics*, *148*, 114–131. <https://doi.org/https://doi.org/10.1016/j.pharmthera.2014.11.016>
- Bhat, R. V., Shanley, J., Correll, M. P., Fieles, W. E., Keith, R. A., Scott, C. W., & Lee, C. M. (2000). Regulation and localization of tyrosine216 phosphorylation of glycogen synthase kinase-3beta in cellular and animal models of neuronal degeneration. *Proceedings of the National Academy of Sciences of the United States of America*, *97*(20), 11074–11079. <https://doi.org/10.1073/pnas.190297597>
- Binder, L. I., Frankfurter, A., & Rebhun, L. I. (1985). The distribution of tau in the mammalian central nervous system. *Journal of Cell Biology*, *101*(4), 1371–1378. <https://doi.org/10.1083/jcb.101.4.1371>
- Blaze, J., Choi, I., Wang, Z., Umali, M., Mendelev, N., Tschiffely, A. E., Ahlers, S. T., Elder, G. A., Ge, Y., & Haghghi, F. (2020). Blast-Related Mild TBI Alters Anxiety-Like Behavior and Transcriptional Signatures in the Rat Amygdala. *Frontiers in Behavioral Neuroscience*, *14*, 1–14. <https://doi.org/10.3389/fnbeh.2020.00160>
- Bolton-Hall, A. N., Hubbard, W. B., & Saatman, K. E. (2019). Experimental Designs for Repeated Mild Traumatic Brain Injury: Challenges and Considerations. *Journal of Neurotrauma*, *36*(8), 1203–1221. <https://doi.org/10.1089/neu.2018.6096>
- Bolton, A. N., & Saatman, K. E. (2014). Regional Neurodegeneration and Gliosis Are Amplified by Mild Traumatic Brain Injury Repeated at 24-Hour Intervals. *Journal of Neuropathology & Experimental Neurology*, *73*(10), 933–947. <https://doi.org/10.1097/NEN.0000000000000115>
- Bramlett, H. M., & Dietrich, W. D. (2015). Long-Term Consequences of Traumatic Brain

- Injury: Current Status of Potential Mechanisms of Injury and Neurological Outcomes. *Journal of Neurotrauma*, 32(23), 1834–1848. <https://doi.org/10.1089/neu.2014.3352>
- Brandt, R., Hundelt, M., & Shahani, N. (2005). Tau alteration and neuronal degeneration in tauopathies: mechanisms and models. *Biochimica et Biophysica Acta (BBA) - Molecular Basis of Disease*, 1739(2), 331–354. <https://doi.org/https://doi.org/10.1016/j.bbadis.2004.06.018>
- Broussard, J. I., Acion, L., De Jesús-Cortés, H., Yin, T., Britt, J. K., Salas, R., Costa-Mattioli, M., Robertson, C., Pieper, A. A., Arciniegas, D. B., & Jorge, R. (2018). Repeated mild traumatic brain injury produces neuroinflammation, anxiety-like behaviour and impaired spatial memory in mice. *Brain Injury*, 32(1), 113–122. <https://doi.org/10.1080/02699052.2017.1380228>
- Buée, L., Bussière, T., Buée-Scherrer, V., Delacourte, A., & Hof, P. R. (2000). Tau protein isoforms, phosphorylation and role in neurodegenerative disorders. *Brain Research Reviews*, 33(1), 95–130. [https://doi.org/https://doi.org/10.1016/S0165-0173\(00\)00019-9](https://doi.org/https://doi.org/10.1016/S0165-0173(00)00019-9)
- Burda, J. E., Bernstein, A. M., & Sofroniew, M. V. (2016). Astrocyte roles in traumatic brain injury. *Experimental Neurology*, 275, 305–315. <https://doi.org/https://doi.org/10.1016/j.expneurol.2015.03.020>
- Cernak, I. (2005). Animal Models of Head Trauma. *NeuroRX*, 2(3), 410–422. <https://doi.org/https://doi.org/10.1602/neurorx.2.3.410>
- Cernak, I., Vink, R., Zapple, D. N., Cruz, M. I., Ahmed, F., Chang, T., Fricke, S. T., & Faden, A. I. (2004). The pathobiology of moderate diffuse traumatic brain injury as identified using a new experimental model of injury in rats. *Neurobiology of Disease*, 17(1), 29–43. <https://doi.org/https://doi.org/10.1016/j.nbd.2004.05.011>
- Chen, T., Liu, W., Chao, X., Zhang, L., Qu, Y., Huo, J., & Fei, Z. (2011). Salvianolic acid B attenuates brain damage and inflammation after traumatic brain injury in

- mice. *Brain Research Bulletin*, 84(2), 163–168.
<https://doi.org/https://doi.org/10.1016/j.brainresbull.2010.11.015>
- Chen, Y.-F., & Zhao, H. (2019). Post - traumatic Stress Disorder : Relationship to Traumatic Brain Injury and Approach to Forensic Psychiatry Evaluation. *Journal of Forensic Science and Medicine*, 5(1), 33–39. <https://doi.org/10.4103/jfsm.jfsm>
- Cheng, G., Kong, R., Zhang, L., & Zhang, J. (2012). Mitochondria in traumatic brain injury and mitochondrial-targeted multipotential therapeutic strategies. *British Journal of Pharmacology*, 167(4), 699–719.
<https://doi.org/https://doi.org/10.1111/j.1476-5381.2012.02025.x>
- Cheng, W. H., Martens, K. M., Bashir, A., Cheung, H., Stukas, S., Gibbs, E., Namjoshi, D. R., Button, E. B., Wilkinson, A., Barron, C. J., Cashman, N. R., Cripton, P. A., & Wellington, C. L. (2019). CHIMERA repetitive mild traumatic brain injury induces chronic behavioural and neuropathological phenotypes in wild-type and APP/PS1 mice. *Alzheimer's Research & Therapy*, 11(1), 6. <https://doi.org/10.1186/s13195-018-0461-0>
- Cho, J.-H., & Johnson, G. V. W. (2003). Glycogen Synthase Kinase 3 β Phosphorylates Tau at Both Primed and Unprimed Sites: DIFFERENTIAL IMPACT ON MICROTUBULE BINDING. *Journal of Biological Chemistry*, 278(1), 187–193.
<https://doi.org/https://doi.org/10.1074/jbc.M206236200>
- Cobb, S., & Battin, B. (2004). Second-Impact Syndrome. *The Journal of School Nursing*, 20(5), 262–267. <https://doi.org/10.1177/10598405040200050401>
- Cohen, P., & Goedert, M. (2004). GSK3 inhibitors: development and therapeutic potential. *Nature Reviews Drug Discovery*, 3(6), 479–487.
<https://doi.org/10.1038/nrd1415>
- Dash, P. K., Johnson, D., Clark, J., Orsi, S. A., Zhang, M., Zhao, J., Grill, R. J., Moore, A. N., & Pati, S. (2011). Involvement of the glycogen synthase kinase-3 signaling pathway in TBI pathology and neurocognitive outcome. *PloS One*, 6(9), e24648–

e24648. <https://doi.org/10.1371/journal.pone.0024648>

- Davis, A. E. (2000). Cognitive Impairments Following Traumatic Brain Injury: Etiologies and Interventions. *Critical Care Nursing Clinics of North America*, 12(4), 447–456. [https://doi.org/https://doi.org/10.1016/S0899-5885\(18\)30081-9](https://doi.org/https://doi.org/10.1016/S0899-5885(18)30081-9)
- Dolan, P. J., & Johnson, G. V. W. (2010). The role of tau kinases in Alzheimer's disease. *Current Opinion in Drug Discovery & Development*, 13(5), 595–603. <https://pubmed.ncbi.nlm.nih.gov/20812151>
- Donovan, V., Kim, C., Anugerah, A. K., Coats, J. S., Oyoyo, U., Pardo, A. C., & Obenaus, A. (2014). Repeated Mild Traumatic Brain Injury Results in Long-Term White-Matter Disruption. *Journal of Cerebral Blood Flow & Metabolism*, 34(4), 715–723. <https://doi.org/10.1038/jcbfm.2014.6>
- Eldar-Finkelman, H., Licht-Murava, A., Pietrokovski, S., & Eisenstein, M. (2010). Substrate Competitive GSK-3 Inhibitors strategy and Implications. *Biochimica et Biophysica Acta (BBA) - Proteins and Proteomics*, 1804(3), 598–603. <https://doi.org/https://doi.org/10.1016/j.bbapap.2009.09.010>
- Engel, T., Goñi-Oliver, P., Lucas, J. J., Avila, J., & Hernández, F. (2006). Chronic lithium administration to FTDP-17 tau and GSK-3 β overexpressing mice prevents tau hyperphosphorylation and neurofibrillary tangle formation, but pre-formed neurofibrillary tangles do not revert. *Journal of Neurochemistry*, 99(6), 1445–1455. <https://doi.org/https://doi.org/10.1111/j.1471-4159.2006.04139.x>
- Erlanger, D. M. (2015). Exposure to sub-concussive head injury in boxing and other sports. *Brain Injury*, 29(2), 171–174. <https://doi.org/10.3109/02699052.2014.965211>
- Fang, X., Yu, S. X., Lu, Y., Bast, R. C., Woodgett, J. R., & Mills, G. B. (2000). Phosphorylation and inactivation of glycogen synthase kinase 3 by protein kinase A. *Proceedings of the National Academy of Sciences*, 97(22), 11960–11965. <https://doi.org/10.1073/pnas.220413597>
- Fann, J. R., Hart, T., & Schomer, K. G. (2009). Treatment for Depression after Traumatic

- Brain Injury: A Systematic Review. *Journal of Neurotrauma*, 26(12), 2383–2402. <https://doi.org/10.1089/neu.2009.1091>
- Fiol, C. J., Mahrenholz, A. M., Wang, Y., Roeske, R. W., & Roach, P. J. (1987). Formation of protein kinase recognition sites by covalent modification of the substrate. Molecular mechanism for the synergistic action of casein kinase II and glycogen synthase kinase 3. *The Journal of Biological Chemistry*, 262(29), 14042–14048. [https://doi.org/10.1016/s0021-9258\(18\)47901-x](https://doi.org/10.1016/s0021-9258(18)47901-x)
- Frame, S., & Cohen, P. (2001). GSK3 takes centre stage more than 20 years after its discovery. *The Biochemical Journal*, 359(Pt 1), 1–16. <https://doi.org/10.1042/0264-6021:3590001>
- Gavett, B. E., Stern, R. A., Cantu, R. C., Nowinski, C. J., & McKee, A. C. (2010). Mild traumatic brain injury: a risk factor for neurodegeneration. *Alzheimer's Research & Therapy*, 2(3), 18. <https://doi.org/10.1186/alzrt42>
- Gavett, B. E., Stern, R. A., & McKee, A. C. (2011). Chronic traumatic encephalopathy: a potential late effect of sport-related concussive and subconcussive head trauma. *Clinics in Sports Medicine*, 30(1), 179–xi. <https://doi.org/10.1016/j.csm.2010.09.007>
- Ghirnikar, R. S., Lee, Y. L., & Eng, L. F. (1998). Inflammation in Traumatic Brain Injury: Role of Cytokines and Chemokines. *Neurochemical Research*, 23(3), 329–340. <https://doi.org/10.1023/A:1022453332560>
- Giarratana, A. O., Teng, S., Reddi, S., Zheng, C., Adler, D., Thakker-Varia, S., & Alder, J. (2019). BDNF Val66Met Genetic Polymorphism Results in Poor Recovery Following Repeated Mild Traumatic Brain Injury in a Mouse Model and Treatment With AAV-BDNF Improves Outcomes . In *Frontiers in Neurology* (Vol. 10, p. 1175). <https://www.frontiersin.org/article/10.3389/fneur.2019.01175>
- Gil, S., Caspi, Y., Ben-Ari, I. Z., Koren, D., & Klein, E. (2005). Does Memory of a Traumatic Event Increase the Risk for Posttraumatic Stress Disorder in Patients With Traumatic Brain Injury? A Prospective Study. *American Journal of Psychiatry*,

162(5), 963–969. <https://doi.org/10.1176/appi.ajp.162.5.963>

- Goedert, M., & Jakes, R. (1990). Expression of separate isoforms of human tau protein: correlation with the tau pattern in brain and effects on tubulin polymerization. *The EMBO Journal*, 9(13), 4225–4230. <https://pubmed.ncbi.nlm.nih.gov/2124967>
- Goedert, M., Spillantini, M. G., & Crowther, R. A. (1992). Cloning of a big tau microtubule-associated protein characteristic of the peripheral nervous system. *Proceedings of the National Academy of Sciences of the United States of America*, 89(5), 1983–1987. <https://doi.org/10.1073/pnas.89.5.1983>
- Goedert, M., Spillantini, M. G., Jakes, R., Rutherford, D., & Crowther, R. A. (1989). Multiple isoforms of human microtubule-associated protein tau: sequences and localization in neurofibrillary tangles of Alzheimer's disease. *Neuron*, 3(4), 519–526. [https://doi.org/10.1016/0896-6273\(89\)90210-9](https://doi.org/10.1016/0896-6273(89)90210-9)
- Goedert, M., Wischik, C. M., Crowther, R. A., Walker, J. E., & Klug, A. (1988). Cloning and sequencing of the cDNA encoding a core protein of the paired helical filament of Alzheimer disease: identification as the microtubule-associated protein tau. *Proceedings of the National Academy of Sciences*, 85(11), 4051 LP – 4055. <https://doi.org/10.1073/pnas.85.11.4051>
- Goedert, Michel, & Jakes, R. (2005). Mutations causing neurodegenerative tauopathies. *Biochimica et Biophysica Acta (BBA) - Molecular Basis of Disease*, 1739(2), 240–250. <https://doi.org/https://doi.org/10.1016/j.bbadis.2004.08.007>
- Götz, J., Probst, A., Spillantini, M. G., Schäfer, T., Jakes, R., Bürki, K., & Goedert, M. (1995). Somatodendritic localization and hyperphosphorylation of tau protein in transgenic mice expressing the longest human brain tau isoform. *The EMBO Journal*, 14(7), 1304–1313. <https://doi.org/https://doi.org/10.1002/j.1460-2075.1995.tb07116.x>
- Haber, M., Hutchinson, E. B., Sadeghi, N., Cheng, W. H., Namjoshi, D., Cripton, P., Irfanoglu, M. O., Wellington, C., Diaz-Arrastia, R., & Pierpaoli, C. (2017). Defining

an Analytic Framework to Evaluate Quantitative MRI Markers of Traumatic Axonal Injury: Preliminary Results in a Mouse Closed Head Injury Model. *ENeuro*, 4(5), ENEURO.0164-17.2017. <https://doi.org/10.1523/ENEURO.0164-17.2017>

Hanes, J., Zilka, N., Bartkova, M., Caletkova, M., Dobrota, D., & Novak, M. (2009). Rat tau proteome consists of six tau isoforms: implication for animal models of human tauopathies. *Journal of Neurochemistry*, 108(5), 1167–1176. <https://doi.org/10.1111/j.1471-4159.2009.05869.x>

Hanger, D. P., Anderton, B. H., & Noble, W. (2009). Tau phosphorylation: the therapeutic challenge for neurodegenerative disease. *Trends in Molecular Medicine*, 15(3), 112–119. <https://doi.org/10.1016/j.molmed.2009.01.003>

Hanger, D. P., Byers, H. L., Wray, S., Leung, K.-Y., Saxton, M. J., Seereeram, A., Reynolds, C. H., Ward, M. A., & Anderton, B. H. (2007). Novel Phosphorylation Sites in Tau from Alzheimer Brain Support a Role for Casein Kinase 1 in Disease Pathogenesis * . *Journal of Biological Chemistry*, 282(32), 23645–23654. <https://doi.org/10.1074/jbc.M703269200>

Hashimoto, S., Matsuba, Y., Kamano, N., Mihira, N., Sahara, N., Takano, J., Muramatsu, S., Saido, T. C., & Saito, T. (2019). Tau binding protein CAPON induces tau aggregation and neurodegeneration. *Nature Communications*, 10(1), 2394. <https://doi.org/10.1038/s41467-019-10278-x>

Hay, J., Johnson, V. E., Smith, D. H., & Stewart, W. (2016). Chronic Traumatic Encephalopathy: The Neuropathological Legacy of Traumatic Brain Injury. *Annual Review of Pathology: Mechanisms of Disease*, 11(1), 21–45. <https://doi.org/10.1146/annurev-pathol-012615-044116>

Hay, J. R., Johnson, V. E., Young, A. M. H., Smith, D. H., & Stewart, W. (2015). Blood-Brain Barrier Disruption Is an Early Event That May Persist for Many Years After Traumatic Brain Injury in Humans. *Journal of Neuropathology & Experimental Neurology*, 74(12), 1147–1157. <https://doi.org/10.1093/jnen/74.12.1147>

- Hernández, F., Merchán-Rubira, J., Vallés-Saiz, L., Rodríguez-Matellán, A., & Avila, J. (2020). Differences Between Human and Murine Tau at the N-terminal End . In *Frontiers in Aging Neuroscience* (Vol. 12, p. 11). <https://www.frontiersin.org/article/10.3389/fnagi.2020.00011>
- Heyburn, L., Sajja, V. S. S. S., & Long, J. B. (2019). The Role of TDP-43 in Military-Relevant TBI and Chronic Neurodegeneration . In *Frontiers in Neurology* (Vol. 10, p. 680). <https://www.frontiersin.org/article/10.3389/fneur.2019.00680>
- Hill, A. A., Hunter, C. P., Tsung, B. T., Tucker-Kellogg, G., & Brown, †E. L. (2000). Genomic Analysis of Gene Expression in *C. elegans*. *Science*, *290*(5492), 809–812. <https://doi.org/10.1126/science.290.5492.809>
- Hiott, D. W., & Labbate, L. (2002). Anxiety disorders associated with traumatic brain injuries. *NeuroRehabilitation*, *17*, 345–355. <https://doi.org/10.3233/NRE-2002-17408>
- Hoge, C. W., McGurk, D., Thomas, J. L., Cox, A. L., Engel, C. C., & Castro, C. A. (2008). Mild Traumatic Brain Injury in U.S. Soldiers Returning from Iraq. *New England Journal of Medicine*, *358*(5), 453–463. <https://doi.org/10.1056/NEJMoa072972>
- Hooper, C., Killick, R., & Lovestone, S. (2008). The GSK3 hypothesis of Alzheimer's disease. *Journal of Neurochemistry*, *104*(6), 1433–1439. <https://doi.org/https://doi.org/10.1111/j.1471-4159.2007.05194.x>
- Irwin, D. J., Cohen, T. J., Grossman, M., Arnold, S. E., McCarty-Wood, E., Van Deerlin, V. M., Lee, V. M.-Y., & Trojanowski, J. Q. (2013). Acetylated Tau Neuropathology in Sporadic and Hereditary Tauopathies. *The American Journal of Pathology*, *183*(2), 344–351. <https://doi.org/https://doi.org/10.1016/j.ajpath.2013.04.025>
- Jeganathan, S., Hascher, A., Chinnathambi, S., Biernat, J., Mandelkow, E.-M., & Mandelkow, E. (2008). Proline-directed Pseudo-phosphorylation at AT8 and PHF1 Epitopes Induces a Compaction of the Paperclip Folding of Tau and Generates a

- Pathological (MC-1) Conformation*. *Journal of Biological Chemistry*, 283(46), 32066–32076. <https://doi.org/https://doi.org/10.1074/jbc.M805300200>
- Jullienne, A., Obenaus, A., Ichkova, A., Savona-Baron, C., Pearce, W. J., & Badaut, J. (2016). Chronic cerebrovascular dysfunction after traumatic brain injury. *Journal of Neuroscience Research*, 94(7), 609–622. <https://doi.org/https://doi.org/10.1002/jnr.23732>
- Katzenberger, R. J., Loewen, C. A., Wassarman, D. R., Petersen, A. J., Ganetzky, B., & Wassarman, D. A. (2013). A Drosophila model of closed head traumatic brain injury. *Proceedings of the National Academy of Sciences*, 110(44), E4152–E4159. <https://doi.org/10.1073/pnas.1316895110>
- Kim, N.-G., Xu, C., & Gumbiner, B. M. (2009). Identification of targets of the Wnt pathway destruction complex in addition to β -catenin. *Proceedings of the National Academy of Sciences*, 106(13), 5165–5170. <https://doi.org/10.1073/pnas.0810185106>
- Kohtala, S., Theilmann, W., Suomi, T., Wigren, H.-K., Porkka-Heiskanen, T., Elo, L. L., Rokka, A., & Rantamäki, T. (2016). Brief Isoflurane Anesthesia Produces Prominent Phosphoproteomic Changes in the Adult Mouse Hippocampus. *ACS Chemical Neuroscience*, 7(6), 749–756. <https://doi.org/10.1021/acchemneuro.6b00002>
- Kokiko-Cochran, O. N., Saber, M., Puntambekar, S., Bemiller, S. M., Katsumoto, A., Lee, Y.-S., Bhaskar, K., Ransohoff, R. M., & Lamb, B. T. (2018). Traumatic Brain Injury in hTau Model Mice: Enhanced Acute Macrophage Response and Altered Long-Term Recovery. *Journal of Neurotrauma*, 35(1), 73–84. <https://doi.org/10.1089/neu.2017.5203>
- Kolarova, M., García-Sierra, F., Bartos, A., Ricny, J., & Ripova, D. (2012). Structure and Pathology of Tau Protein in Alzheimer Disease. *International Journal of Alzheimer Disease*, 2012, 731526. <https://doi.org/10.1155/2012/731526>

- Koponen, S., Taiminen, T., Portin, R., Himanen, L., Isoniemi, H., Heinonen, H., Hinkka, S., & Tenovuo, O. (2002). Axis I and II Psychiatric Disorders After Traumatic Brain Injury: A 30-Year Follow-Up Study. *American Journal of Psychiatry*, *159*(8), 1315–1321. <https://doi.org/10.1176/appi.ajp.159.8.1315>
- Kosik, K. S., Orecchio, L. D., Bakalis, S., & Neve, R. L. (1989). Developmentally regulated expression of specific tau sequences. *Neuron*, *2*(4), 1389–1397. [https://doi.org/10.1016/0896-6273\(89\)90077-9](https://doi.org/10.1016/0896-6273(89)90077-9)
- Kovacs, G. G. (2018). Chapter 25 - Tauopathies. In G. G. Kovacs & I. B. T.-H. of C. N. Alafuzoff (Eds.), *Neuropathology* (Vol. 145, pp. 355–368). Elsevier. <https://doi.org/https://doi.org/10.1016/B978-0-12-802395-2.00025-0>
- Krishnamurthy K, & Laskowitz DT. (2016). Chapter 5: Cellular and Molecular Mechanisms of Secondary Neuronal Injury following Traumatic Brain Injury. In *Translational Research in Traumatic Brain Injury*. Boca Raton (FL): CRC Press/Taylor and Francis Group. <https://www.ncbi.nlm.nih.gov/books/NBK326718/>
- Krishnankutty, A., Kimura, T., Saito, T., Aoyagi, K., Asada, A., Takahashi, S.-I., Ando, K., Ohara-Imaizumi, M., Ishiguro, K., & Hisanaga, S. (2017). In vivo regulation of glycogen synthase kinase 3 β activity in neurons and brains. *Scientific Reports*, *7*(1), 8602. <https://doi.org/10.1038/s41598-017-09239-5>
- Kumar, H., & Udgaonkar, J. B. (2018). Mechanistic and Structural Origins of the Asymmetric Barrier to Prion-like Cross-Seeding between Tau-3R and Tau-4R. *Journal of Molecular Biology*, *430*(24), 5304–5312. <https://doi.org/https://doi.org/10.1016/j.jmb.2018.09.010>
- Laurer, H. L., Bareyre, F. M., Lee, V. M. Y. C., Trojanowski, J. Q., Longhi, L., Hoover, R., Saatman, K. E., Raghupathi, R., Hoshino, S., Grady, M. S., & McIntosh, T. K. (2001). Mild head injury increasing the brain's vulnerability to a second concussive impact. *Journal of Neurosurgery*, *95*(5), 859–870. <https://doi.org/10.3171/jns.2001.95.5.0859>

- Lazarus, R. C., Buonora, J. E., Jacobowitz, D. M., & Mueller, G. P. (2015). Protein carbonylation after traumatic brain injury: cell specificity, regional susceptibility, and gender differences. *Free Radical Biology and Medicine*, 78, 89–100. <https://doi.org/https://doi.org/10.1016/j.freeradbiomed.2014.10.507>
- Lee, G., Thangavel, R., Sharma, V. M., Litersky, J. M., Bhaskar, K., Fang, S. M., Do, L. H., Andreadis, A., Van Hoesen, G., & Ksiezak-Reding, H. (2004). Phosphorylation of Tau by Fyn: Implications for Alzheimer's Disease. *The Journal of Neuroscience*, 24(9), 2304–2312. <https://doi.org/10.1523/JNEUROSCI.4162-03.2004>
- Lee, V. M.-Y., Goedert, M., & Trojanowski, J. Q. (2001). Neurodegenerative Tauopathies. *Annual Review of Neuroscience*, 24(1), 1121–1159. <https://doi.org/10.1146/annurev.neuro.24.1.1121>
- Leikas, J. V, Kohtala, S., Theilmann, W., Jalkanen, A. J., Forsberg, M. M., & Rantamäki, T. (2017). Brief isoflurane anesthesia regulates striatal AKT-GSK3 β signaling and ameliorates motor deficits in a rat model of early-stage Parkinson's disease. *Journal of Neurochemistry*, 142(3), 456–463. <https://doi.org/10.1111/jnc.14066>
- Leong Bin Abdullah, M. F. I., Ng, Y. P., & Sidi, H. Bin. (2018). Depression and anxiety among traumatic brain injury patients in Malaysia. *Asian Journal of Psychiatry*, 37, 67–70. <https://doi.org/https://doi.org/10.1016/j.ajp.2018.08.017>
- Linding, R., Jensen, L. J., Ostheimer, G. J., van Vugt, M. A. T. M., Jørgensen, C., Miron, I. M., Diella, F., Colwill, K., Taylor, L., Elder, K., Metalnikov, P., Nguyen, V., Pasculescu, A., Jin, J., Park, J. G., Samson, L. D., Woodgett, J. R., Russell, R. B., Bork, P., ... Pawson, T. (2007). Systematic Discovery of In Vivo Phosphorylation Networks. *Cell*, 129(7), 1415–1426. <https://doi.org/https://doi.org/10.1016/j.cell.2007.05.052>
- Ling, H., Hardy, J., & Zetterberg, H. (2015). Neurological consequences of traumatic brain injuries in sports. *Molecular and Cellular Neuroscience*, 66, 114–122. <https://doi.org/https://doi.org/10.1016/j.mcn.2015.03.012>

- Longhi, L., Saatman, K. E., Fujimoto, S., Raghupathi, R., Meaney, D. F., Davis, J., McMillan, A., Conte, V., Laurer, H. L., Stein, S., Stocchetti, N., & McIntosh, T. K. (2005). Temporal Window of Vulnerability to Repetitive Experimental Concussive Brain Injury. *Neurosurgery*, *56*(2), 364–374. <https://doi.org/10.1227/01.NEU.0000149008.73513.44>
- Lucas, J. J., Hernández, F., Gómez-Ramos, P., Morán, M. A., Hen, R., & Avila, J. (2001). Decreased nuclear beta-catenin, tau hyperphosphorylation and neurodegeneration in GSK-3beta conditional transgenic mice. *The EMBO Journal*, *20*(1–2), 27–39. <https://doi.org/10.1093/emboj/20.1.27>
- Lucke-Wold, B. P., Turner, R. C., Logsdon, A. F., Bailes, J. E., Huber, J. D., & Rosen, C. L. (2014). Linking Traumatic Brain Injury to Chronic Traumatic Encephalopathy: Identification of Potential Mechanisms Leading to Neurofibrillary Tangle Development. *Journal of Neurotrauma*, *31*(13), 1129–1138. <https://doi.org/10.1089/neu.2013.3303>
- Luo, J., Nguyen, A., Villeda, S., Zhang, H., Ding, Z., Lindsey, D., Bieri, G., Castellano, J. M., Beaupre, G. S., & Wyss-Coray, T. (2014). Long-term cognitive impairments and pathological alterations in a mouse model of repetitive mild traumatic brain injury. *Frontiers in Neurology*, *5*, 12. <https://doi.org/10.3389/fneur.2014.00012>
- Mannix, R., Berglass, J., Berkner, J., Moleus, P., Qiu, J., Andrews, N., Gunner, G., Berglass, L., Jantzie, L. L., Robinson, S., & Meehan, W. P. (2014). Chronic gliosis and behavioral deficits in mice following repetitive mild traumatic brain injury. *Journal of Neurosurgery JNS*, *121*(6), 1342–1350. <https://doi.org/10.3171/2014.7.JNS14272>
- Maroon, J. C., LePere, D. B., Blaylock, R. L., & Bost, J. W. (2012). Postconcussion Syndrome: A Review of Pathophysiology and Potential Nonpharmacological Approaches to Treatment. *The Physician and Sportsmedicine*, *40*(4), 73–87. <https://doi.org/10.3810/psm.2012.11.1990>
- Martland, H. S. (1928). PUNCH DRUNK. *Journal of the American Medical Association*,

91(15), 1103–1107. <https://doi.org/10.1001/jama.1928.02700150029009>

- Mauri, M. C., Paletta, S., Colasanti, A., Misericocchi, G., & Altamura, A. C. (2014). Clinical and neuropsychological correlates of major depression following post-traumatic brain injury, a prospective study. *Asian Journal of Psychiatry*, *12*, 118–124. <https://doi.org/https://doi.org/10.1016/j.ajp.2014.07.003>
- Mbye, L. H., Singh, I. N., Sullivan, P. G., Springer, J. E., & Hall, E. D. (2008). Attenuation of acute mitochondrial dysfunction after traumatic brain injury in mice by NIM811, a non-immunosuppressive cyclosporin A analog. *Experimental Neurology*, *209*(1), 243–253. <https://doi.org/https://doi.org/10.1016/j.expneurol.2007.09.025>
- McAllister, T. W. (2010). Genetic Factors Modulating Outcome After Neurotrauma. *PM&R*, *2*(12), S241–S252. <https://doi.org/https://doi.org/10.1016/j.pmrj.2010.10.005>
- McKee, A. C., Cantu, R. C., Nowinski, C. J., Hedley-Whyte, E. T., Gavett, B. E., Budson, A. E., Santini, V. E., Lee, H.-S., Kubilus, C. A., & Stern, R. A. (2009). Chronic traumatic encephalopathy in athletes: progressive tauopathy after repetitive head injury. *Journal of Neuropathology and Experimental Neurology*, *68*(7), 709–735. <https://doi.org/10.1097/NEN.0b013e3181a9d503>
- McKee, A. C., Gavett, B. E., Stern, R. A., Nowinski, C. J., Cantu, R. C., Kowall, N. W., Perl, D. P., Hedley-Whyte, E. T., Price, B., Sullivan, C., Morin, P., Lee, H.-S., Kubilus, C. A., Daneshvar, D. H., Wulff, M., & Budson, A. E. (2010). TDP-43 Proteinopathy and Motor Neuron Disease in Chronic Traumatic Encephalopathy. *Journal of Neuropathology & Experimental Neurology*, *69*(9), 918–929. <https://doi.org/10.1097/NEN.0b013e3181ee7d85>
- McKee, A. C., Stein, T. D., Nowinski, C. J., Stern, R. A., Daneshvar, D. H., Alvarez, V. E., Lee, H.-S., Hall, G., Wojtowicz, S. M., Baugh, C. M., Riley, D. O., Kubilus, C. A., Cormier, K. A., Jacobs, M. A., Martin, B. R., Abraham, C. R., Ikezu, T., Reichard, R. R., Wolozin, B. L., ... Cantu, R. C. (2013). The spectrum of disease in

- chronic traumatic encephalopathy. *Brain*, *136*(1), 43–64.
<https://doi.org/10.1093/brain/aws307>
- Medina, M., & Wandosell, F. (2011). Deconstructing GSK-3: The Fine Regulation of Its Activity. *International Journal of Alzheimer's Disease*, *2011*, 479249.
<https://doi.org/10.4061/2011/479249>
- Miansari, M., Mehta, M. D., Schilling, J. M., Kurashina, Y., Patel, H. H., & Friend, J. (2019). Inducing Mild Traumatic Brain Injury in *C. elegans* via Cavitation-Free Surface Acoustic Wave-Driven Ultrasonic Irradiation. *Scientific Reports*, *9*(1), 12775. <https://doi.org/10.1038/s41598-019-47295-1>
- Monson, K. L., Converse, M. I., & Manley, G. T. (2019). Cerebral blood vessel damage in traumatic brain injury. *Clinical Biomechanics*, *64*, 98–113.
<https://doi.org/https://doi.org/10.1016/j.clinbiomech.2018.02.011>
- Montenigro, P. H., Alosco, M. L., Martin, B. M., Daneshvar, D. H., Mez, J., Chaisson, C. E., Nowinski, C. J., Au, R., McKee, A. C., Cantu, R. C., McClean, M. D., Stern, R. A., & Tripodis, Y. (2017). Cumulative Head Impact Exposure Predicts Later-Life Depression, Apathy, Executive Dysfunction, and Cognitive Impairment in Former High School and College Football Players. *Journal of Neurotrauma*, *34*(2), 328–340. <https://doi.org/10.1089/neu.2016.4413>
- Montenigro, P. H., Corp, D. T., Stein, T. D., Cantu, R. C., & Stern, R. A. (2015). Chronic Traumatic Encephalopathy: Historical Origins and Current Perspective. *Annual Review of Clinical Psychology*, *11*(1), 309–330. <https://doi.org/10.1146/annurev-clinpsy-032814-112814>
- Monteserin-Garcia, J., Al-Massadi, O., Seoane, L. M., Alvarez, C. V., Shan, B., Stalla, J., Paez-Pereda, M., Casanueva, F. F., Stalla, G. K., & Theodoropoulou, M. (2013). Sirt1 inhibits the transcription factor CREB to regulate pituitary growth hormone synthesis. *The FASEB Journal*, *27*(4), 1561–1571.
<https://doi.org/https://doi.org/10.1096/fj.12-220129>

- Morganti-Kossmann, M. C., Rancan, M., Otto, V. I., Stahel, P. F., & Kossmann, T. (2001). Role of Cerebral Inflammation After Traumatic Brain Injury: A Revisited Concept. *Shock*, *16*(3), 165–177. https://journals.lww.com/shockjournal/Fulltext/2001/16030/ROLE_OF_CEREBRAL_INFLAMMATION_AFTER_TRAUMATIC.1.aspx
- Morris, M., Knudsen, G. M., Maeda, S., Trinidad, J. C., Ioanoviciu, A., Burlingame, A. L., & Mucke, L. (2015). Tau post-translational modifications in wild-type and human amyloid precursor protein transgenic mice. *Nature Neuroscience*, *18*(8), 1183–1189. <https://doi.org/10.1038/nn.4067>
- Moszczynski, A. J., Gohar, M., Volkening, K., Leystra-Lantz, C., Strong, W., & Strong, M. J. (2015). Thr175-phosphorylated tau induces pathologic fibril formation via GSK3 β -mediated phosphorylation of Thr231 in vitro. *Neurobiology of Aging*, *36*(3), 1590–1599. <https://doi.org/https://doi.org/10.1016/j.neurobiolaging.2014.12.001>
- Moszczynski, A. J., Harvey, M., Fulcher, N., de Oliveira, C., McCunn, P., Donison, N., Bartha, R., Schmid, S., Strong, M. J., & Volkening, K. (2019). Synergistic toxicity in an in vivo model of neurodegeneration through the co-expression of human TDP-43M337V and tauT175D protein. *Acta Neuropathologica Communications*, *7*(1), 170. <https://doi.org/10.1186/s40478-019-0816-1>
- Moszczynski, A. J., Strong, W., Xu, K., McKee, A., Brown, A., & Strong, M. J. (2018). Pathologic Thr(175) tau phosphorylation in CTE and CTE with ALS. *Neurology*, *90*(5), e380–e387. <https://doi.org/10.1212/WNL.0000000000004899>
- Mudher, A., Colin, M., Dujardin, S., Medina, M., Dewachter, I., Alavi Naini, S. M., Mandelkow, E.-M., Mandelkow, E., Buée, L., Goedert, M., & Brion, J.-P. (2017). What is the evidence that tau pathology spreads through prion-like propagation? *Acta Neuropathologica Communications*, *5*(1), 99. <https://doi.org/10.1186/s40478-017-0488-7>
- Niblock, M., & Gallo, J.-M. (2012). Tau alternative splicing in familial and sporadic tauopathies. *Biochemical Society Transactions*, *40*(4), 677–680.

<https://doi.org/10.1042/BST20120091>

- Noble, W., Planel, E., Zehr, C., Olm, V., Meyerson, J., Suleman, F., Gaynor, K., Wang, L., LaFrancois, J., Feinstein, B., Burns, M., Krishnamurthy, P., Wen, Y., Bhat, R., Lewis, J., Dickson, D., & Duff, K. (2005). Inhibition of glycogen synthase kinase-3 by lithium correlates with reduced tauopathy and degeneration in vivo. *Proceedings of the National Academy of Sciences of the United States of America*, *102*(19), 6990–6995. <https://doi.org/10.1073/pnas.0500466102>
- Ojo, J.-O., Mouzon, B., Greenberg, M. B., Bachmeier, C., Mullan, M., & Crawford, F. (2013). Repetitive Mild Traumatic Brain Injury Augments Tau Pathology and Glial Activation in Aged hTau Mice. *Journal of Neuropathology & Experimental Neurology*, *72*(2), 137–151. <https://doi.org/10.1097/NEN.0b013e3182814cdf>
- Park, S. A., Ahn, S. Il, & Gallo, J.-M. (2016). Tau mis-splicing in the pathogenesis of neurodegenerative disorders. *BMB Reports*, *49*(8), 405–413. <https://doi.org/10.5483/bmbrep.2016.49.8.084>
- Parker, H. L. (1934). Traumatic Encephalopathy ('Punch Drunk') of Professional Pugilists. *The Journal of Neurology and Psychopathology*, *15*(57), 20–28. <https://doi.org/10.1136/jnnp.s1-15.57.20>
- Pierce, J. E. S., Smith, D. H., Trojanowski, J. Q., & McIntosh, T. K. (1998). Enduring cognitive, neurobehavioral and histopathological changes persist for up to one year following severe experimental brain injury in rats. *Neuroscience*, *87*(2), 359–369. [https://doi.org/https://doi.org/10.1016/S0306-4522\(98\)00142-0](https://doi.org/https://doi.org/10.1016/S0306-4522(98)00142-0)
- Polydoro, M., Acker, C. M., Duff, K., Castillo, P. E., & Davies, P. (2009). Age-Dependent Impairment of Cognitive and Synaptic Function in the htau Mouse Model of Tau Pathology. *The Journal of Neuroscience*, *29*(34), 10741 LP – 10749. <https://doi.org/10.1523/JNEUROSCI.1065-09.2009>
- Popovitz, J., Mysore, S. P., & Adwanikar, H. (2019). Long-Term Effects of Traumatic Brain Injury on Anxiety-Like Behaviors in Mice: Behavioral and Neural Correlates

- . In *Frontiers in Behavioral Neuroscience* (Vol. 13, p. 6).
<https://www.frontiersin.org/article/10.3389/fnbeh.2019.00006>
- Rehman, S. U., Ikram, M., Ullah, N., Alam, S. I., Park, H. Y., Badshah, H., Choe, K., & Ok Kim, M. (2019). Neurological Enhancement Effects of Melatonin against Brain Injury-Induced Oxidative Stress, Neuroinflammation, and Neurodegeneration via AMPK/CREB Signaling. In *Cells* (Vol. 8, Issue 7, p. 760).
<https://doi.org/10.3390/cells8070760>
- Reynolds, C. H., Betts, J. C., Blackstock, W. P., Nebreda, A. R., & Anderton, B. H. (2000). Phosphorylation Sites on Tau Identified by Nanoelectrospray Mass Spectrometry. *Journal of Neurochemistry*, 74(4), 1587–1595.
<https://doi.org/https://doi.org/10.1046/j.1471-4159.2000.0741587.x>
- Risling, M., Smith, D., Stein, T. D., Thelin, E. P., Zanier, E. R., Ankarcrona, M., & Nilsson, P. (2019). Modelling human pathology of traumatic brain injury in animal models. *Journal of Internal Medicine*, 285(6), 594–607.
<https://doi.org/https://doi.org/10.1111/joim.12909>
- Roberts, G. W., Allsop, D., & Bruton, C. (1990). The occult aftermath of boxing. *Journal of Neurology, Neurosurgery, and Psychiatry*, 53(5), 373–378.
<https://doi.org/10.1136/jnnp.53.5.373>
- Rola, R., Mizumatsu, S., Otsuka, S., Morhardt, D. R., Noble-Haeusslein, L. J., Fishman, K., Potts, M. B., & Fike, J. R. (2006). Alterations in hippocampal neurogenesis following traumatic brain injury in mice. *Experimental Neurology*, 202(1), 189–199.
<https://doi.org/https://doi.org/10.1016/j.expneurol.2006.05.034>
- Saito, T., Mihira, N., Matsuba, Y., Sasaguri, H., Hashimoto, S., Narasimhan, S., Zhang, B., Murayama, S., Higuchi, M., Lee, V. M. Y., Trojanowski, J. Q., & Saido, T. C. (2019). Humanization of the entire murine *Mapt* gene provides a murine model of pathological human tau propagation. *Journal of Biological Chemistry*, 294(34), 12754–12765. <https://doi.org/10.1074/jbc.RA119.009487>

- Sánchez-Juan, P., Moreno, S., de Rojas, I., Hernández, I., Valero, S., Alegret, M., Montreal, L., García González, P., Lage, C., López-García, S., Rodríguez-Rodríguez, E., Orellana, A., Tárraga, L., Boada, M., & Ruiz, A. (2019). The MAPT H1 Haplotype Is a Risk Factor for Alzheimer's Disease in APOE ϵ 4 Non-carriers. *Frontiers in Aging Neuroscience*, *11*, 327. <https://doi.org/10.3389/fnagi.2019.00327>
- Sanders, D. W., Kaufman, S. K., DeVos, S. L., Sharma, A. M., Mirbaha, H., Li, A., Barker, S. J., Foley, A. C., Thorpe, J. R., Serpell, L. C., Miller, T. M., Grinberg, L. T., Seeley, W. W., & Diamond, M. I. (2014). Distinct Tau Prion Strains Propagate in Cells and Mice and Define Different Tauopathies. *Neuron*, *82*(6), 1271–1288. <https://doi.org/https://doi.org/10.1016/j.neuron.2014.04.047>
- Schultz, M. K., Gentzel, R., Usenovic, M., Gretzula, C., Ware, C., Parmentier-Batteur, S., Schachter, J. B., & Zariwala, H. A. (2018). Pharmacogenetic neuronal stimulation increases human tau pathology and trans-synaptic spread of tau to distal brain regions in mice. *Neurobiology of Disease*, *118*, 161–176. <https://doi.org/https://doi.org/10.1016/j.nbd.2018.07.003>
- Serenó, L., Coma, M., Rodríguez, M., Sánchez-Ferrer, P., Sánchez, M. B., Gich, I., Agulló, J. M., Pérez, M., Avila, J., Guardia-Laguarta, C., Clarimón, J., Lleó, A., & Gómez-Isla, T. (2009). A novel GSK-3 β inhibitor reduces Alzheimer's pathology and rescues neuronal loss in vivo. *Neurobiology of Disease*, *35*(3), 359–367. <https://doi.org/https://doi.org/10.1016/j.nbd.2009.05.025>
- Sergeant, N., Delacourte, A., & Buée, L. (2005). Tau protein as a differential biomarker of tauopathies. *Biochimica et Biophysica Acta (BBA) - Molecular Basis of Disease*, *1739*(2), 179–197. <https://doi.org/https://doi.org/10.1016/j.bbadis.2004.06.020>
- Shah, E. J., Gurdziel, K., & Ruden, D. M. (2019). Mammalian Models of Traumatic Brain Injury and a Place for Drosophila in TBI Research . In *Frontiers in Neuroscience* (Vol. 13, p. 409). <https://www.frontiersin.org/article/10.3389/fnins.2019.00409>
- Shitaka, Y., Tran, H. T., Bennett, R. E., Sanchez, L., Levy, M. A., Dikranian, K., &

- Brody, D. L. (2011). Repetitive Closed-Skull Traumatic Brain Injury in Mice Causes Persistent Multifocal Axonal Injury and Microglial Reactivity. *Journal of Neuropathology & Experimental Neurology*, 70(7), 551–567. <https://doi.org/10.1097/NEN.0b013e31821f891f>
- Shultz, S. R., McDonald, S. J., Corrigan, F., Semple, B. D., Salberg, S., Zamani, A., Jones, N. C., & Mychasiuk, R. (2020). Clinical Relevance of Behavior Testing in Animal Models of Traumatic Brain Injury. *Journal of Neurotrauma*, 37(22), 2381–2400. <https://doi.org/10.1089/neu.2018.6149>
- Siebold, L., Obenaus, A., & Goyal, R. (2018). Criteria to define mild, moderate, and severe traumatic brain injury in the mouse controlled cortical impact model. *Experimental Neurology*, 310, 48–57. <https://doi.org/https://doi.org/10.1016/j.expneurol.2018.07.004>
- Soutar, M. P. M., Kim, W.-Y., Williamson, R., Peggie, M., Hastie, C. J., McLauchlan, H., Snider, W. D., Gordon-Weeks, P. R., & Sutherland, C. (2010). Evidence that glycogen synthase kinase-3 isoforms have distinct substrate preference in the brain. *Journal of Neurochemistry*, 115(4), 974–983. <https://doi.org/https://doi.org/10.1111/j.1471-4159.2010.06988.x>
- Spillantini, M. G., & Goedert, M. (1998). Tau protein pathology in neurodegenerative diseases. *Trends in Neurosciences*, 21(10), 428–433. [https://doi.org/https://doi.org/10.1016/S0166-2236\(98\)01337-X](https://doi.org/https://doi.org/10.1016/S0166-2236(98)01337-X)
- Stambolic, V., & Woodgett, J. R. (1994). Mitogen inactivation of glycogen synthase kinase-3 beta in intact cells via serine 9 phosphorylation. *The Biochemical Journal*, 303(Pt 3), 701–704. <https://doi.org/10.1042/bj3030701>
- Stein, T. D., Alvarez, V. E., & McKee, A. C. (2014). Chronic traumatic encephalopathy: a spectrum of neuropathological changes following repetitive brain trauma in athletes and military personnel. *Alzheimer's Research & Therapy*, 6(1), 4. <https://doi.org/10.1186/alzrt234>

- Tagge, C. A., Fisher, A. M., Minaeva, O. V, Gaudreau-Balderrama, A., Moncaster, J. A., Zhang, X.-L., Wojnarowicz, M. W., Casey, N., Lu, H., Kokiko-Cochran, O. N., Saman, S., Ericsson, M., Onos, K. D., Veksler, R., Senatorov Jr, V. V, Kondo, A., Zhou, X. Z., Miry, O., Vose, L. R., ... Goldstein, L. E. (2018). Concussion, microvascular injury, and early tauopathy in young athletes after impact head injury and an impact concussion mouse model. *Brain*, *141*(2), 422–458. <https://doi.org/10.1093/brain/awx350>
- Tate, D. F., Wade, B. S. C., Velez, C. S., Drennon, A. M., Bolzenius, J., Gutman, B. A., Thompson, P. M., Lewis, J. D., Wilde, E. A., Bigler, E. D., Shenton, M. E., Ritter, J. L., & York, G. E. (2016). Volumetric and shape analyses of subcortical structures in United States service members with mild traumatic brain injury. *Journal of Neurology*, *263*(10), 2065–2079. <https://doi.org/10.1007/s00415-016-8236-7>
- Thornton, T. M., Pedraza-Alva, G., Deng, B., Wood, C. D., Aronshtam, A., Clements, J. L., Sabio, G., Davis, R. J., Matthews, D. E., Doble, B., & Rincon, M. (2008). Phosphorylation by p38 MAPK as an alternative pathway for GSK3beta inactivation. *Science*, *320*(5876), 667–670. <https://doi.org/10.1126/science.1156037>
- Tomkins, O., Feintuch, A., Benifla, M., Cohen, A., Friedman, A., & Shelef, I. (2011). Blood-brain barrier breakdown following traumatic brain injury: a possible role in posttraumatic epilepsy. *Cardiovascular Psychiatry and Neurology*, *2011*, 765923. <https://doi.org/10.1155/2011/765923>
- Trinczek, B., Biernat, J., Baumann, K., Mandelkow, E. M., & Mandelkow, E. (1995). Domains of tau protein, differential phosphorylation, and dynamic instability of microtubules. *Molecular Biology of the Cell*, *6*(12), 1887–1902. <https://doi.org/10.1091/mbc.6.12.1887>
- Tsujio, I., Tanaka, T., Kudo, T., Nishikawa, T., Shinozaki, K., Grundke-Iqbal, I., Iqbal, K., & Takeda, M. (2000). Inactivation of glycogen synthase kinase-3 by protein kinase C δ : implications for regulation of τ phosphorylation. *FEBS Letters*, *469*(1), 111–117. [https://doi.org/https://doi.org/10.1016/S0014-5793\(00\)01234-5](https://doi.org/https://doi.org/10.1016/S0014-5793(00)01234-5)

- Turner, R. C., Lucke-Wold, B. P., Robson, M. J., Lee, J. M., & Bailes, J. E. (2016). Alzheimer's disease and chronic traumatic encephalopathy: Distinct but possibly overlapping disease entities. *Brain Injury*, 30(11), 1279–1292. <https://doi.org/10.1080/02699052.2016.1193631>
- Tyurin, V. A., Tyurina, Y. Y., Borisenko, G. G., Sokolova, T. V, Ritov, V. B., Quinn, P. J., Rose, M., Kochanek, P., Graham, S. H., & Kagan, V. E. (2000). Oxidative Stress Following Traumatic Brain Injury in Rats. *Journal of Neurochemistry*, 75(5), 2178–2189. <https://doi.org/https://doi.org/10.1046/j.1471-4159.2000.0752178.x>
- Uzan, M., Erman, H., Tanriverdi, T., Sanus, G. Z., Kafadar, A., & Uzun, H. (2006). Evaluation of apoptosis in cerebrospinal fluid of patients with severe head injury. *Acta Neurochirurgica*, 148(11), 1157–1164. <https://doi.org/10.1007/s00701-006-0887-1>
- Waller, K. A., Zhang, L. X., & Jay, G. D. (2017). Friction-Induced Mitochondrial Dysregulation Contributes to Joint Deterioration in Prg4 Knockout Mice. *International Journal of Molecular Sciences*, 18(6). <https://doi.org/10.3390/ijms18061252>
- Walt, G. S., Burriss, H. M., Brady, C. B., Spencer, K. R., Alvarez, V. E., Huber, B. R., Guilderson, L., Abdul Rauf, N., Collins, D., Singh, T., Mathias, R., Averill, J. G., Walker, S. E., Robey, I., McKee, A. C., Kowall, N. W., & Stein, T. D. (2018). Chronic Traumatic Encephalopathy Within an Amyotrophic Lateral Sclerosis Brain Bank Cohort. *Journal of Neuropathology and Experimental Neurology*, 77(12), 1091–1100. <https://doi.org/10.1093/jnen/nly092>
- Washington, P. M., Forcelli, P. A., Wilkins, T., Zapple, D. N., Parsadonian, M., & Burns, M. P. (2012). The Effect of Injury Severity on Behavior: A Phenotypic Study of Cognitive and Emotional Deficits after Mild, Moderate, and Severe Controlled Cortical Impact Injury in Mice. *Journal of Neurotrauma*, 29(13), 2283–2296. <https://doi.org/10.1089/neu.2012.2456>
- Wei, J. C. J., Edwards, G. A., Martin, D. J., Huang, H., Crichton, M. L., & Kendall, M.

- A. F. (2017). Allometric scaling of skin thickness, elasticity, viscoelasticity to mass for micro-medical device translation: from mice, rats, rabbits, pigs to humans. *Scientific Reports*, 7(1), 15885. <https://doi.org/10.1038/s41598-017-15830-7>
- Weissberg, I., Veksler, R., Kamintsky, L., Saar-Ashkenazy, R., Milikovsky, D. Z., Shelef, I., & Friedman, A. (2014). Imaging Blood-Brain Barrier Dysfunction in Football Players. *JAMA Neurology*, 71(11), 1453–1455. <https://doi.org/10.1001/jamaneurol.2014.2682>
- Williams, A. J., Hartings, J. A., Lu, X.-C. M., Rolli, M. L., & Tortella, F. C. (2006). Penetrating ballistic-like brain injury in the rat: differential time courses of hemorrhage, cell death, inflammation, and remote degeneration. In *Journal of Neurotrauma* (Vol. 23, Issue 12, pp. 1828–1846). Mary Ann Liebert., <https://doi.org/10.1089/neu.2006.23.1828>
- Wong, J., Hoe, N. W., Zhiwei, F., & Ng, I. (2005). Apoptosis and traumatic brain injury. *Neurocritical Care*, 3(2), 177–182. <https://doi.org/10.1385/NCC:3:2:177>
- Xiong, Y., Mahmood, A., & Chopp, M. (2013). Animal models of traumatic brain injury. *Nature Reviews Neuroscience*, 14(2), 128–142. <https://doi.org/10.1038/nrn3407>
- Xu, X., Cowan, M., Beraldo, F., Schranz, A., McCunn, P., Geremia, N., Brown, Z., Patel, M., Nygard, K. L., Khazaei, R., Lu, L., Liu, X., Strong, M. J., Dekaban, G. A., Menon, R., Bartha, R., Daley, M., Mao, H., Prado, V., ... Brown, A. (2021). Repetitive mild traumatic brain injury in mice triggers a slowly developing cascade of long-term and persistent behavioral deficits and pathological changes. *Acta Neuropathologica Communications*, 9(1), 60. <https://doi.org/10.1186/s40478-021-01161-2>
- Yap, Y. C., King, A. E., Guijt, R. M., Jiang, T., Blizzard, C. A., Breadmore, M. C., & Dickson, T. C. (2017). Mild and repetitive very mild axonal stretch injury triggers cytoskeletal mislocalization and growth cone collapse. *PloS One*, 12(5), e0176997–e0176997. <https://doi.org/10.1371/journal.pone.0176997>

- Yuan, S. H., & Wang, S. G. (2018). Alzheimer's Dementia due to Suspected CTE from Subconcussive Head Impact. *Case Reports in Neurological Medicine*, 2018, 7890269. <https://doi.org/10.1155/2018/7890269>
- Zhang, X., Chen, Y., Jenkins, L. W., Kochanek, P. M., & Clark, R. S. B. (2004). Bench-to-bedside review: Apoptosis/programmed cell death triggered by traumatic brain injury. *Critical Care*, 9(1), 66–75. <https://doi.org/10.1186/cc2950>
- Zhang, Y., Wu, F., Iqbal, K., Gong, C.-X., Hu, W., & Liu, F. (2019). Subacute to chronic Alzheimer-like alterations after controlled cortical impact in human tau transgenic mice. *Scientific Reports*, 9(1), 3789. <https://doi.org/10.1038/s41598-019-40678-4>
- Ziebell, J. M., & Morganti-Kossmann, M. C. (2010). Involvement of pro- and anti-inflammatory cytokines and chemokines in the pathophysiology of traumatic brain injury. *Neurotherapeutics: The Journal of the American Society for Experimental NeuroTherapeutics*, 7(1), 22–30. <https://doi.org/10.1016/j.nurt.2009.10.016>

Curriculum Vitae

Morgan Walker

EDUCATION

Bachelor of Sciences 2014-2018

The University of Western (Western) Ontario, London, ON

- Honors Specialization in Biology

Candidate of Masters of Science in Neuroscience 2018-Present

The University of Western (Western) Ontario, London, ON

- Degree Status: In Progress

PRESENTATIONS

Ontario Biology Day

The University of Waterloo, Waterloo, ON

- Mining The Clones: Improving The Phylogenetic Information From A Set Of Clones Of Soil-Derived Fungal rNDA

Dean's Undergraduate Research Opportunities Program (DUROP)

The University of Western Ontario, London, ON

- Quantifying Markers of Inflammation in a Mouse Model of Concussion
- 3MT Presentation

Concussion Awareness Conference

The University of Western Ontario, London, ON

- Concussion Awareness Speaker Series
- Presentation and Panel discussions

PUBLICATIONS

Journal Article

Hryciw, T, Geremia, N, **Walker, M**, Xu X, Brown A. (2018). Anti-Chondroitin Sulfate Proteoglycan Strategies in Spinal Cord Injury: Temporal and Spatial Considerations Explain the Balance between Neuroplasticity and Neuroprotection. *Journal of Neurotrauma*. 35(16): 1958-1969.

Thesis/Dissertation

Mining The Clones: Improving The Phylogenetic Information From A Set Of Clones Of Soil-Derived Fungal rNDA. (2018). University of Western Ontario. Bachelor's Honors. Number of Pages: 49 Supervisor: Thorn, Greg

RECOGNITIONS

The Western Scholarship of Excellence

2014-2015

The University of Western Ontario, London, ON

Freedom 55 Financial Scholar Athlete Award Winner The University of Western Ontario, London, ON	2016-2017
Dean's Honor List The University of Western Ontario, London, ON	2016-2018
Dean's Undergraduate Research Opportunities Program (DUROP) The University of Western Ontario, London, ON	2018
Canada Graduate Scholarships (CGS-M) Canadian Institutes of Health Research (CIHR)	2019-2020

COURSES TAUGHT

Graduate Teaching Assistant, Biology The University of Western Ontario, London, ON Course Title: 1201A General Biology 1 Course Level: Undergraduate	2018, 2019
Graduate Teaching Assistant, Biology The University of Western Ontario, London, ON Course Title: 1001A Biology for Science 1 Course Level: Undergraduate	2018, 2019
Graduate Teaching Assistant, Biology The University of Western Ontario, London, ON Course Title: 1202B General Biology 2 Course Level: Undergraduate	2020
Graduate Teaching Assistant, Biology The University of Western Ontario, London, ON Course Title: 1002B Biology for Science 2 Course Level: Undergraduate	2020